

PIERRE
AUGER
OBSERVATORY

Anisotropy studies of the arrival directions of cosmic rays at the highest energies with the Pierre Auger Observatory



João de Mello Neto^a for the Pierre Auger Collaboration^b

^a Federal University of Rio de Janeiro - Brazil

^b Observatorio Pierre Auger, Malargüe, Argentina

HEP2023

Valparaiso - Chile, 9-13 Jan 2023

The highest energy particles



The highest energy particles

Unanswered questions about UHECRs:

The highest energy particles

Unanswered questions about UHECRs:

- ★ **What are those particles?**
- ★ **Where do they come from?**
- ★ **How they reach $E > 10^{20}$ eV = 100 EeV?**
- ★ **Can we extrapolate hadronic models orders of magnitude in energy?**

The highest energy particles

Unanswered questions about UHECRs:

- ★ What are those particles?
- ★ Where do they come from?
- ★ How they reach $E > 10^{20}$ eV = 100 EeV?
- ★ Can we extrapolate hadronic models orders of magnitude in energy?

See talk by Eva Santos
(yesterday)

The highest energy particles

Unanswered questions about UHECRs:

- ★ What are those particles?
- ★ Where do they come from?
- ★ How they reach $E > 10^{20}$ eV = 100 EeV?
- ★ Can we extrapolate hadronic models orders of magnitude in energy?

See talk by Eva Santos
(yesterday)

We need to understand:

- ★ Composition
- ★ Production sources
- ★ Acceleration mechanisms
- ★ Fundamental interactions

The highest energy particles

Unanswered questions about UHECRs:

- ★ What are those particles?
- ★ Where do they come from?
- ★ How they reach $E > 10^{20}$ eV = 100 EeV?
- ★ Can we extrapolate hadronic models orders of magnitude in energy?

See talk by Eva Santos
(yesterday)

We need to understand:

- ★ Composition
- ★ Production sources
- ★ Acceleration mechanisms
- ★ Fundamental interactions

See talk by Belén Andrada

The search for UHECR sources

The search for UHECR sources

- ★ Cosmic rays: observed at energies of more than **10^{20} eV**
- ★ Most **energetic** particles known in the universe

The search for UHECR sources

- ★ Cosmic rays: observed at energies of more than **10^{20} eV**
- ★ Most **energetic** particles known in the universe
 - ★ Search for sources is challenging: charged particles deflected by **magnetic fields**
 - ★ Magnetic fields: **difficult to study** and their modeling is far from being complete

The search for UHECR sources

- ★ Cosmic rays: observed at energies of more than **10^{20} eV**
- ★ Most **energetic** particles known in the universe
 - ★ Search for sources is challenging: charged particles deflected by **magnetic fields**
 - ★ Magnetic fields: **difficult to study** and their modeling is far from being complete
- ★ Above a few tens of EeV: **deflections small enough**, directional information for small charges
- ★ The cosmological **volume** within which UHECRs sources should be sought is **limited**
- ★ CR interact with photon backgrounds, **mean free path** for energy losses depends on their mass and energies
- ★ At 100 EeV, protons and iron: **200-300 Mpc**, intermediate nuclei He, N: **3-6 Mpc**
- ★ Sources of UHECRs must be in the **local universe!**

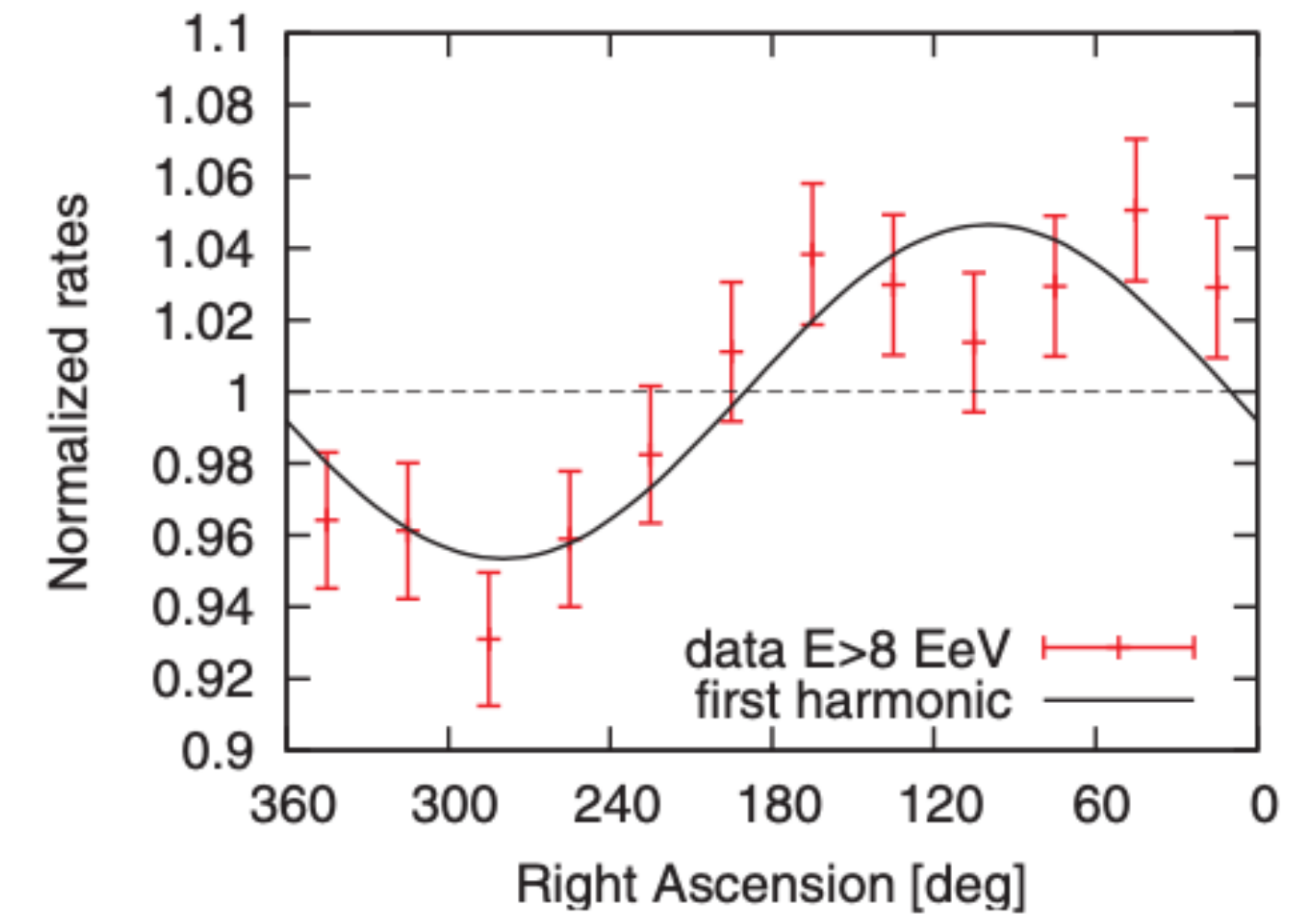
Two approaches to search for anisotropies

Large scale anisotropies can be present at all energies

- ★ **Propagation** from **extragalactic sources** distributed anisotropically
- ★ **Diffusion** from individual extragalactic sources
- ★ **Diffusive escape** from Galaxy of CRs from galactic sources
- ★ **Compton-Getting** effect due to the Earth motion in the CR rest frame

Method: Rayleigh analysis in right ascension (and azimuth)

Challenge: control exposure and event rate down below $< 1\%$ level



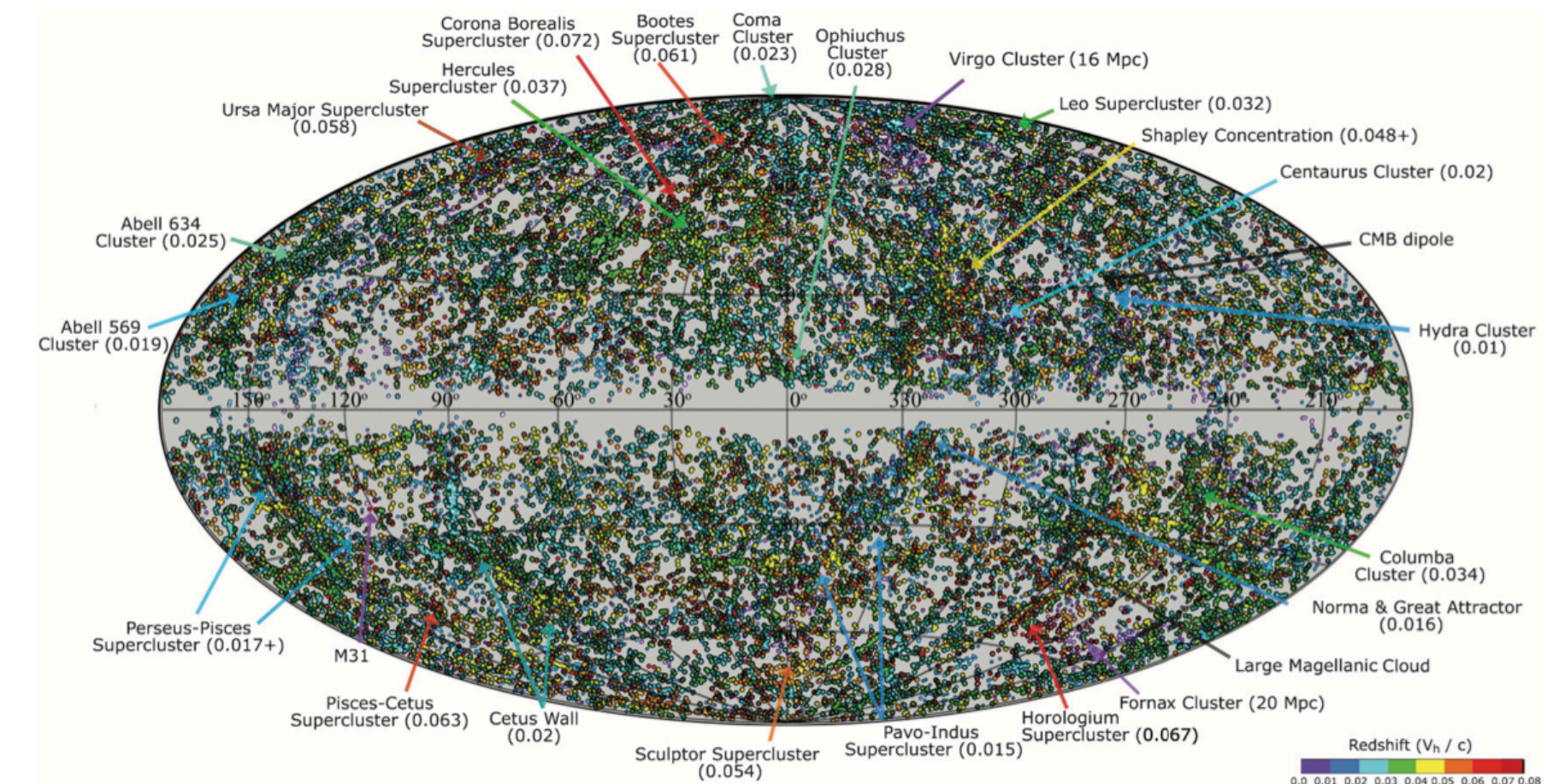
[Pierre Auger Collab., Science, 2017](#)

Small-intermediate scale anisotropies can be present in the suppression region

At UHE, cosmic rays have reduced horizon and maybe enough rigidity **to point back to their sources**

Method: Comparison of UHECR arrival directions with catalogues of astronomical objects

Challenge: control of exposure and trial factor (energy, angle...)



[2MASS Survey, Astrophys. J., 2011](#)

Large scale: weighted harmonic analysis

★ Search for harmonic modulation in right ascension and azimuth: $x = \alpha$ or ϕ

★ Fourier coefficients of order k (1 or 2) $a_x^k = \frac{2}{\mathcal{N}} \sum_{i=1}^N w_i \cos(kx_i), b_x^k = \frac{2}{\mathcal{N}} \sum_{i=1}^N w_i \sin(kx_i)$

★ Amplitude, $r_k^x = \sqrt{(a_k^x)^2 + (b_k^x)^2}$, phase $\varphi_k^x = \frac{1}{k} \tan^{-1} \frac{b_k^x}{a_k^x}$

★ Weights: small variations in coverage and tilt of the array

$$w_i = \left[\Delta N_{cell}(\alpha_i^0) (1 + 0.003 \tan \theta_i \cos(\phi_i - \phi_0)) \right]^{-1}$$

number of active
detector cells

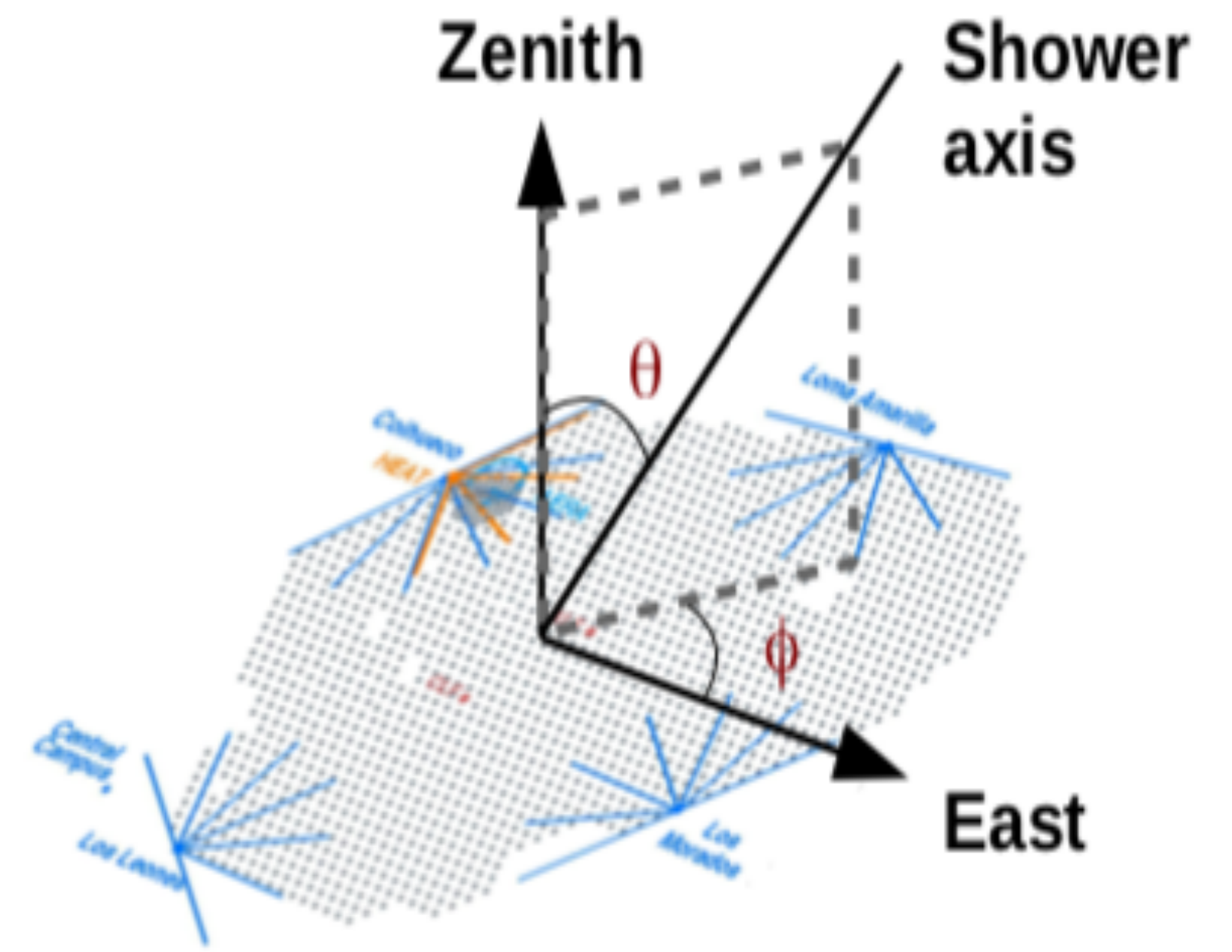
right ascension of the
zenith of the observatory

average tilt of
the array $\phi_0 = -30^\circ$

Dipolar modulation:

$$d_{\perp} \simeq \frac{r_1^{\alpha}}{\langle \cos \delta \rangle}$$

$$d_z \simeq \frac{b_1^{\phi}}{\cos \ell_{obs} \langle \sin \theta \rangle}$$



Harmonic analysis above 4 EeV

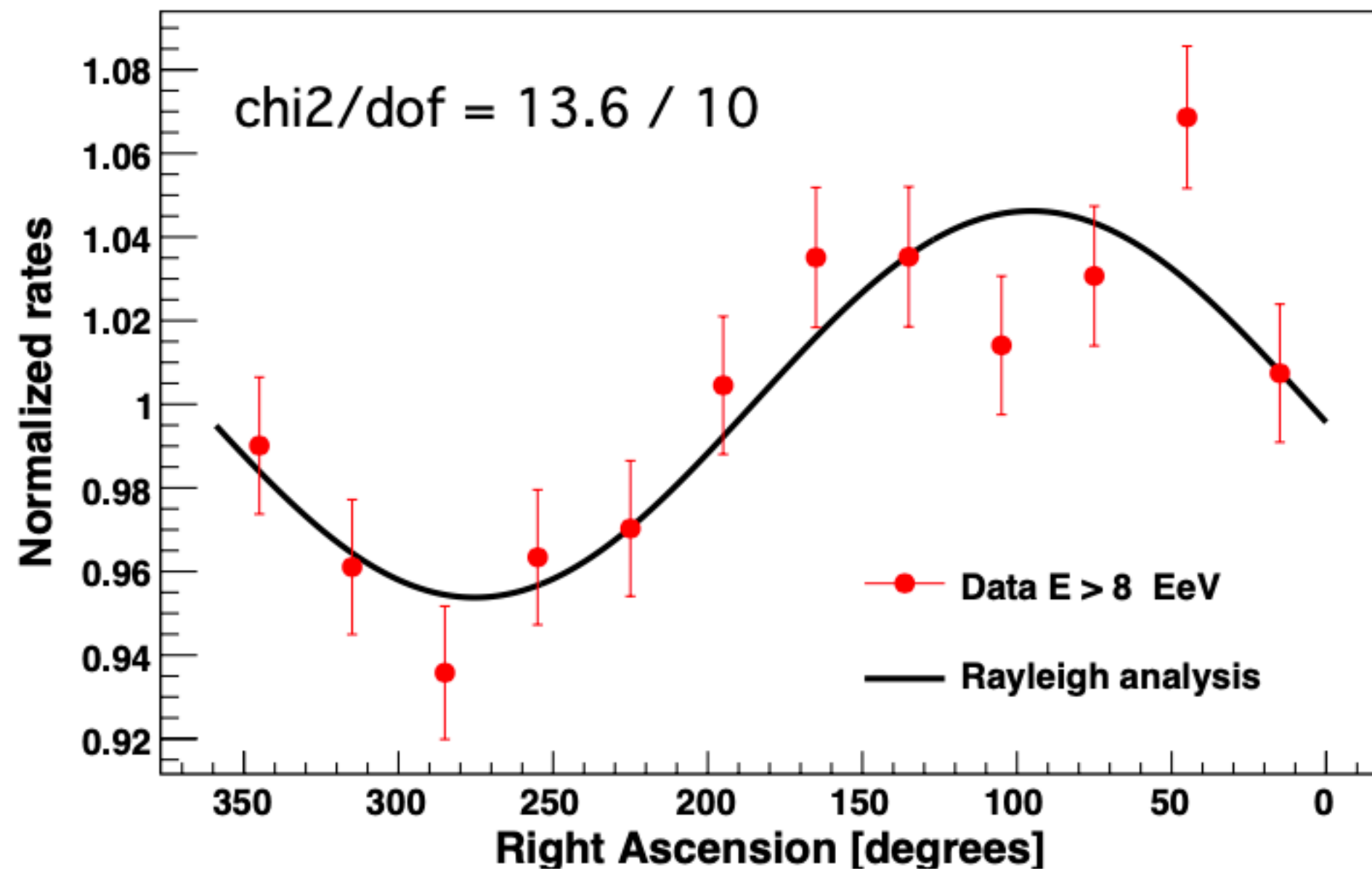
E (EeV)	N	d_{\perp}	d_z	d	$\alpha_d [^{\circ}]$	$\delta_d [^{\circ}]$	$P(\geq r_1^{\alpha})$
4-8	106, 290	$0.01^{+0.006}_{-0.004}$	-0.012 ± 0.008	$0.016^{+0.008}_{-0.005}$	97 ± 29	-48^{+23}_{-22}	1.4×10^{-1}
8-16	32, 794	$0.055^{+0.011}_{-0.009}$	-0.03 ± 0.01	$0.063^{+0.013}_{-0.009}$	95 ± 10	-28^{+12}_{-13}	3.1×10^{-7}
16-32	9, 156	$0.072^{+0.021}_{-0.016}$	-0.07 ± 0.03	$0.10^{+0.03}_{-0.02}$	81 ± 15	-43^{+14}_{-14}	7.5×10^{-4}
≥ 8	44, 398	$0.059^{+0.009}_{-0.008}$	-0.042 ± 0.013	$0.073^{+0.011}_{-0.009}$	95 ± 8	-36^{+9}_{-9}	5.1×10^{-11}
≥ 32	2, 448	$0.11^{+0.04}_{-0.03}$	-0.12 ± 0.05	$0.16^{+0.05}_{-0.04}$	139 ± 19	-47^{+16}_{-15}	1.0×10^{-2}

R. de Almeida, for P. Auger Collab., ICRC 2021

→ 6, 6 σ

Significance of the first harmonic modulation became larger as the exposure increase

1.4×10^{-9} [ApJ 2020](#)
 2.6×10^{-8} [Science 2017](#)
 6×10^{-5} [ApJ 2015](#)



4-8 EeV bin: consistent with isotropy $P(\geq r) = 1.4 \times 10^{-1}$
 > 8 EeV bin: $P(\geq r) = 5 \times 10^{-11}$, $\alpha = 95^{\circ} \pm 8^{\circ}$

Evidence of large scale anisotropies above 8 EeV

(detection above 5σ accounting for the null results in the other energy bins)

Dipole reconstruction

E (EeV)	N	d_{\perp}	d_z	d	α_d [°]	δ_d [°]	$P(\geq r_1^{\alpha})$
4-8	106,290	$0.01^{+0.006}_{-0.004}$	-0.012 ± 0.008	$0.016^{+0.008}_{-0.005}$	97 ± 29	-48^{+23}_{-22}	1.4×10^{-1}
8-16	32,794	$0.055^{+0.011}_{-0.009}$	-0.03 ± 0.01	$0.063^{+0.013}_{-0.009}$	95 ± 10	-28^{+12}_{-13}	3.1×10^{-7}
16-32	9,156	$0.072^{+0.021}_{-0.016}$	-0.07 ± 0.03	$0.10^{+0.03}_{-0.02}$	81 ± 15	-43^{+14}_{-14}	7.5×10^{-4}
≥ 8	44,398	$0.059^{+0.009}_{-0.008}$	-0.042 ± 0.013	$0.073^{+0.011}_{-0.009}$	95 ± 8	-36^{+9}_{-9}	5.1×10^{-11}
≥ 32	2,448	$0.11^{+0.04}_{-0.03}$	-0.12 ± 0.05	$0.16^{+0.05}_{-0.04}$	139 ± 19	-47^{+16}_{-15}	1.0×10^{-2}

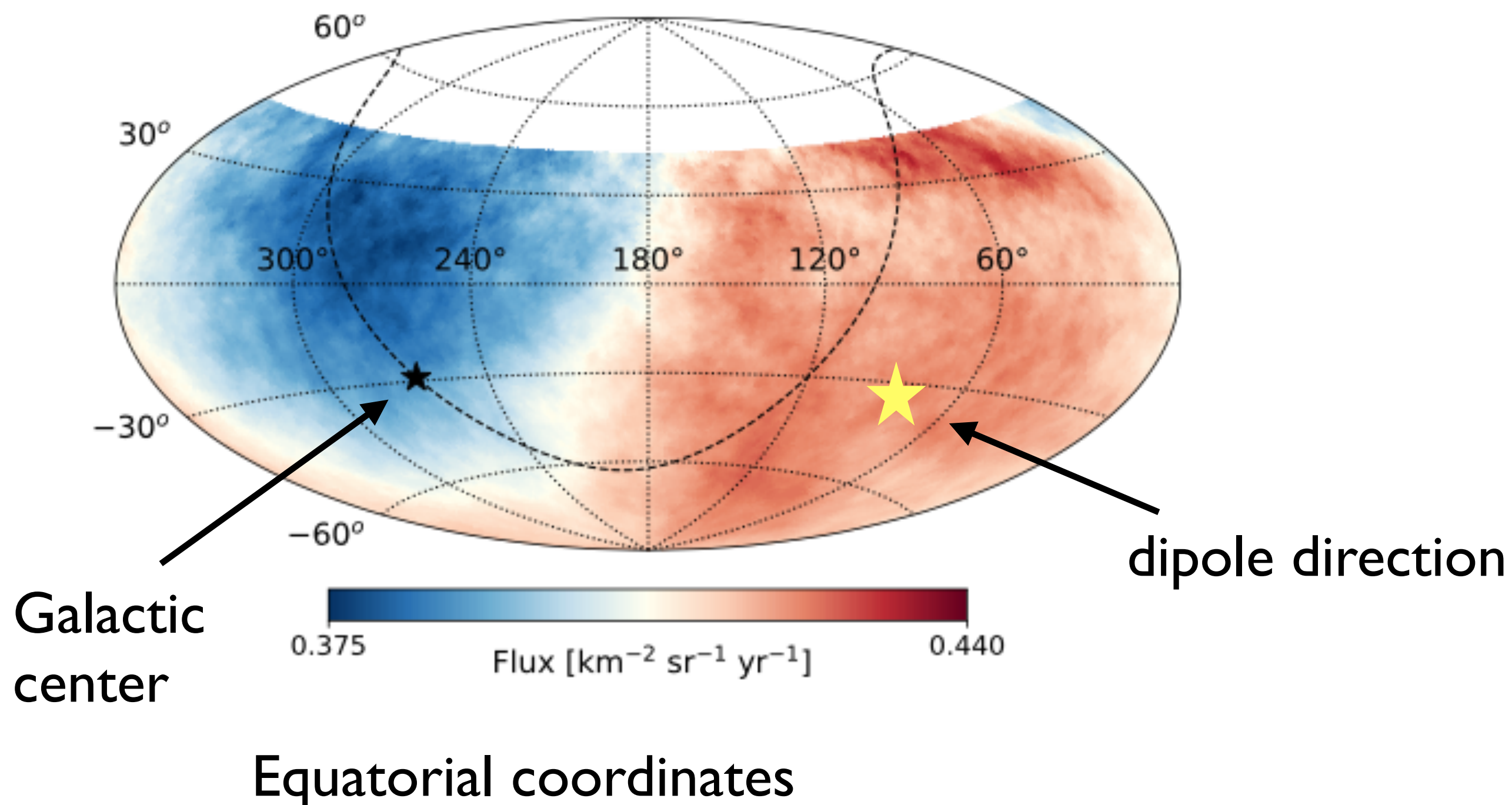
suposing a pure dipolar distribution

$E > 8$ EeV:

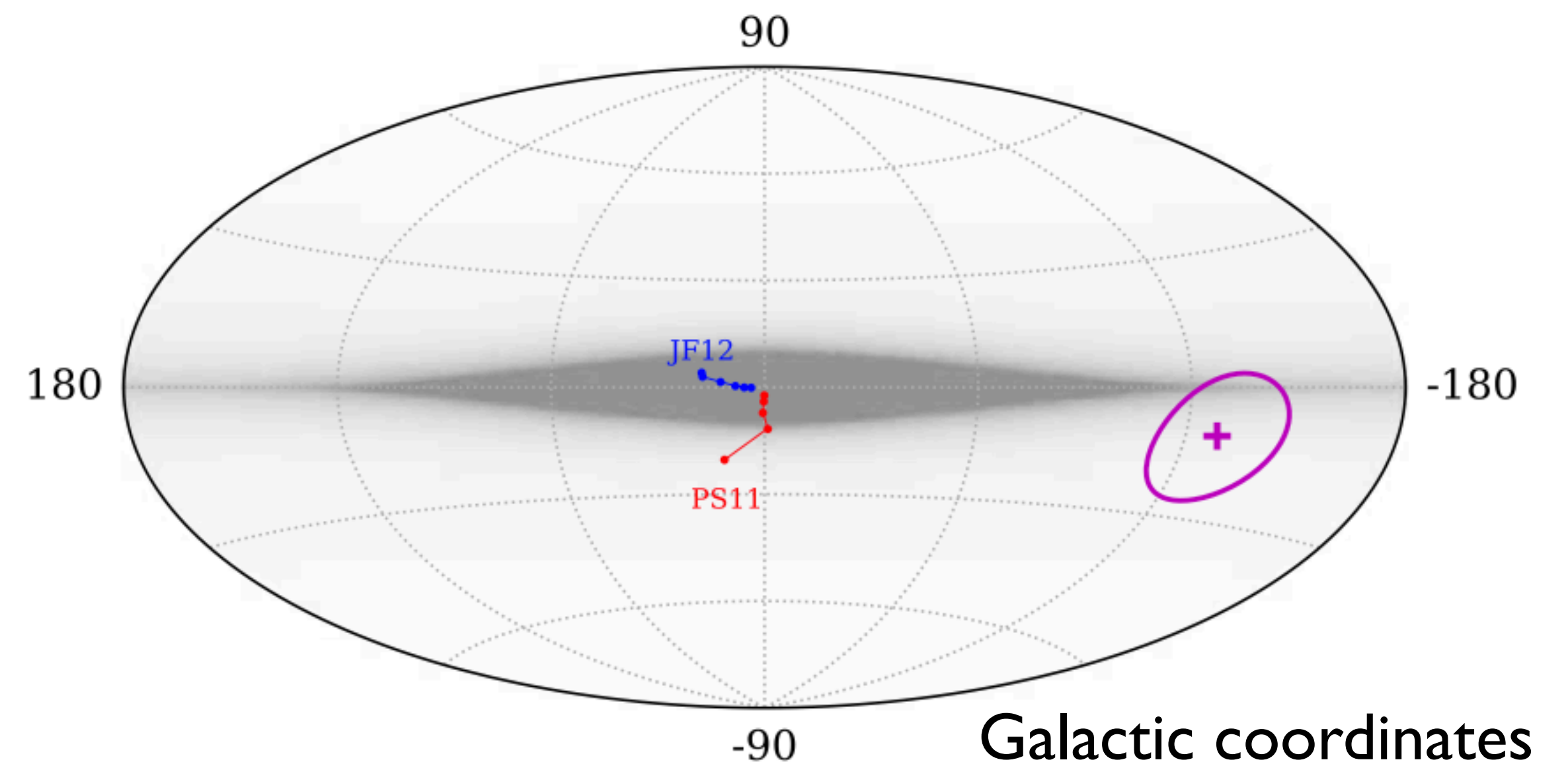
dipole amplitude:

$7.3\%^{+1.1\%}_{-0.9\%}$

Flux sky map $E > 8$ EeV

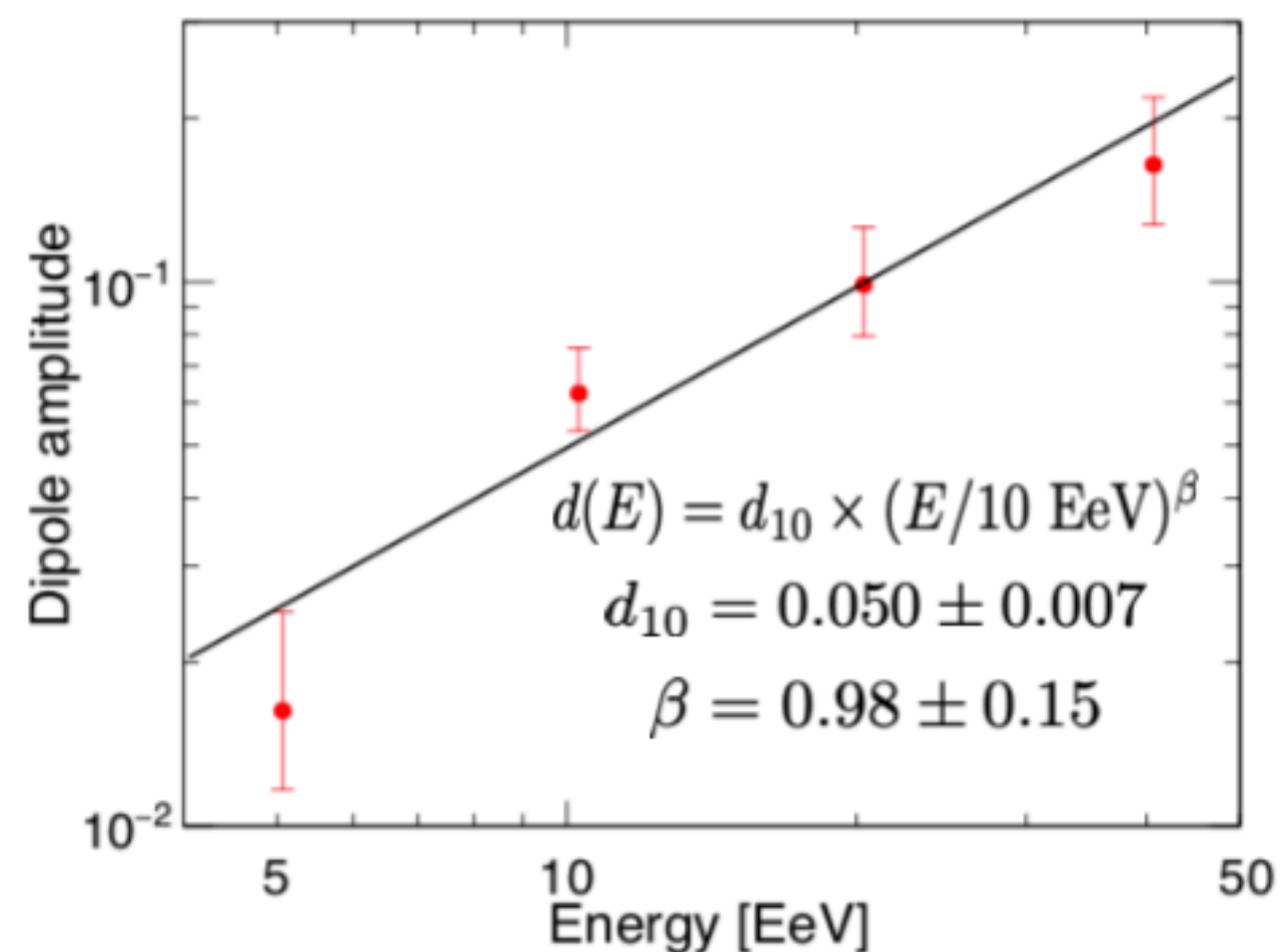


Dipole directions in galactic scenario

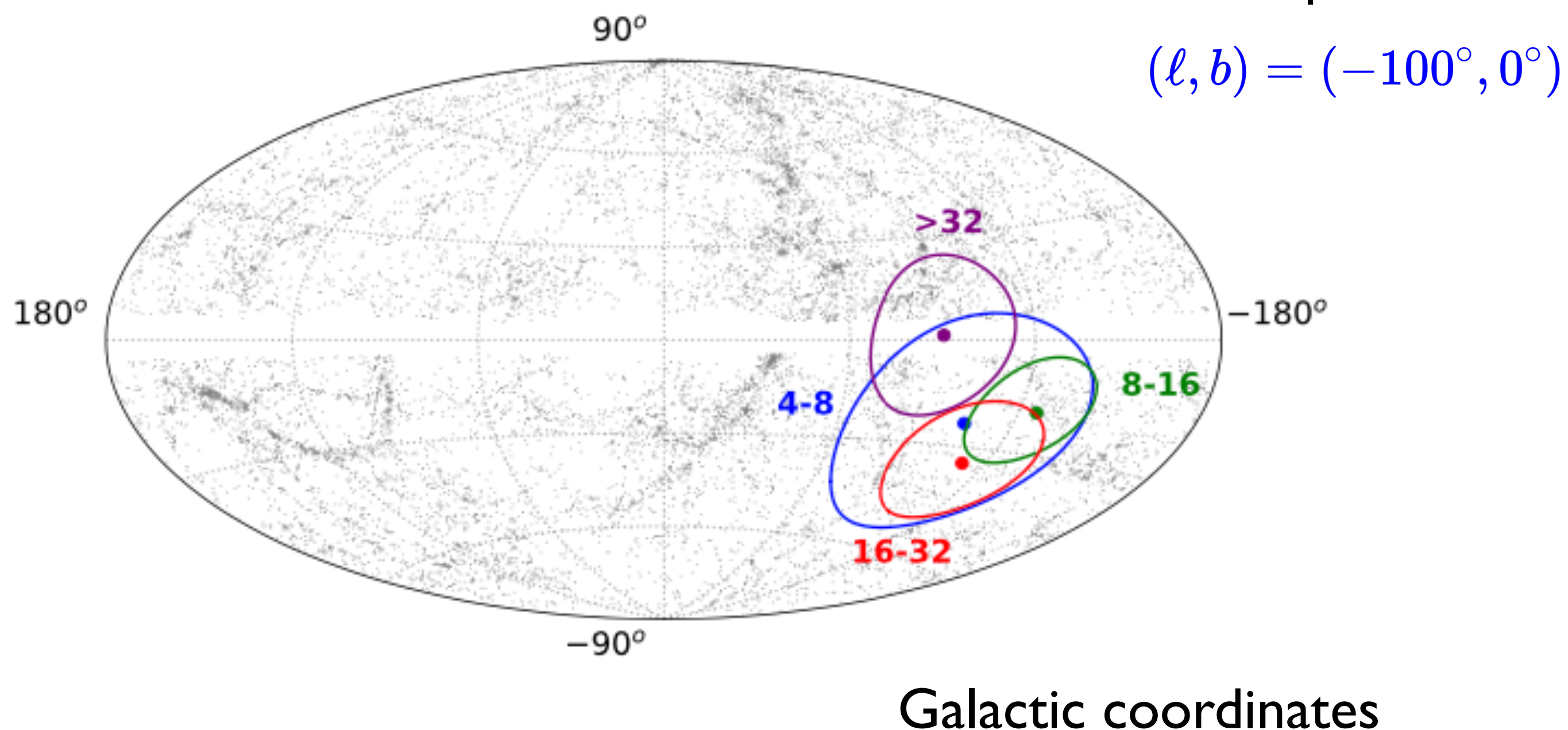


Energy dependence of dipolar modulation

Split the $E > 8$ EeV bin in three



Dipole directions above 4 EeV



dipole amplitude increases with energy

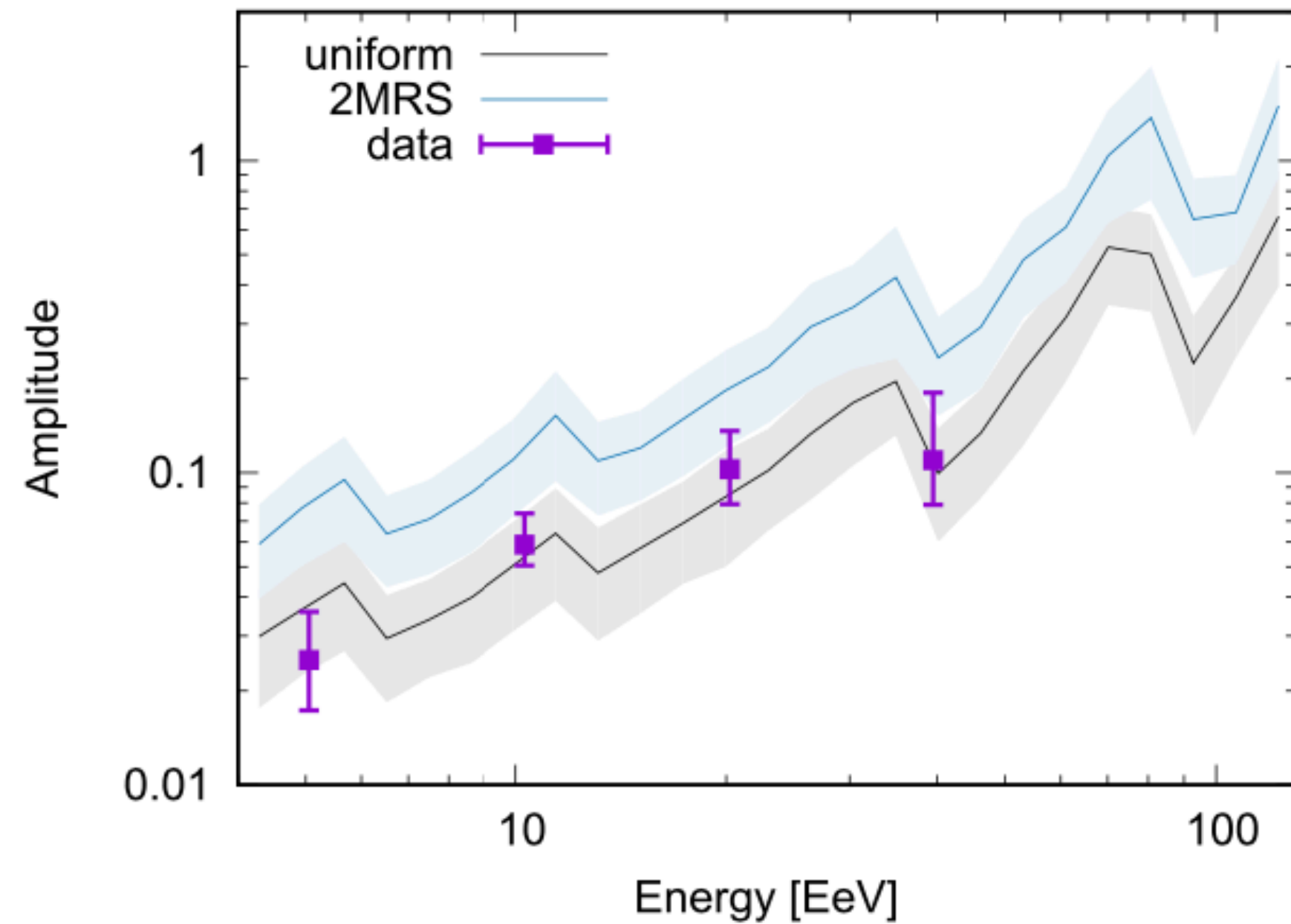
(energy-independent fit disfavored above 5σ)

No clear trend in the evolution of dipole direction with energy

Dipole interpretation

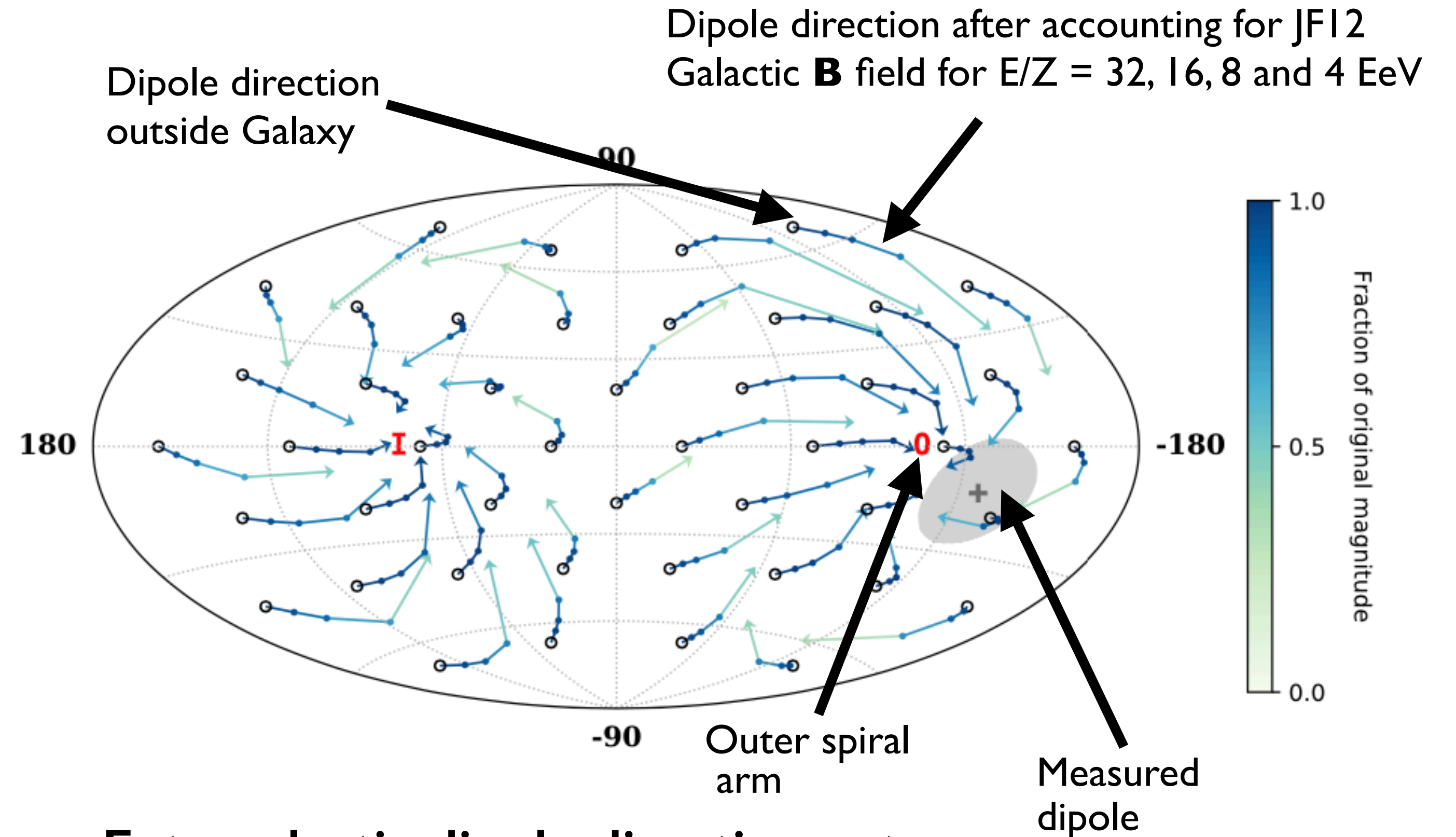
Models with mixed composition,

$R_{\max} = 6 \text{ EV}$, source density 10^{-4} Mpc^{-3}



Consistent with expectations

Extragalactic Dipole and GMF



Extragalactic dipole direction gets shifted towards spiral arms

Possibly due to the larger relative contribution from nearby sources to the flux at higher energies

Highest energies: blind searches for overdensities

Search for excesses not specifying a priori the targeted regions of the sky

- ★ **Li-Ma**: compare cumulative number of events (N_{obs}) given the expected on average from isotropic simulations (N_{exp})
- ★ Scan in **energy** threshold in [32; 80] EeV, step of 1 EeV
- ★ Scan in top-hat search **angle** Ψ in [1° ; 30°], steps of 1°

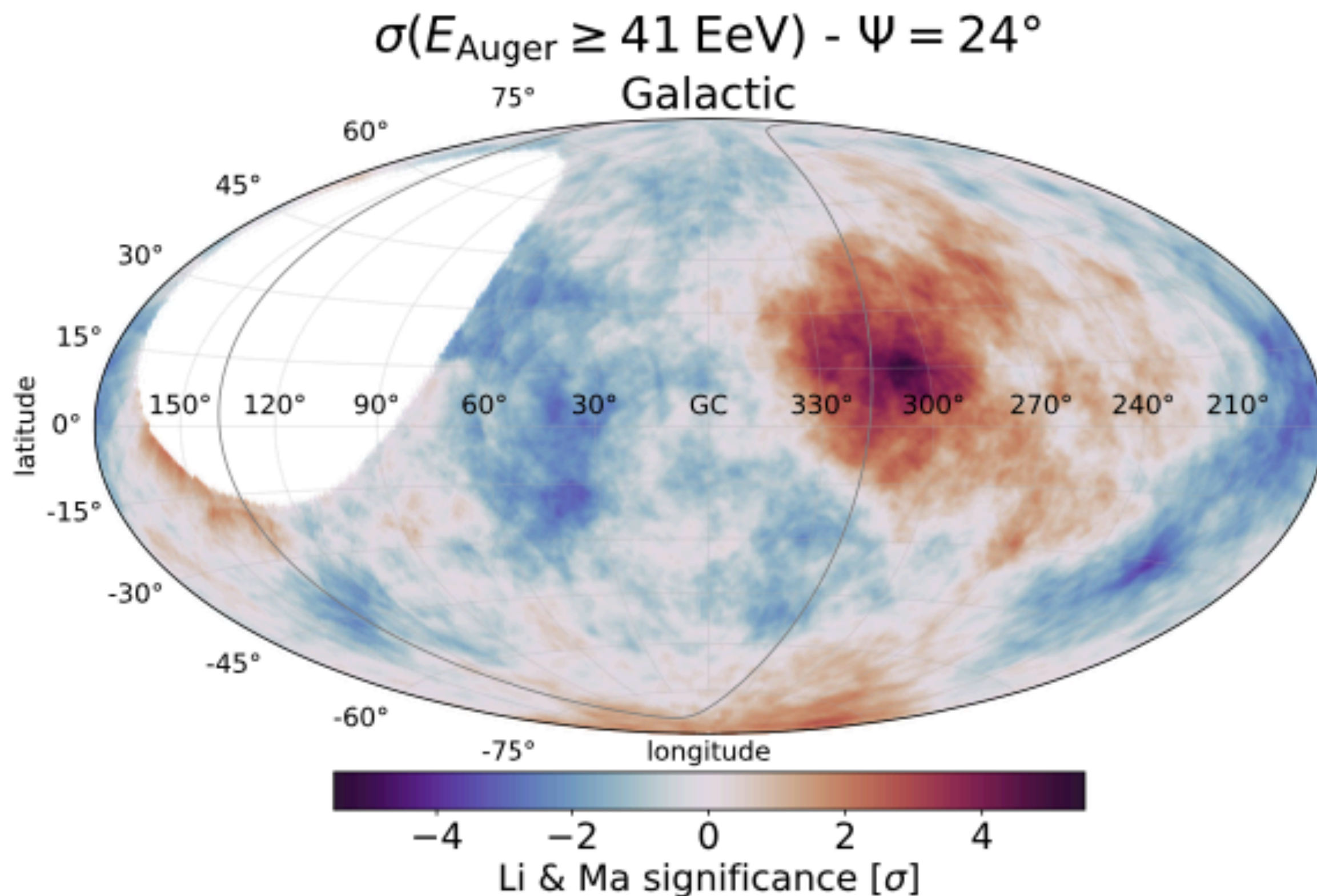
Most significant local excess over whole observable sky

- ★ $E_{\text{th}} \geq 41 \text{ EeV}$, $\Psi = 24^\circ$
- ★ $(\alpha, \delta) = (196.3^\circ, -46.6^\circ)$, $(l, b) = (305.4^\circ, 16.2^\circ)$
- ★ Local p -value 3.7×10^{-8} , Li&Ma significance = 5.4σ
- ★ **Global p -value = 3%**
(after accounting the scan, penalty factor $\sim O(10^5)$)

The dataset above 32 EeV is available for public use

- ★ with the code to reproduce the results [\(link\)](#)

[P. Auger Collab, ApJ, 2022](#)



Autocorrelation and correlation with astrophysical structures

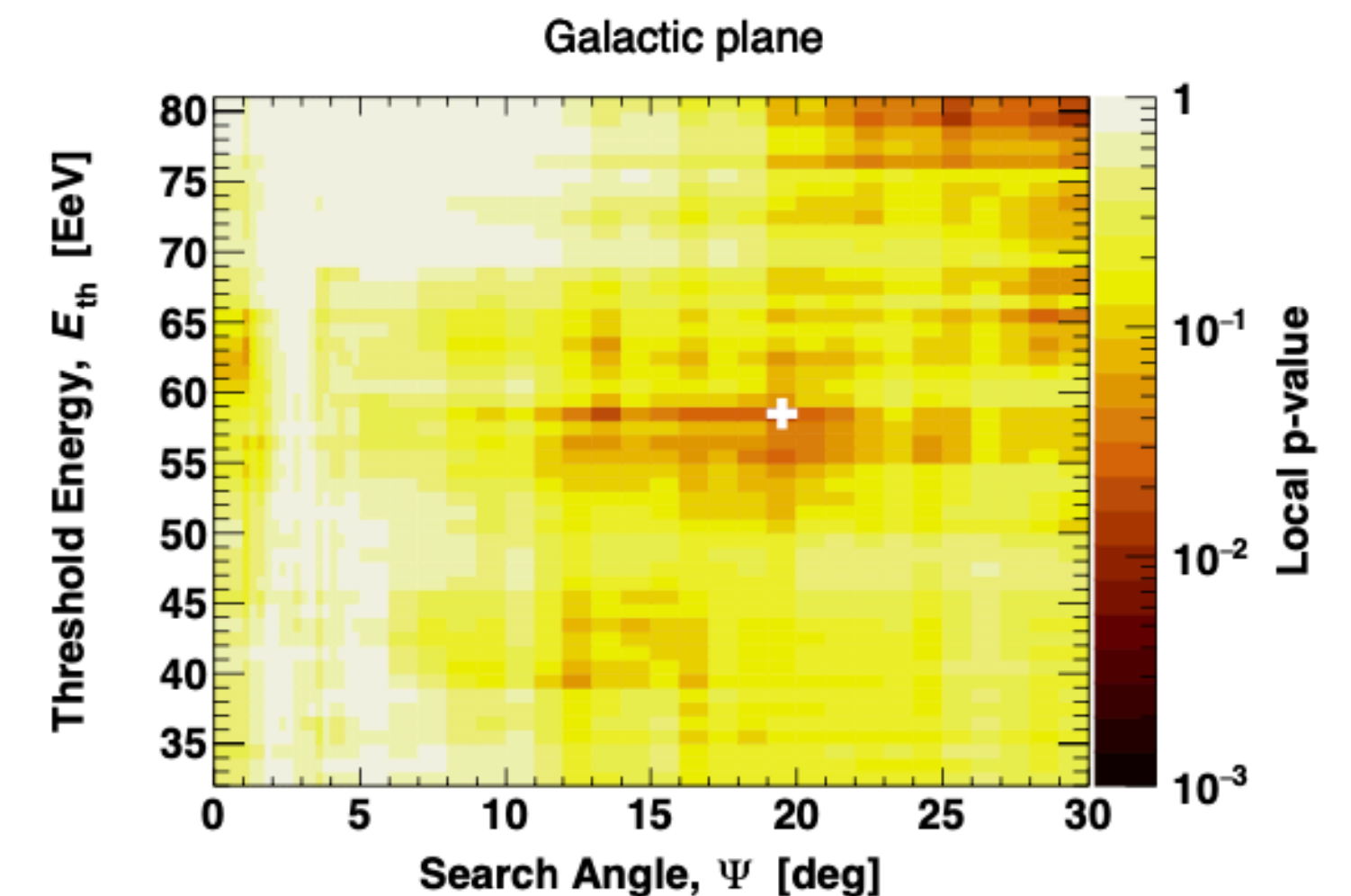
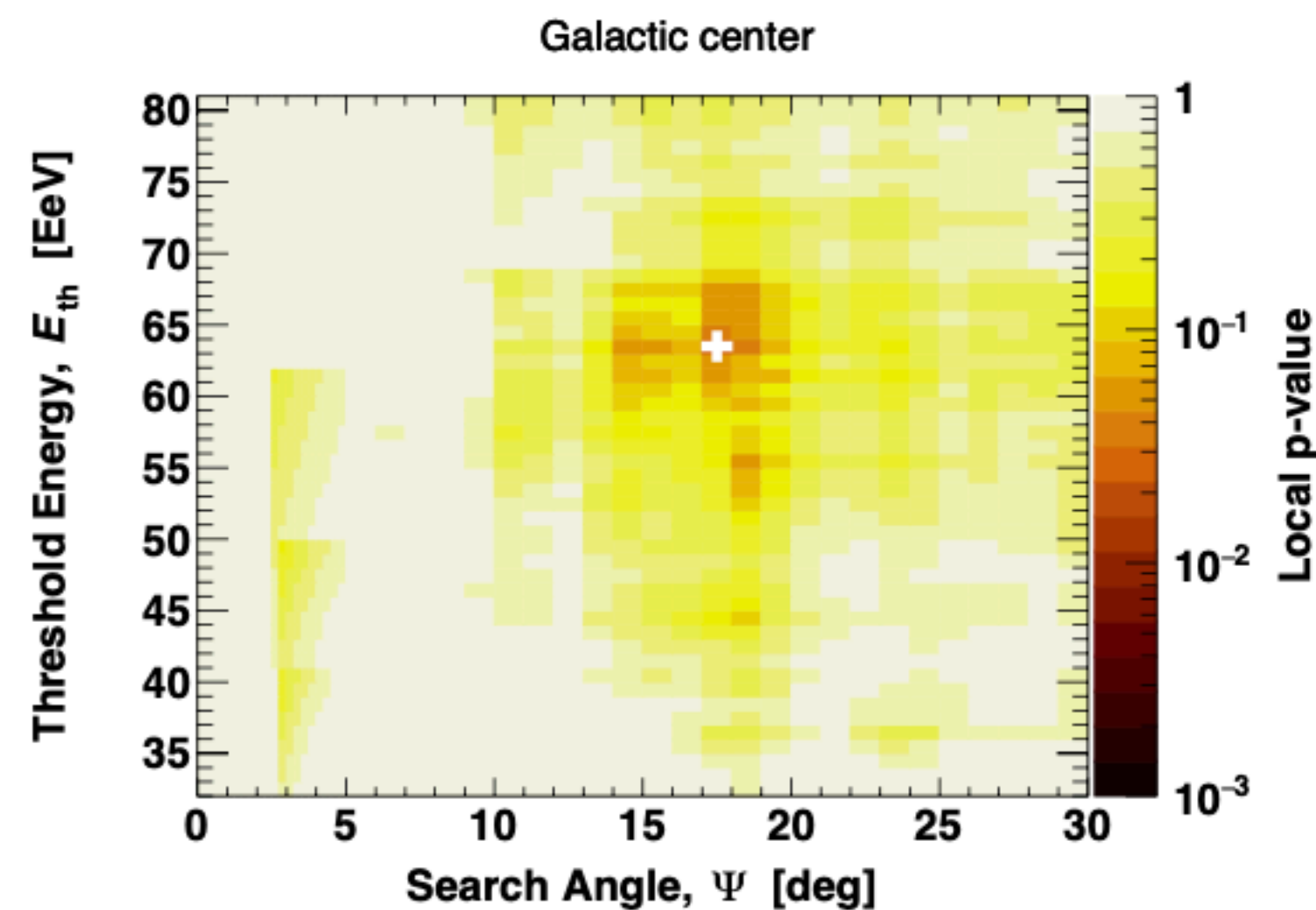
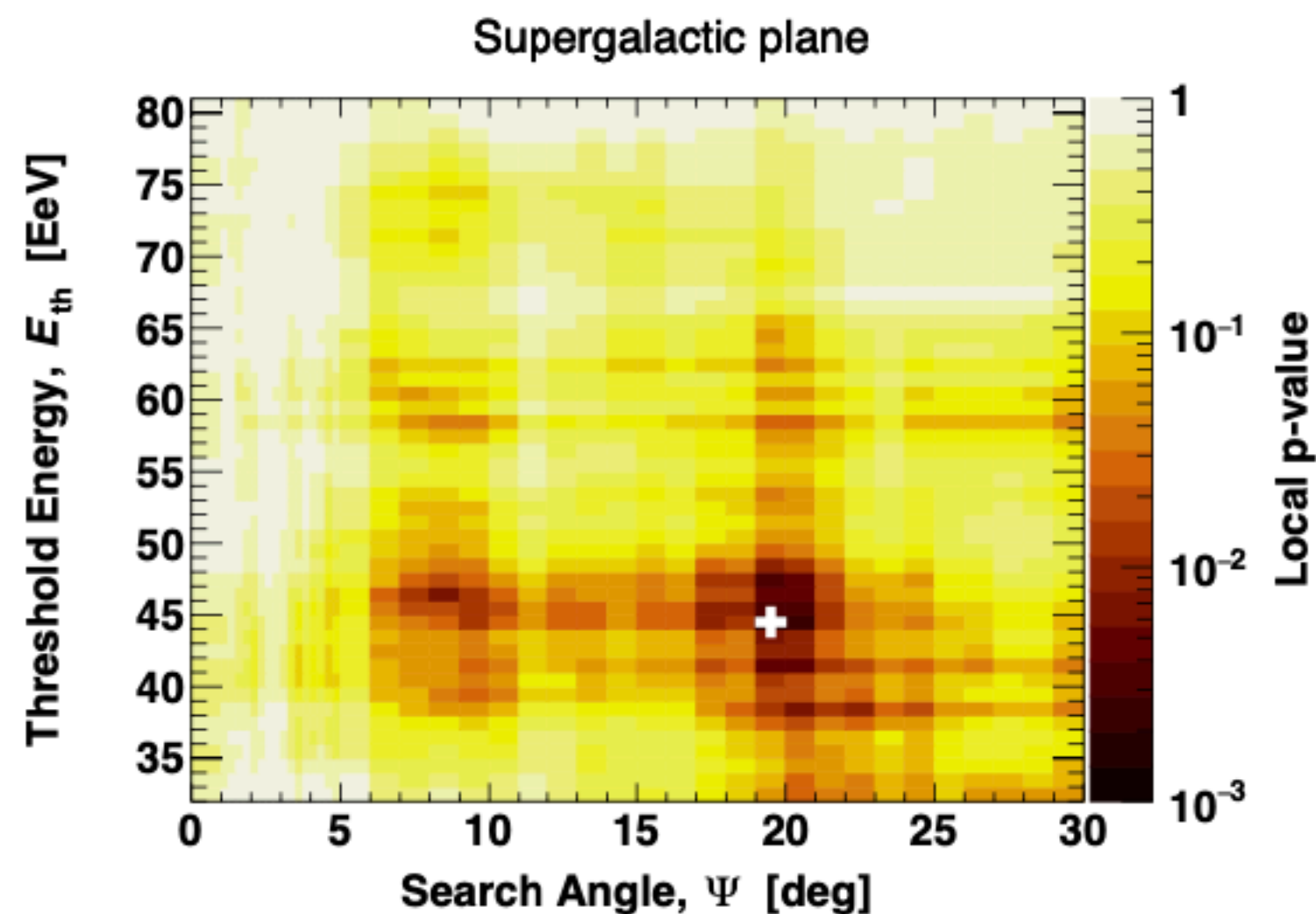
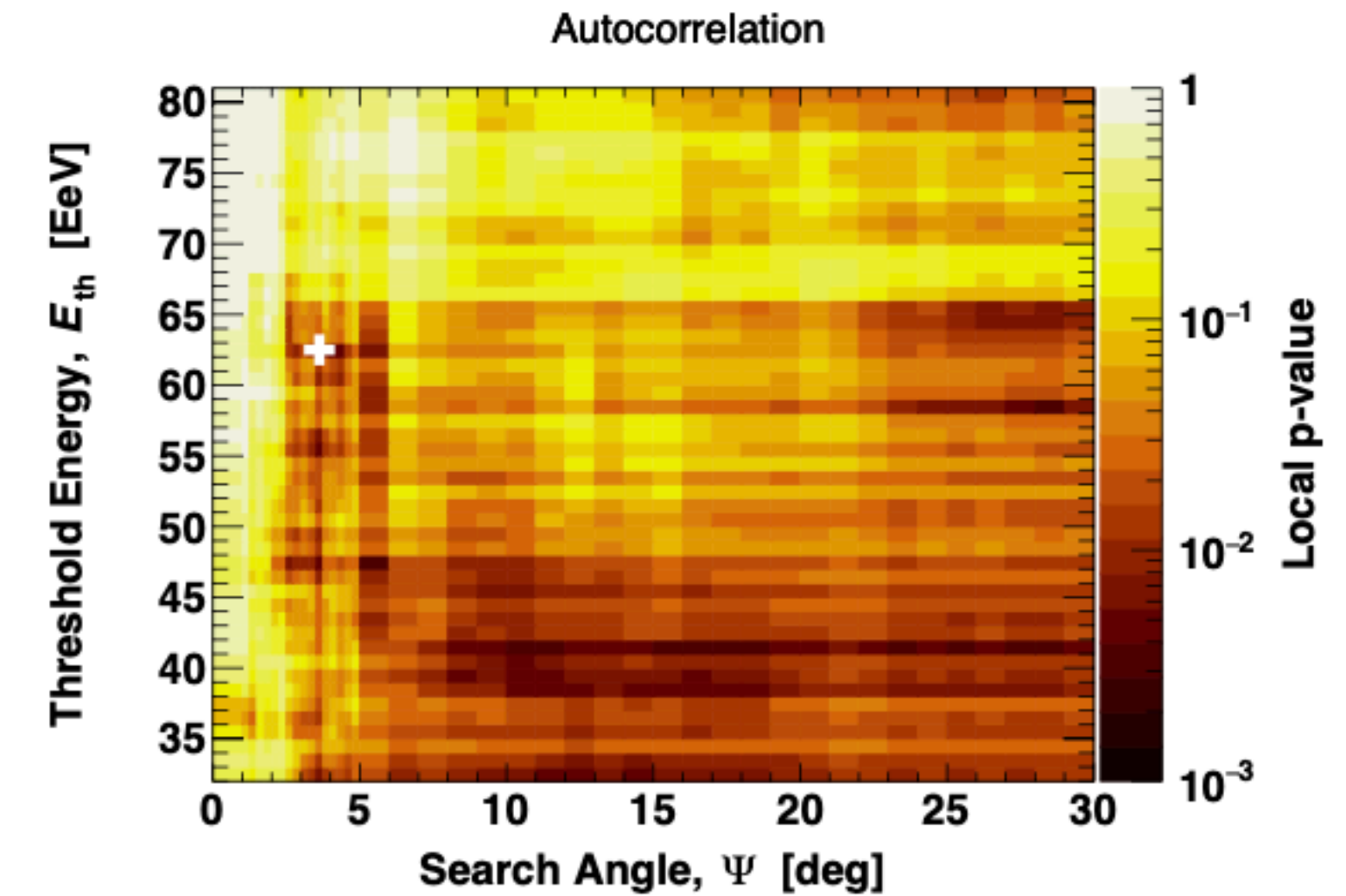
Structures

- ★ Events in proximity of **local astrophysical structures**
- ★ Scan in threshold **energy, angle** Ψ

Autocorrelation

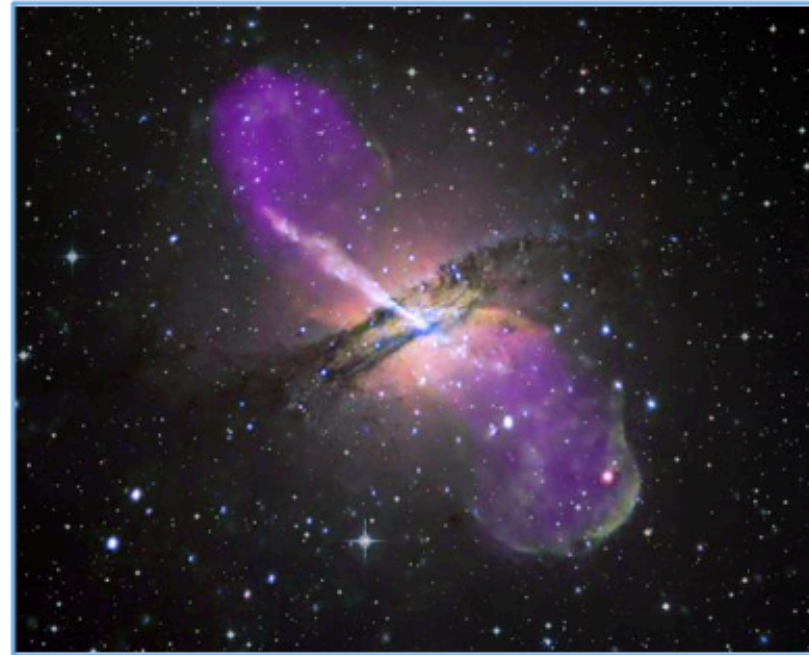
- ★ **Pairs** of events separated by given angular distance
- ★ Scan in threshold **energy, angle** Ψ

Search	E_{th} [EeV]	Angle, Ψ [deg]	N_{obs}	N_{exp}	Local p -value, f_{min}	Post-trial p -value
Autocorrelation	62	3.75	93	66.4	2.5×10^{-3}	0.24
Supergalactic plane	44	20	394	349.1	1.8×10^{-3}	0.13
Galactic plane	58	20	151	129.8	1.4×10^{-2}	0.44
Galactic center	63	18	17	10.1	2.6×10^{-2}	0.57



Catalog-based searches

CenA, jetted AGN



NGC415, non-jetted AGN



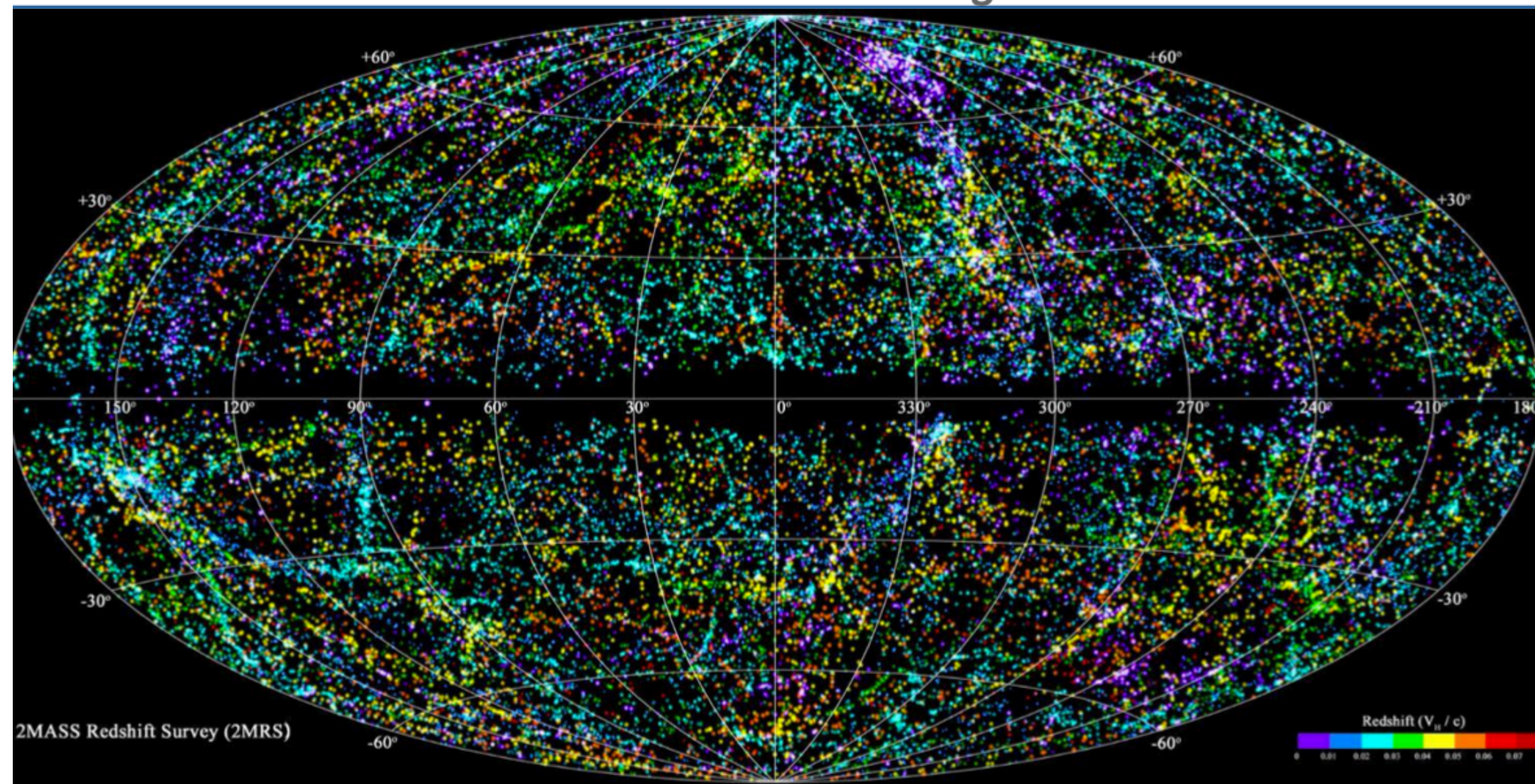
M82, starburst



Each source weighted based on

- ★ **luminosity distance** to account for propagation effects (supposing an average composition above 32 EeV)
- ★ **electromagnetic emission** to estimate UHECR flux

Uncut 2MRS catalog color coded in redshift



AGN activity

- ★ Accretion = X-rays from SwiftBAT (523 galaxies at 14- 195 keV)
- ★ Jet = γ -rays from 3FHL (26 galaxies at 10 GeV- 1 TeV)

Star formation

- ★ Generic/stellar mass = IR from 2MRS (>40000 galaxies 2.2 μ m)
- ★ Burst = radio from Lunardini+19 (44 galaxies, 1.4 GHz)

Result: 4 flux- limited samples: Jetted AGNs, all AGNs, Starburst galaxies, all galaxies

Catalogue searches for intermediate scale anisotropies

Analysis strategy

Sky model probability maps:

Null hypothesis H_0 : **isotropy**

$$n^{H_0}(\mathbf{u}) = \frac{\omega(\mathbf{u})}{\sum_i \omega(\mathbf{u}_i)}$$

Single population **signal** model H_1 :

$$n^{H_1}(\mathbf{u}) = (1 - \alpha) \times n^{H_0}(\mathbf{u}) + \alpha \times \frac{\sum_j s_j(\mathbf{u}; \Theta)}{\sum_i \sum_j s_j(\mathbf{u}_i; \Theta)}$$

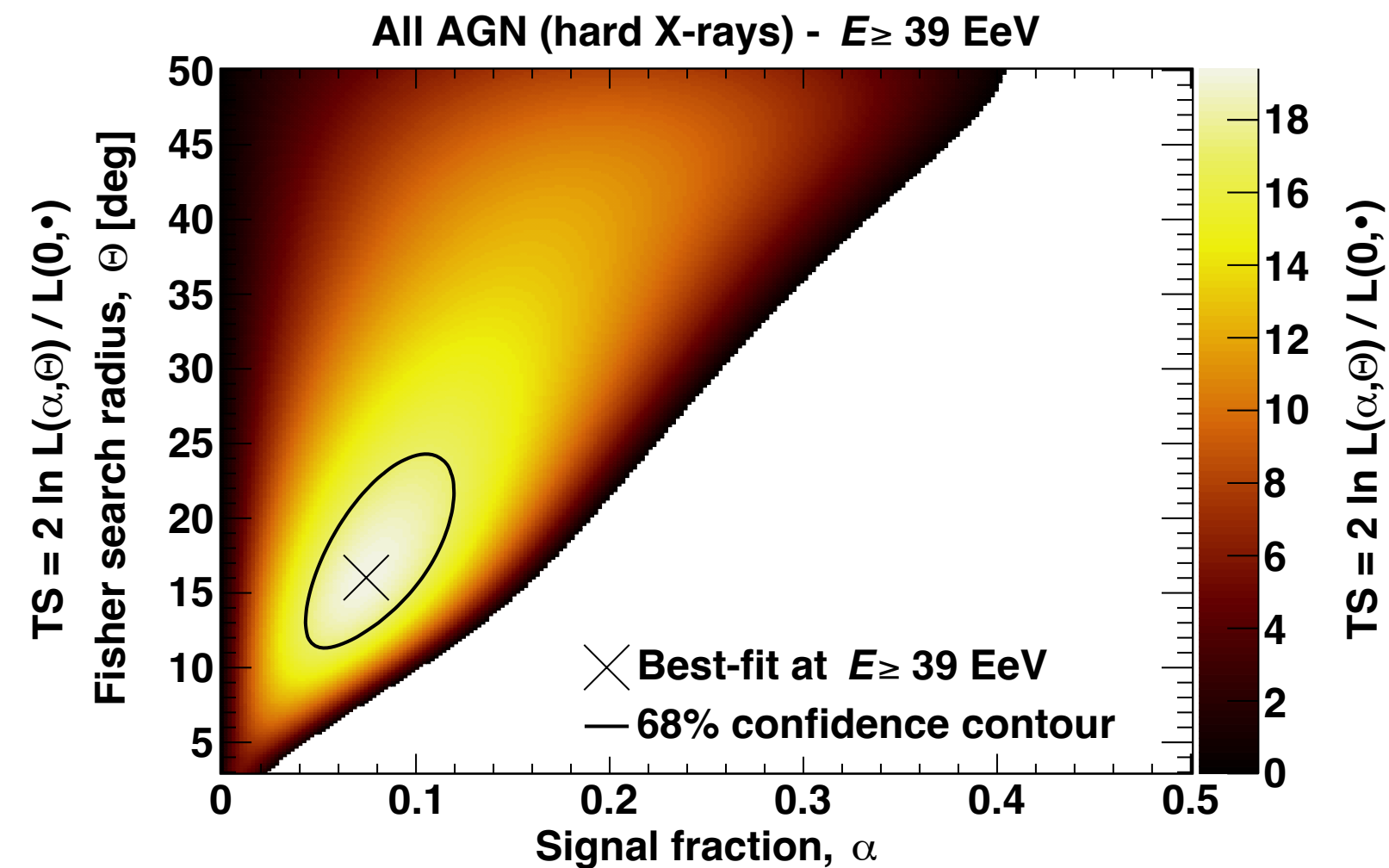
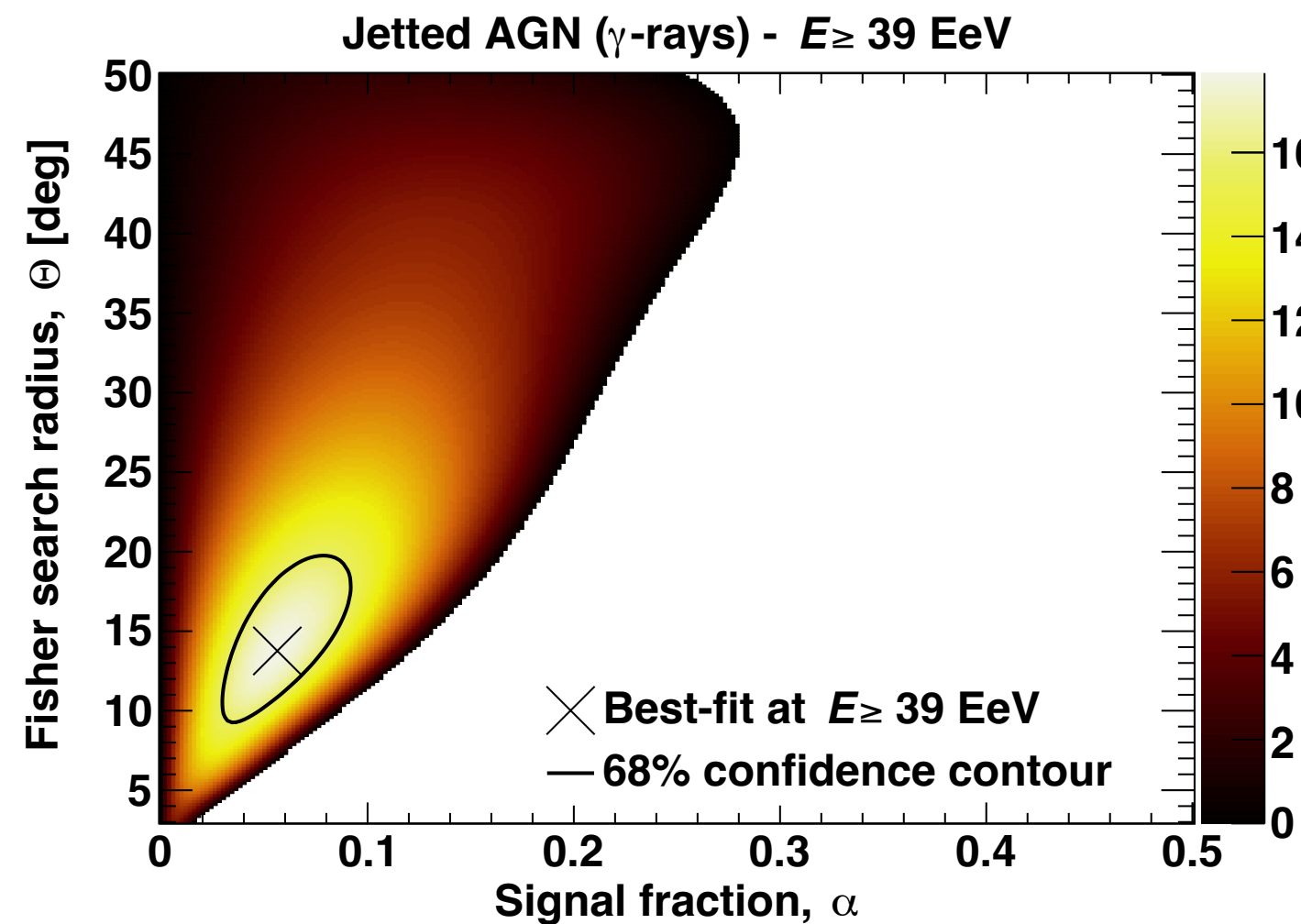
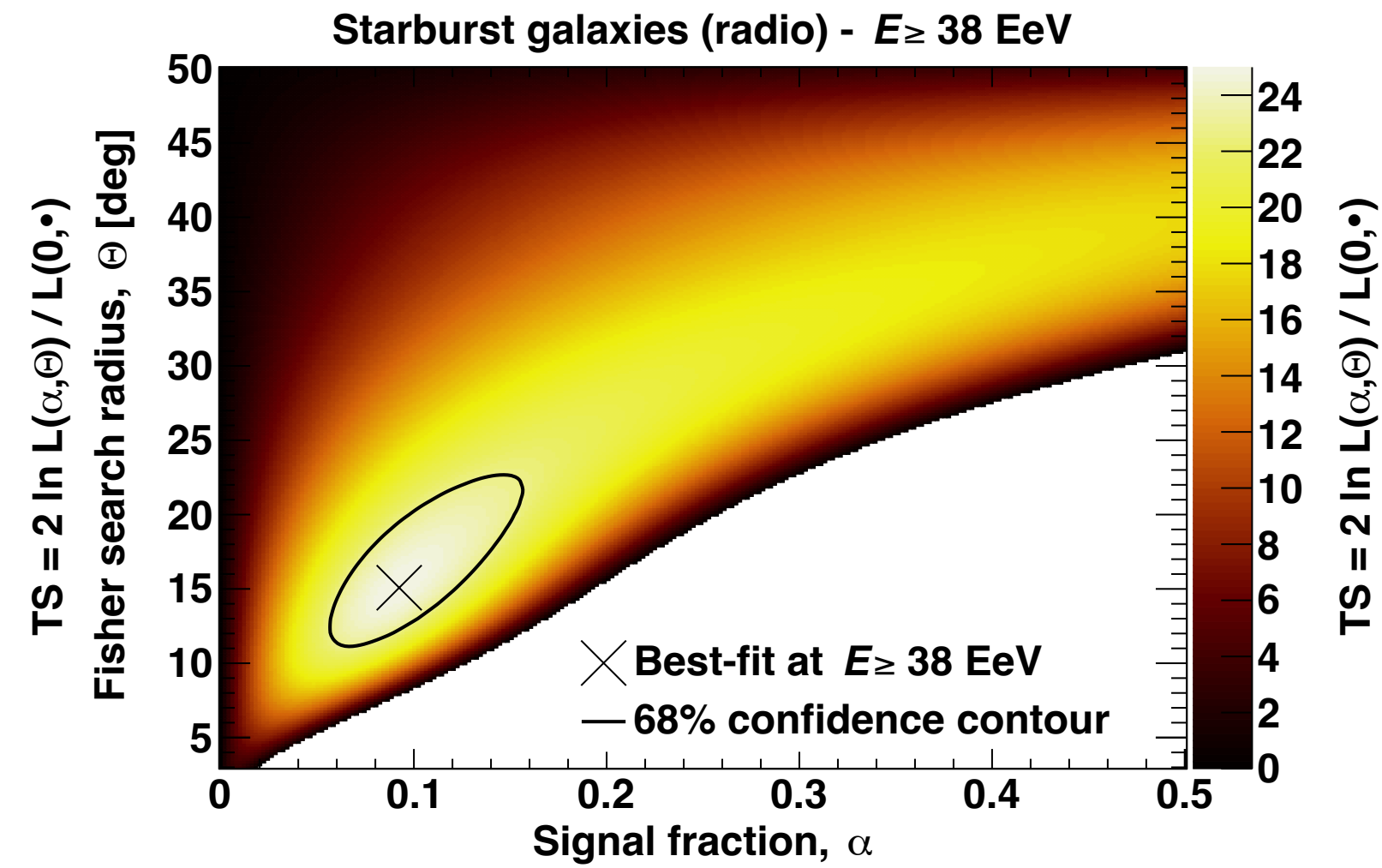
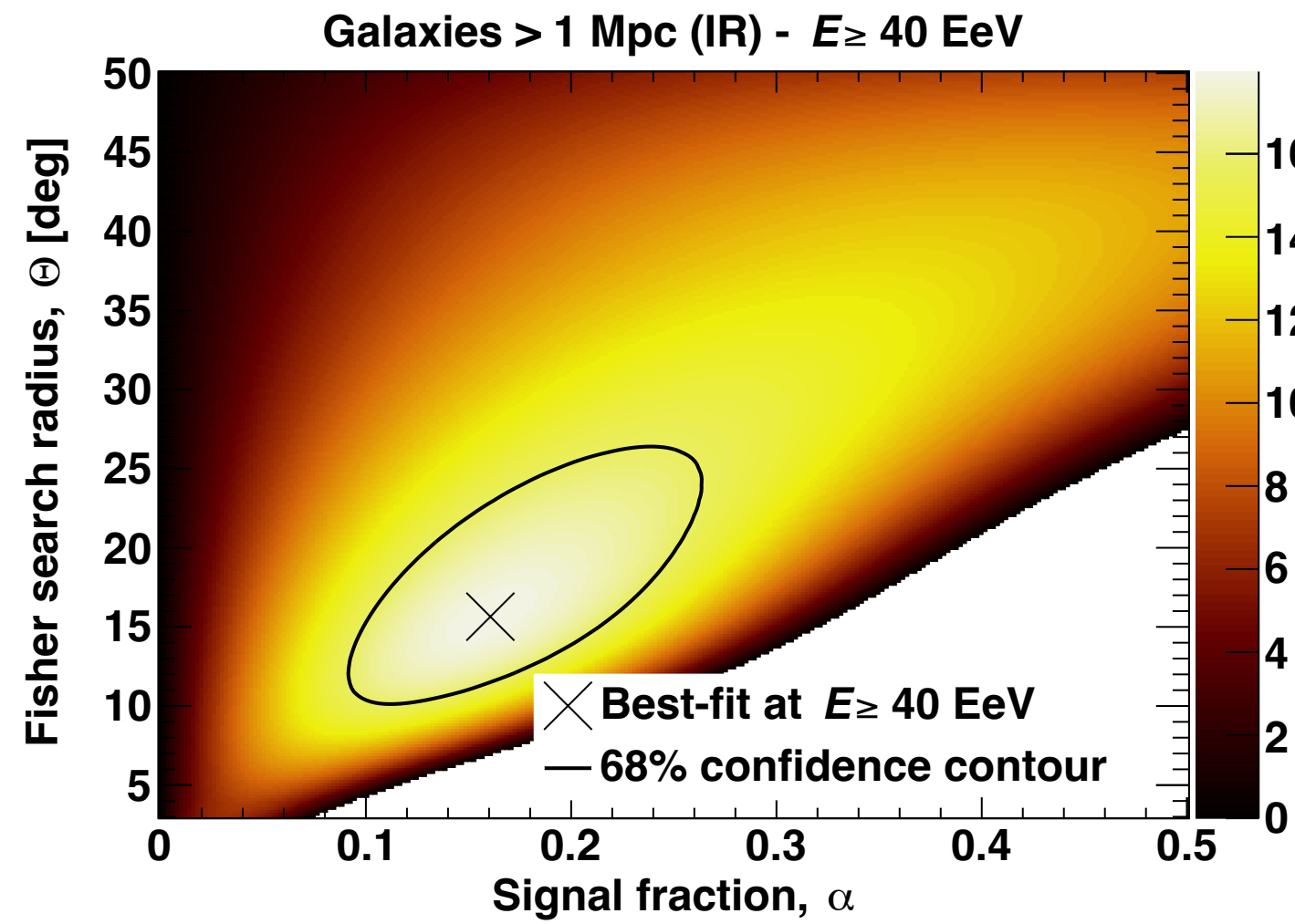
(free parameters: α and Θ)

Contribution to the UHECR flux from each galaxy: $s_j(\mathbf{u}; \Theta) = \omega(\mathbf{u}) \times \phi_j a(d_j) \times \exp\left(\frac{\mathbf{u} \cdot \mathbf{u}_j}{2(1 - \cos \Theta)}\right)$

Modeled as a von Mises-Fisher distribution centered on the direction of the galaxy with a smearing angle Θ

Test statistics: $TS = 2 \log(H_1/H_0)$ $TS = 2 \sum_i k_i \times \ln \frac{n^{H_1}(\mathbf{u}_i)}{n^{H_0}(\mathbf{u}_i)}$

Catalogue searches for intermediate scale anisotropies

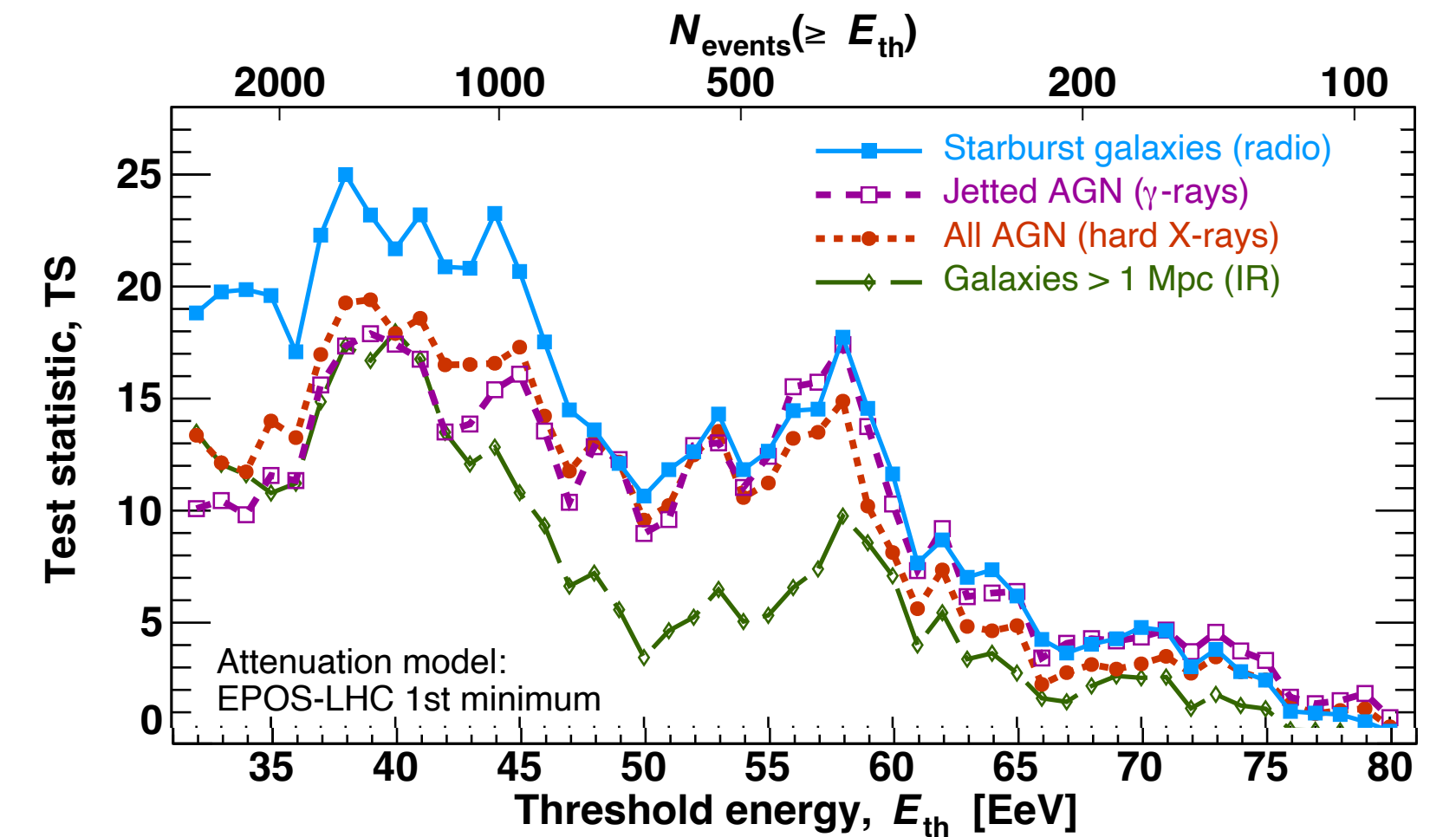


All catalogs have highest test statistics at $E_{th}=38-41$ EeV, scale $\Psi=23^\circ-27^\circ$, signal fraction $\alpha=6-15\%$

Post-trial significance

3.1σ for jetted AGNs

4.0σ for Starburst galaxies



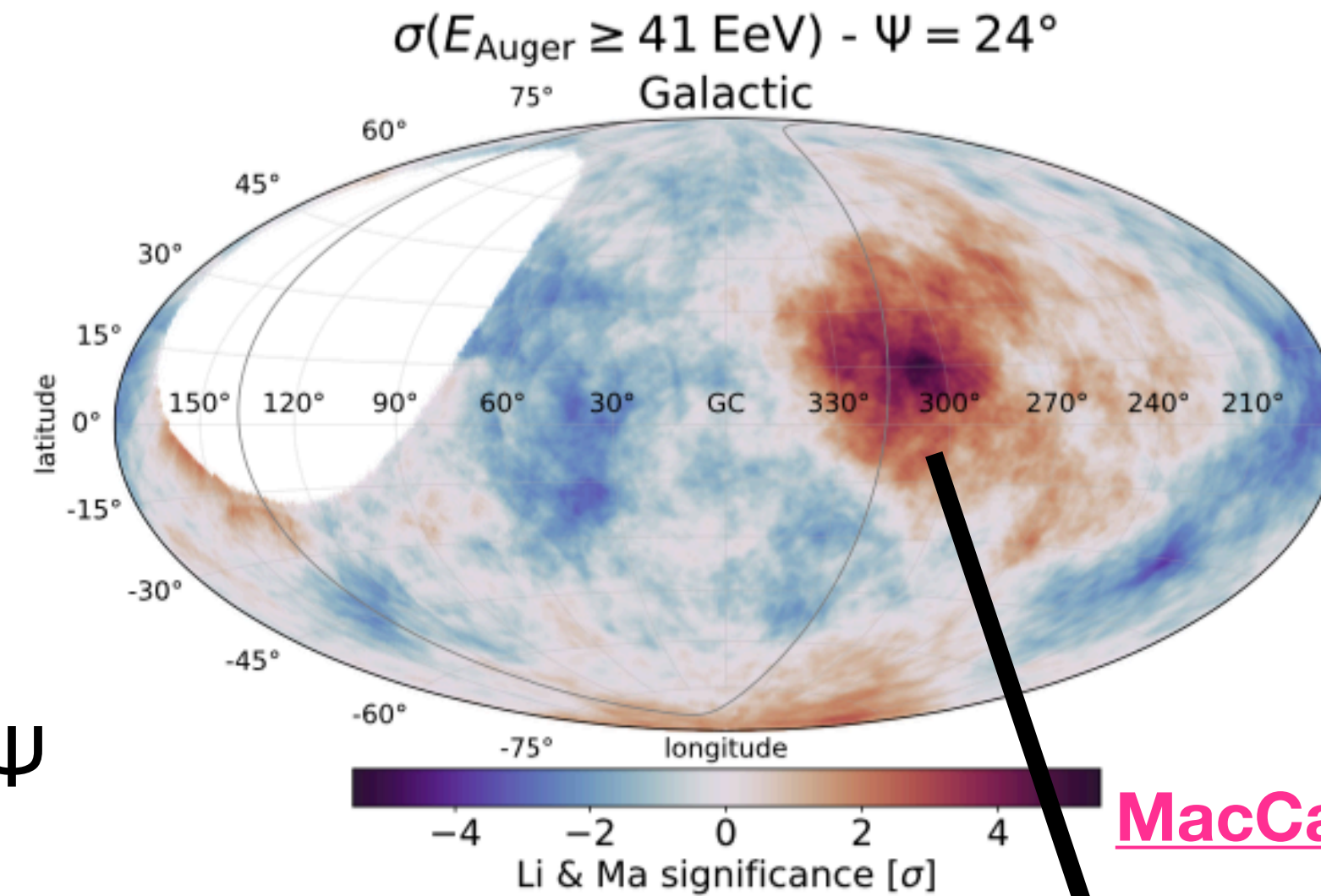
Excess in the Centaurus region

Motivation:

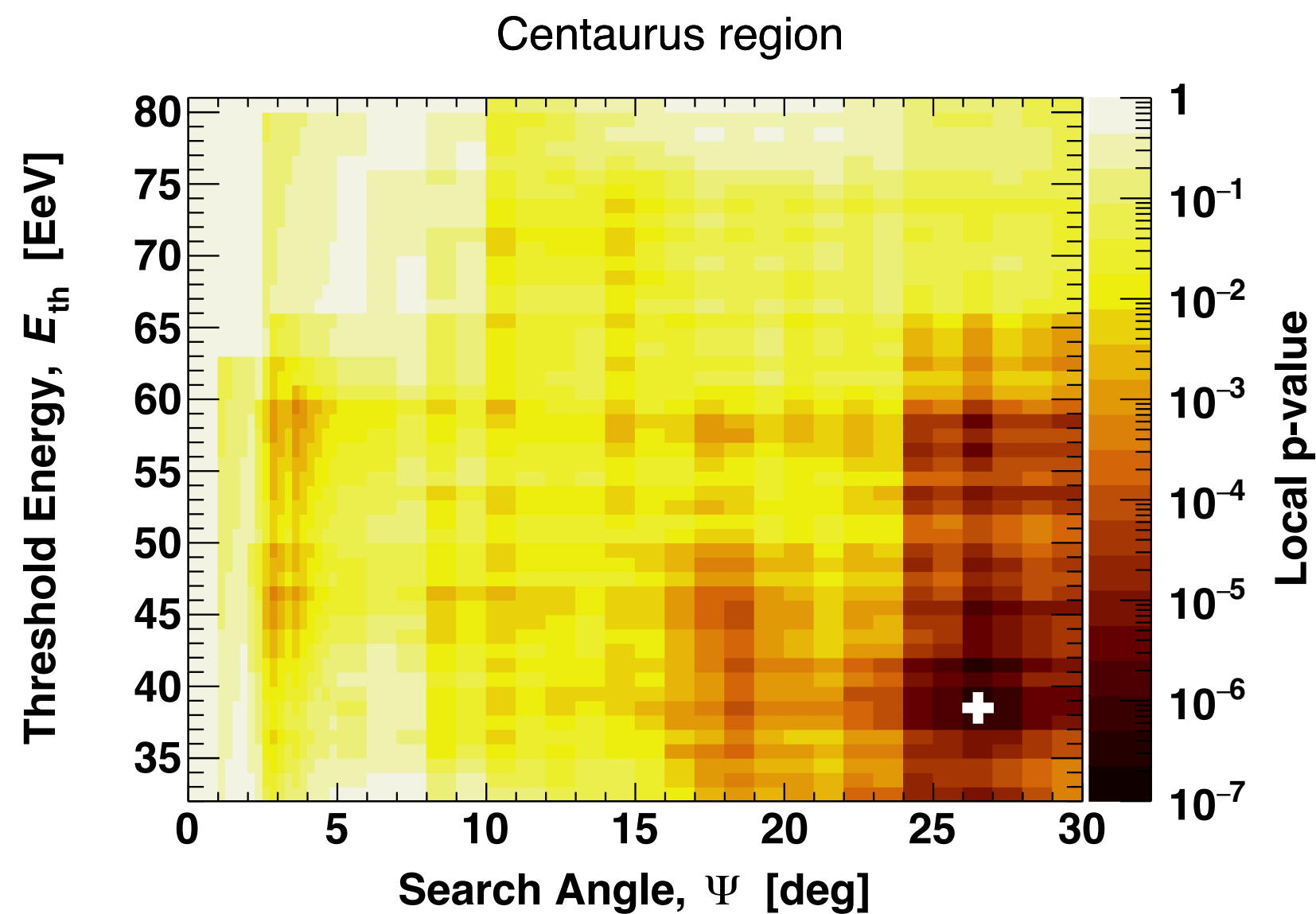
- ★ A priori: prominent area in the **Council of Giants**
- ★ Flagged area since the first anisotropy results (7% of current exposure)
- ★ Most significant **overdensity** present in the blind search
- ★ Driving **hotspot** in all the catalog based models

Results

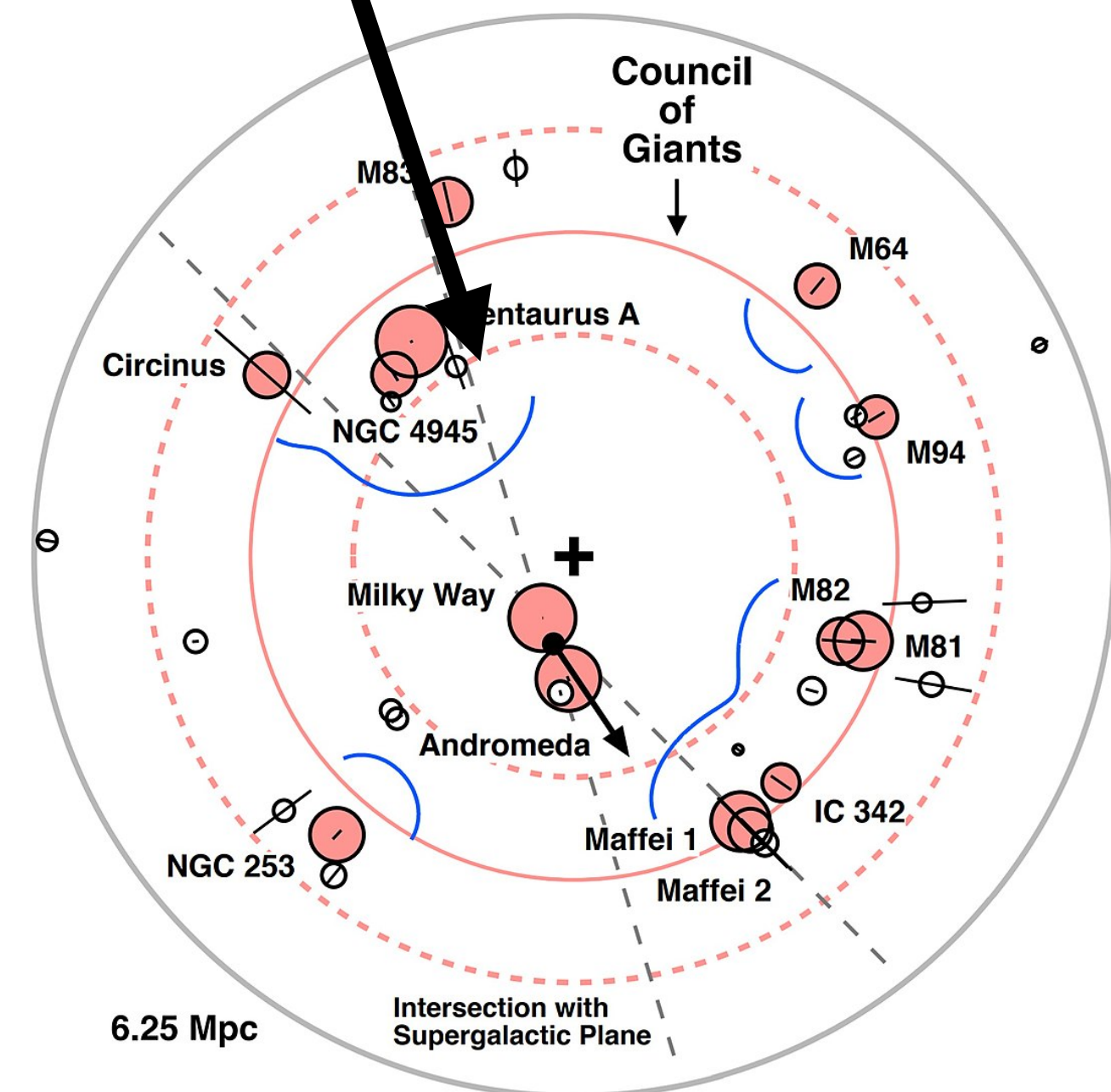
- ★ Correlation with structure (Cen A)
- ★ Direction fixed to CenA, scan in threshold energy and angle Ψ
- ★ **3.9 σ post-trial**
- ★ for $E_{th}=38$ EeV, $\Psi=27^\circ$ $Excess=N_{obs}-N_{exp}=215-152=63$



[MacCaI, MNRAS, 2014](#)

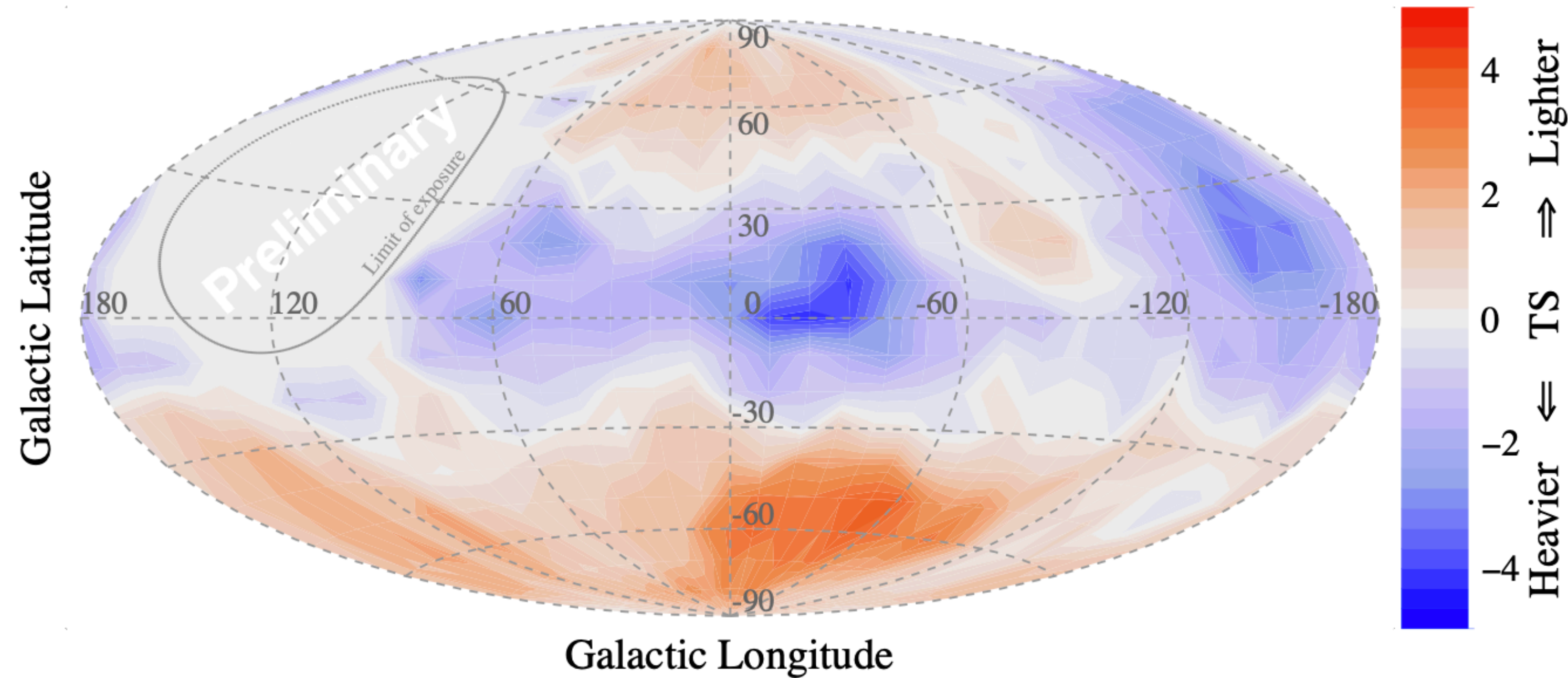


Council of Giants is a ring of twelve large galaxies surrounding the Local Group in the Local Sheet, with a radius of 3.75 Mpc



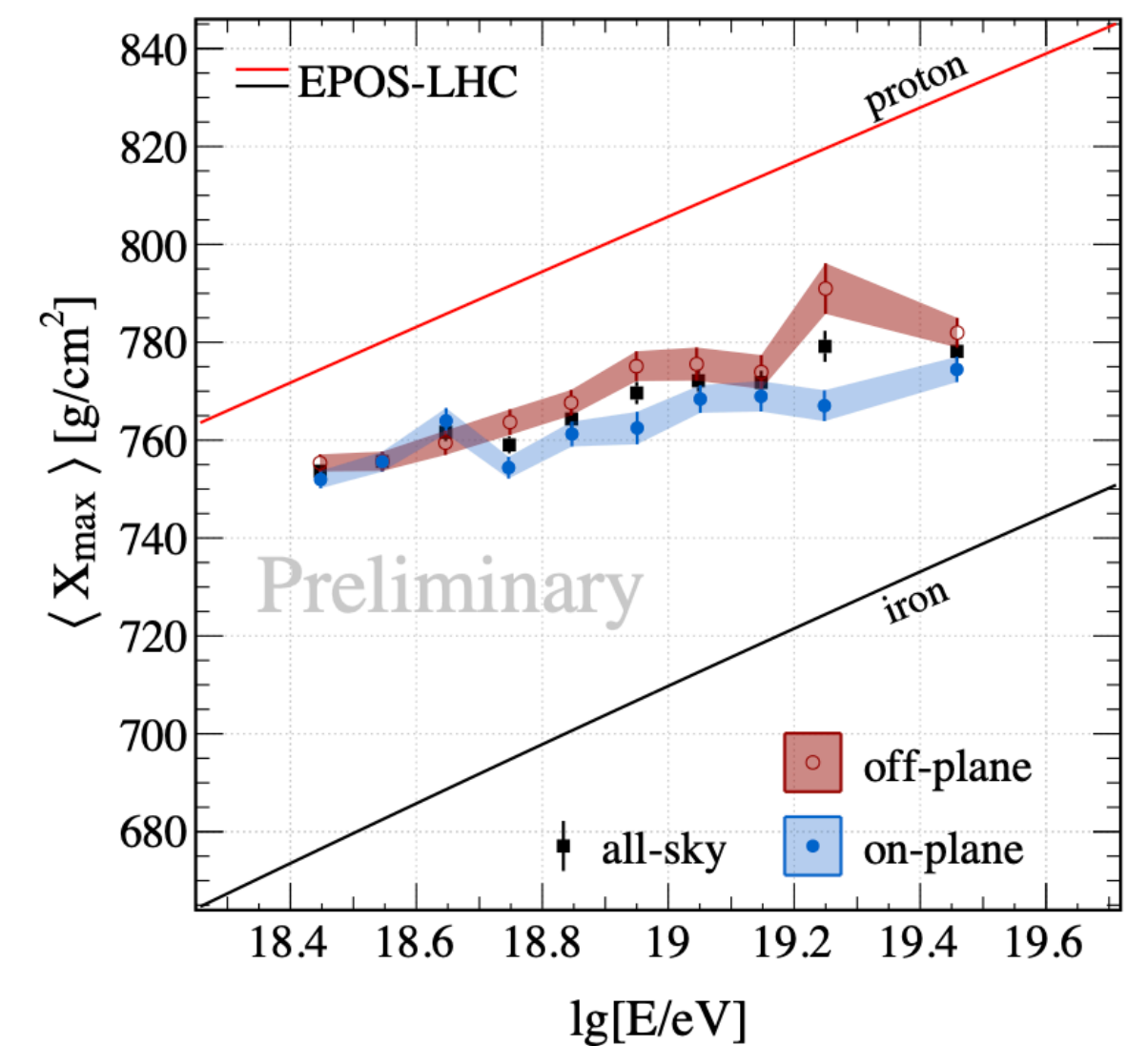
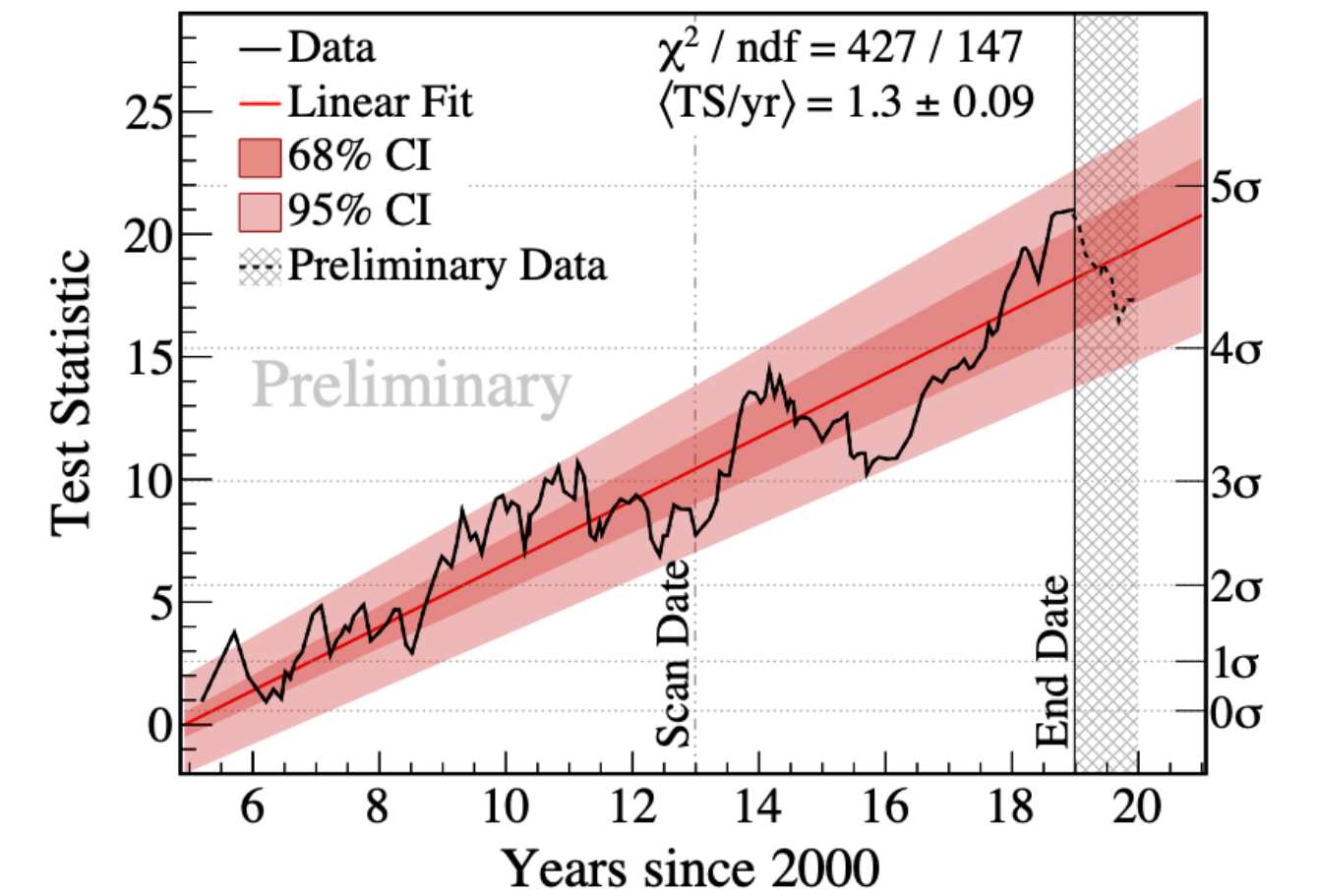
Indication of mass-dependent anisotropy above $10^{18.7}$ eV

Hybrid events



Heavier composition on the Galactic Plane with 3.3σ significance.

Rate of growth of test statistics : 1.3 TS/yr



Conclusions and prospects with Auger Phase 1 data (2004-2020)

Large scale anisotropy:

- ★ The first evidence of **anisotropy** at UHE.
- ★ First observational **evidence** that the origin of UHECRs is **extragalactic**.
- ★ Above 4 EeV, **dipole amplitude** grows with energy.
- ★ **Phases** close to **outer spiral**.

Small-intermediate scale anisotropy searches in the suppression region

- ★ Indication of **departure** from **isotropy** $\sim 4\sigma$ from search in Centaurus region confirmed also by catalog-based searches
- ★ **Starburst galaxy model** provides the most significant indication that UHECRs are **not isotropically** distributed.
- ★ The **largest** available dataset of **ultra-high-energy** cosmic rays **above 32 EeV!**

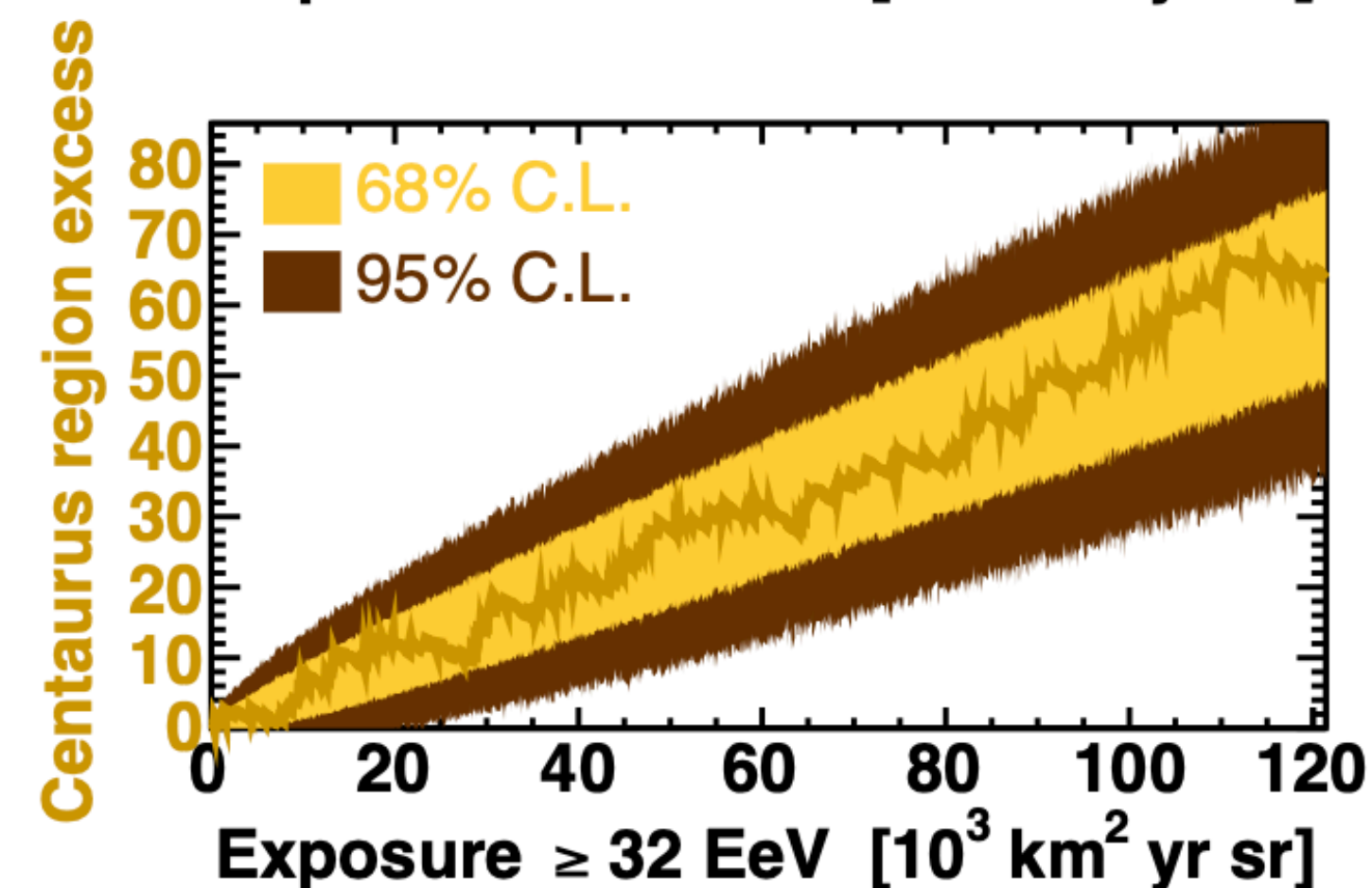
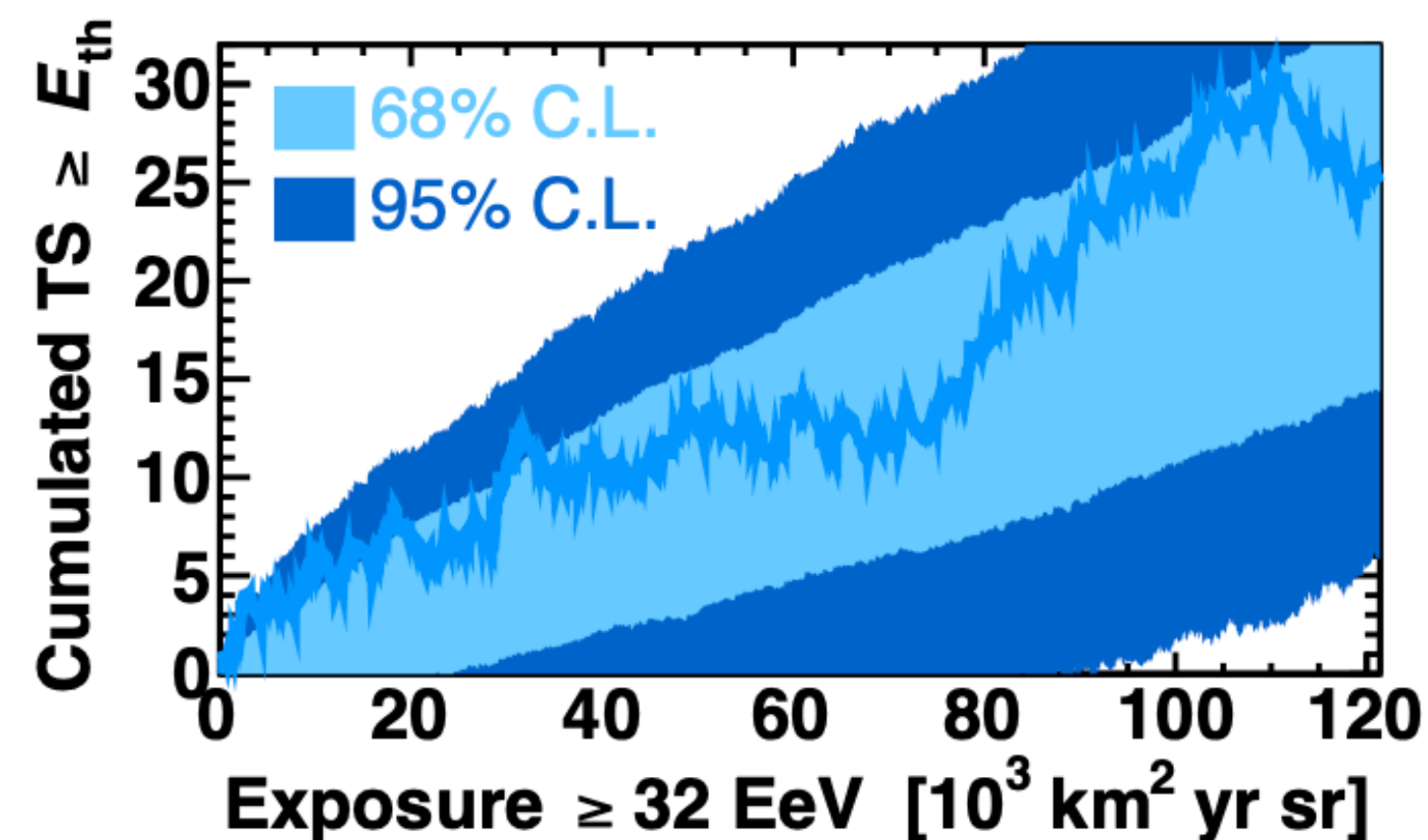
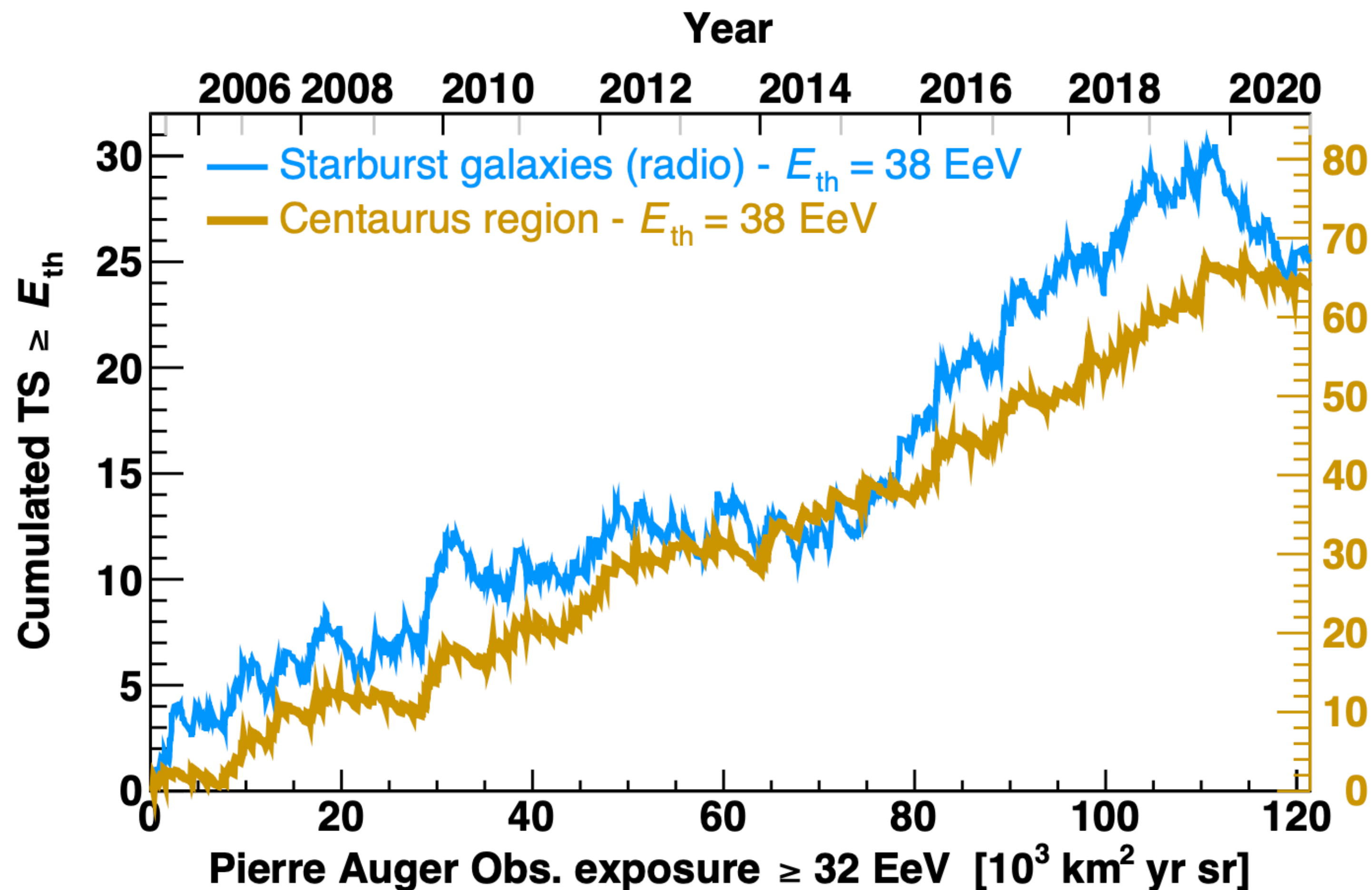
Thank you!



Backup slides

Evolution of the signal

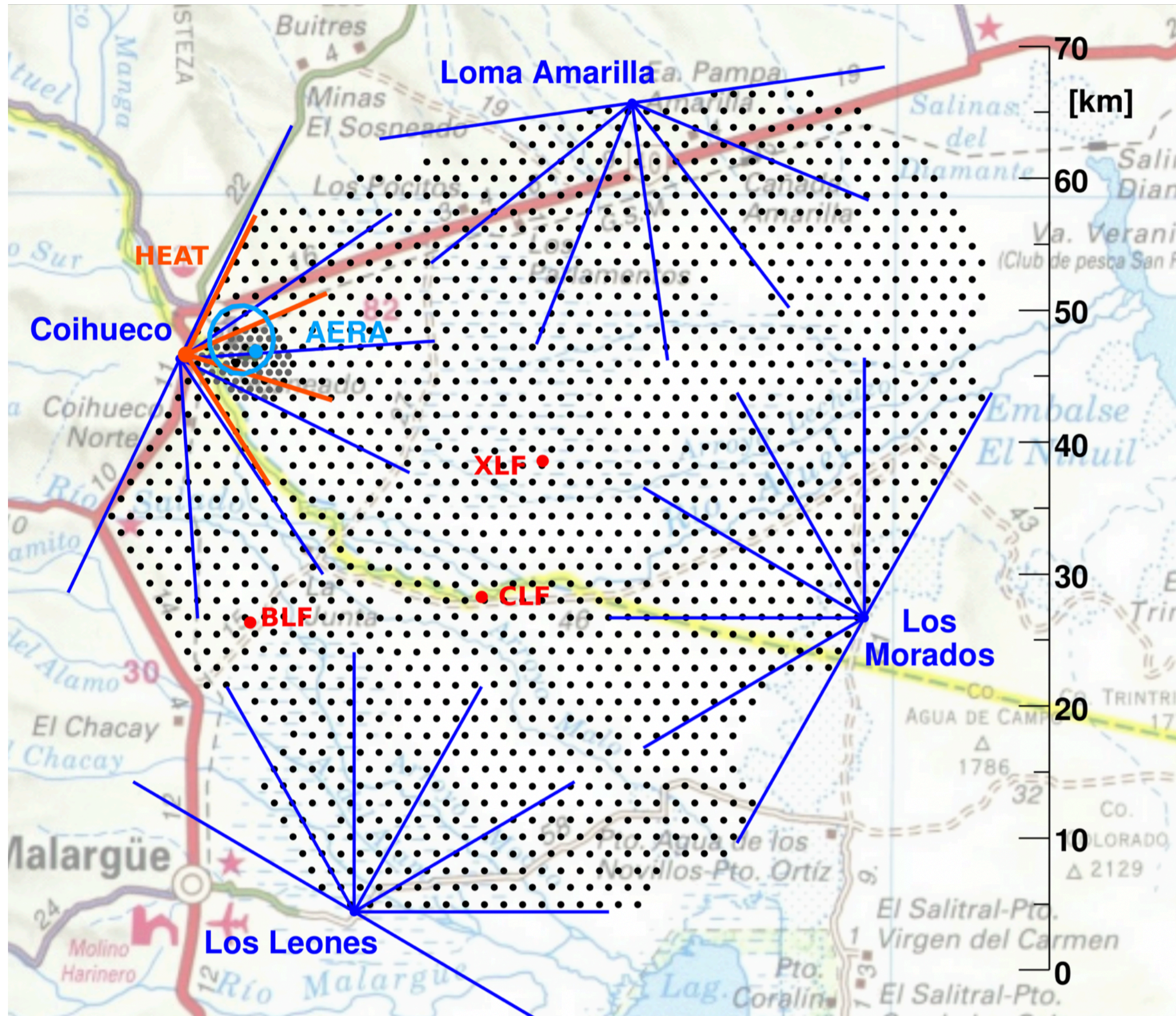
Considering the best-fit parameters of the Centaurus region search



Compatible with linear growth within the expected variance

5 sigma deviation from isotropy at 2025 ± 2 years

Pierre Auger Observatory: state-of-the art cosmic ray detector



★ Water Cherenkov stations

- ★ SD1500: 1600, 1.5 km grid, 3000 km²
- ★ SD750: 61, 0.75 km grid, 23.5 km²
- ★ **Live time ~ 100%**

★ 4 Fluorescence sites

- ★ 24 telescopes, 1-30° FOV
- ★ 3 high elevation FD 30°-60° FOV
- ★ **Live time ~ 13%**

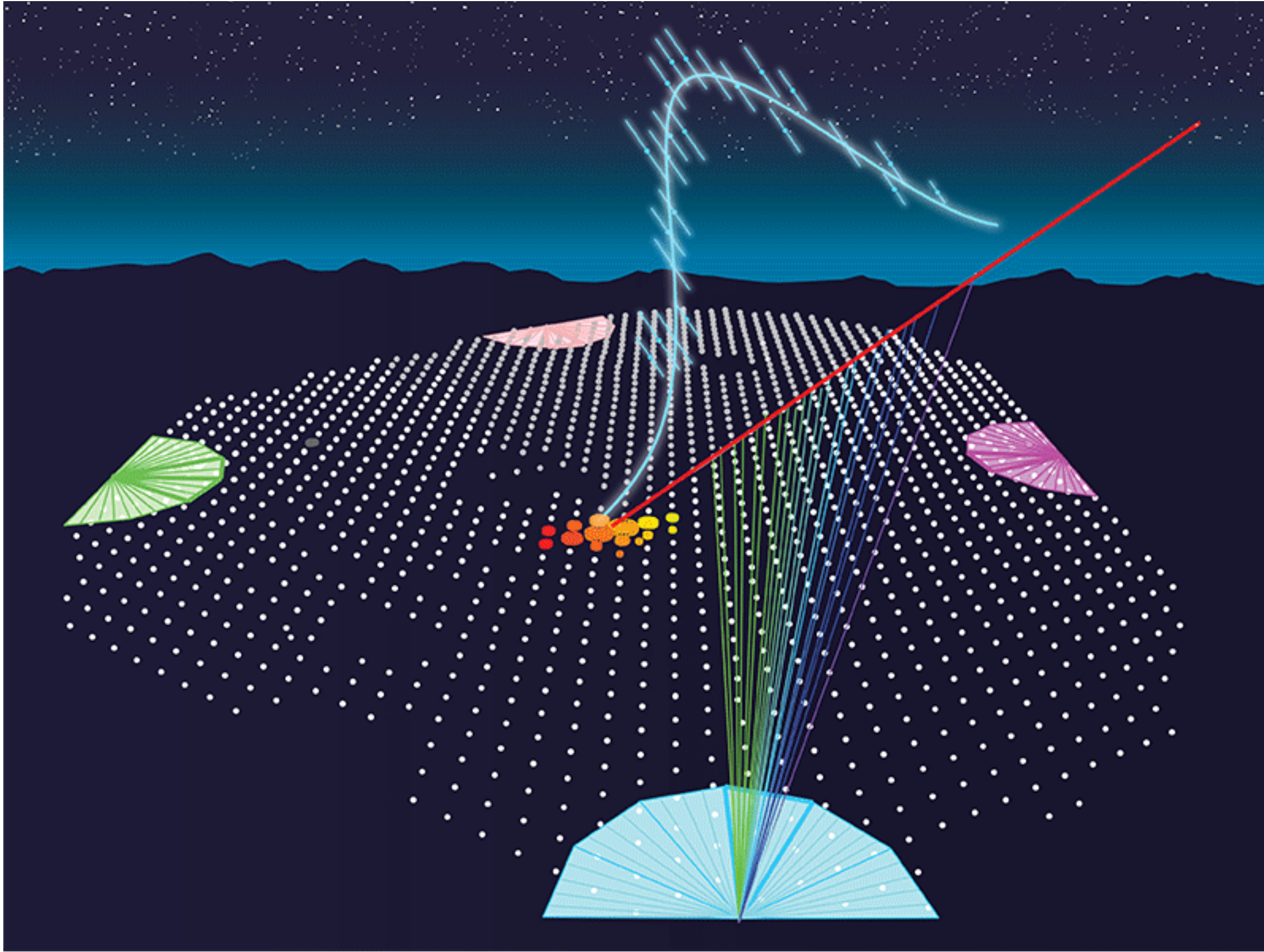
★ Underground Muon Detectors

- ★ 7 in engineering array phase
- ★ 61 aside the Infill stations

★ AERA radio antennas

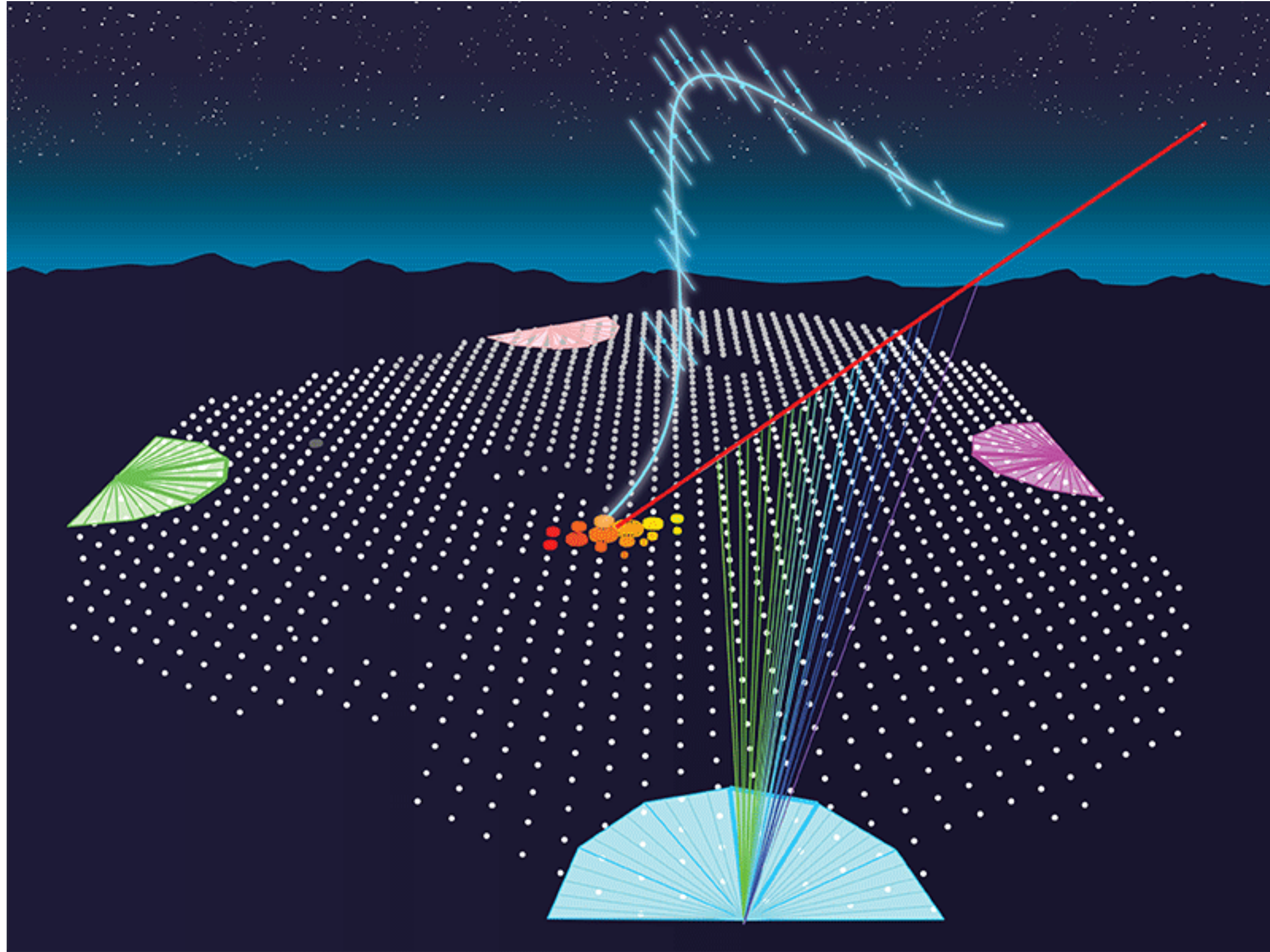
- ★ 153 antennas in 17 km²

Schema of a cosmic ray detection at the Pierre Auger Obs.



APS/Karin Cain

Schema of a cosmic ray detection at the Pierre Auger Obs.

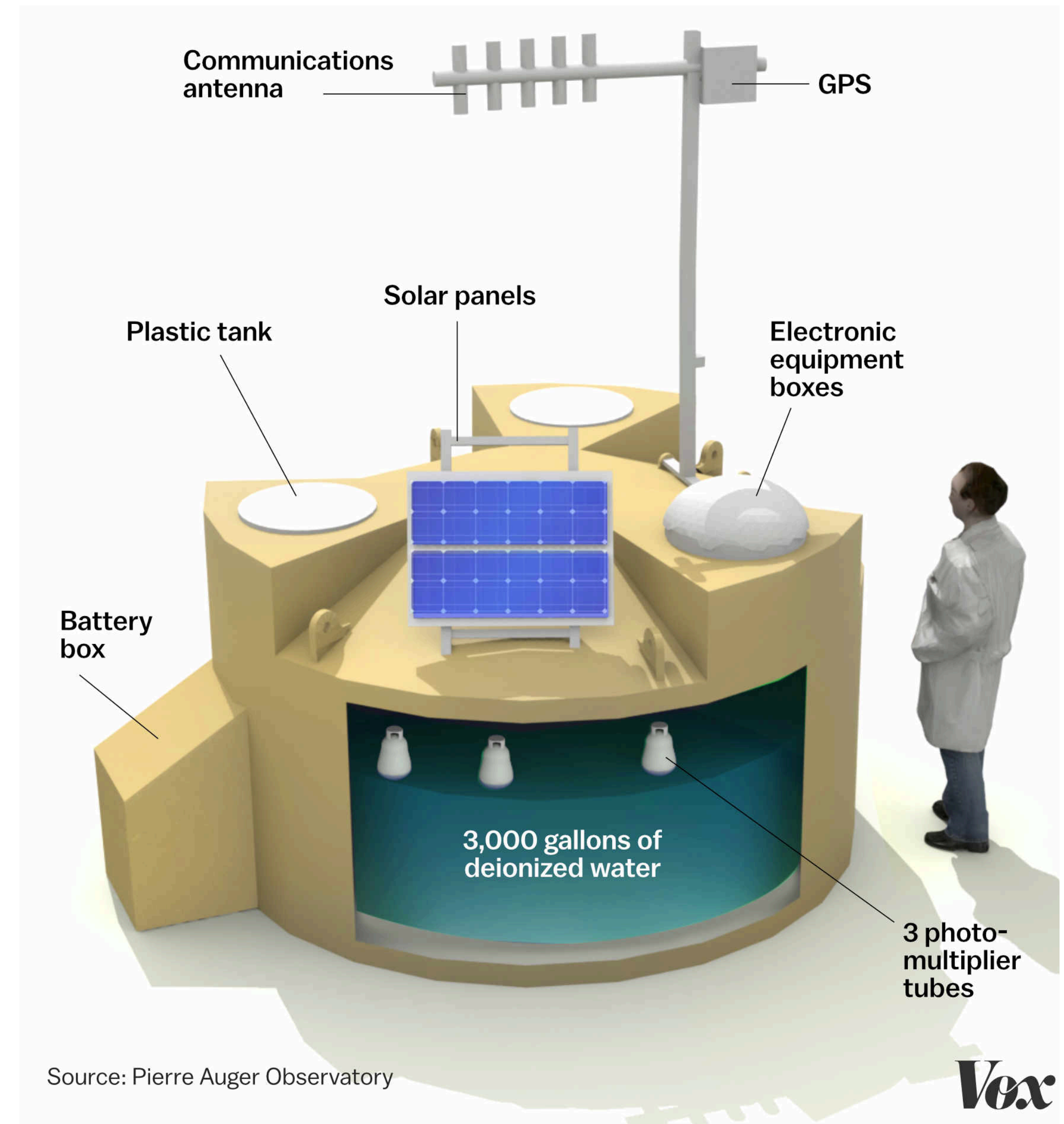
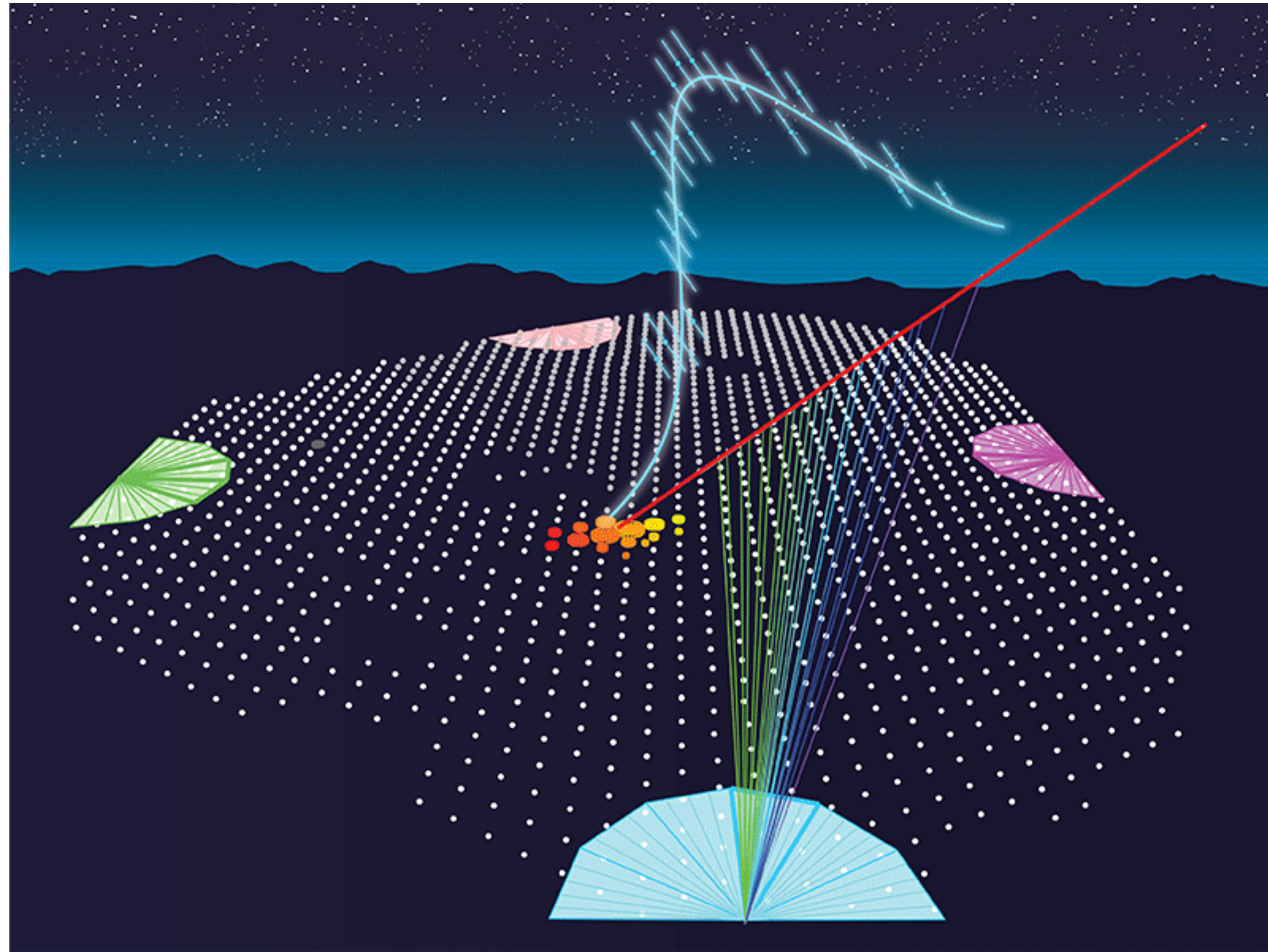


Hybrid design

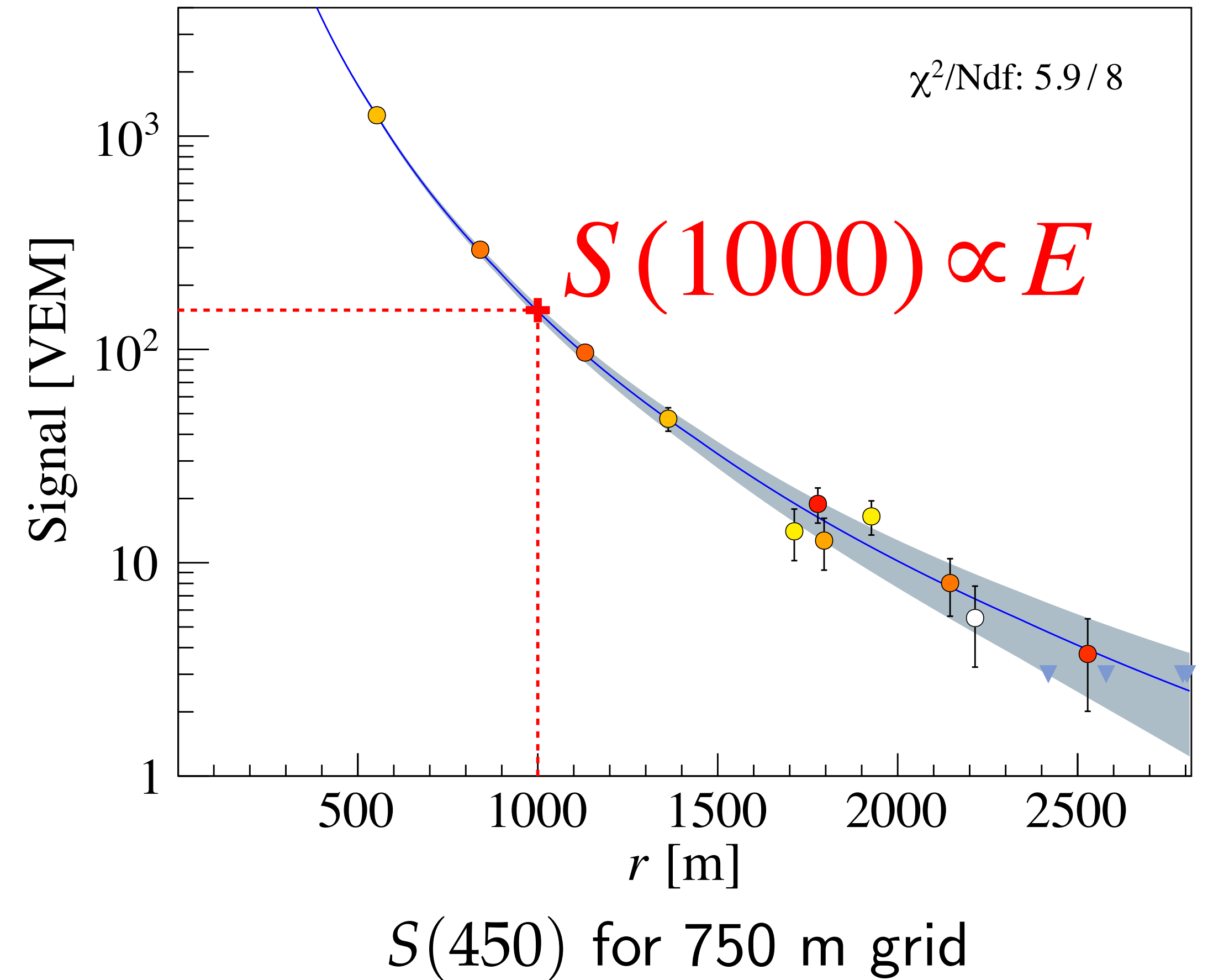
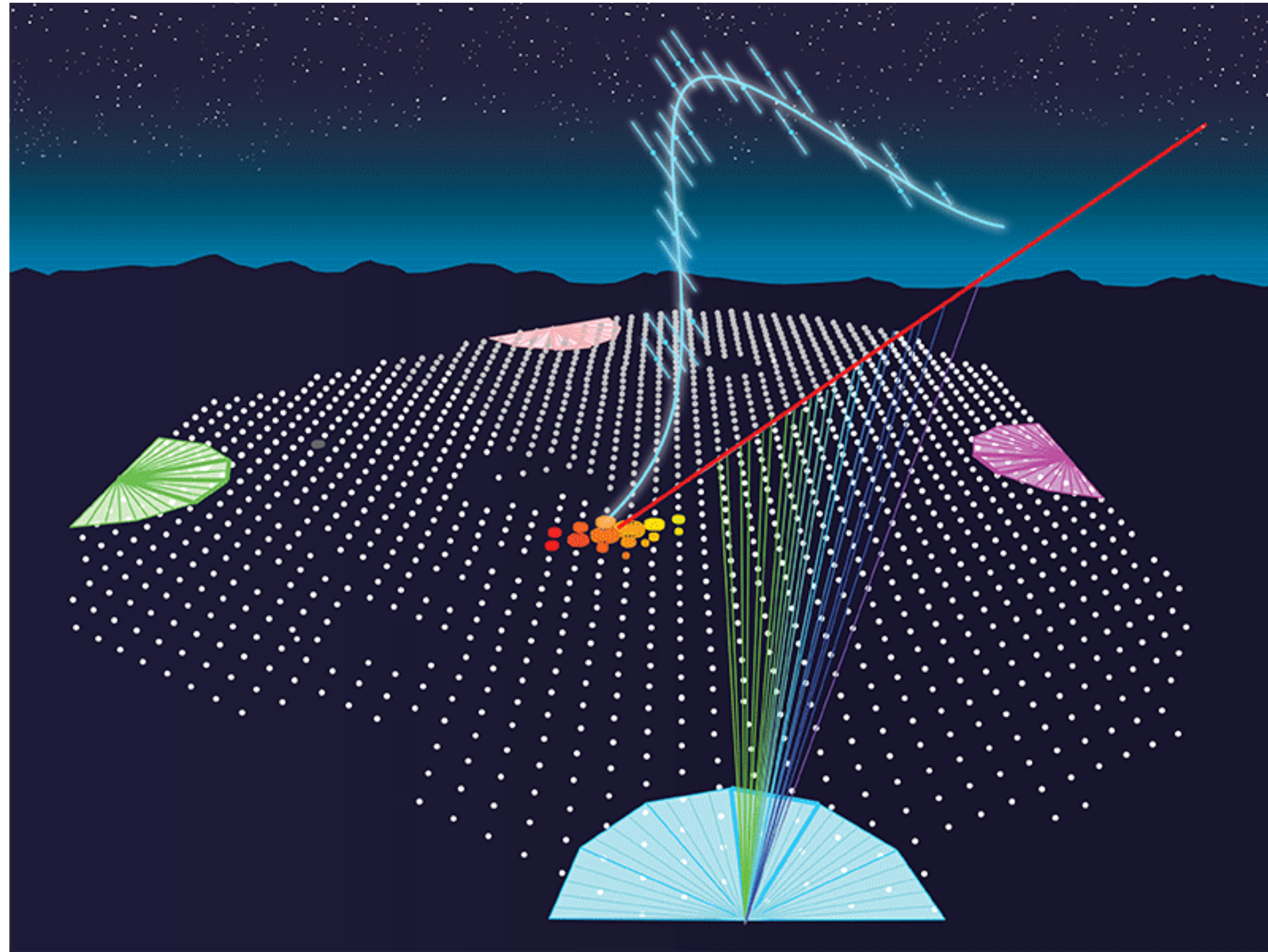
simultaneous detection by a surface array and by fluorescence telescopes

APS/Karin Cain

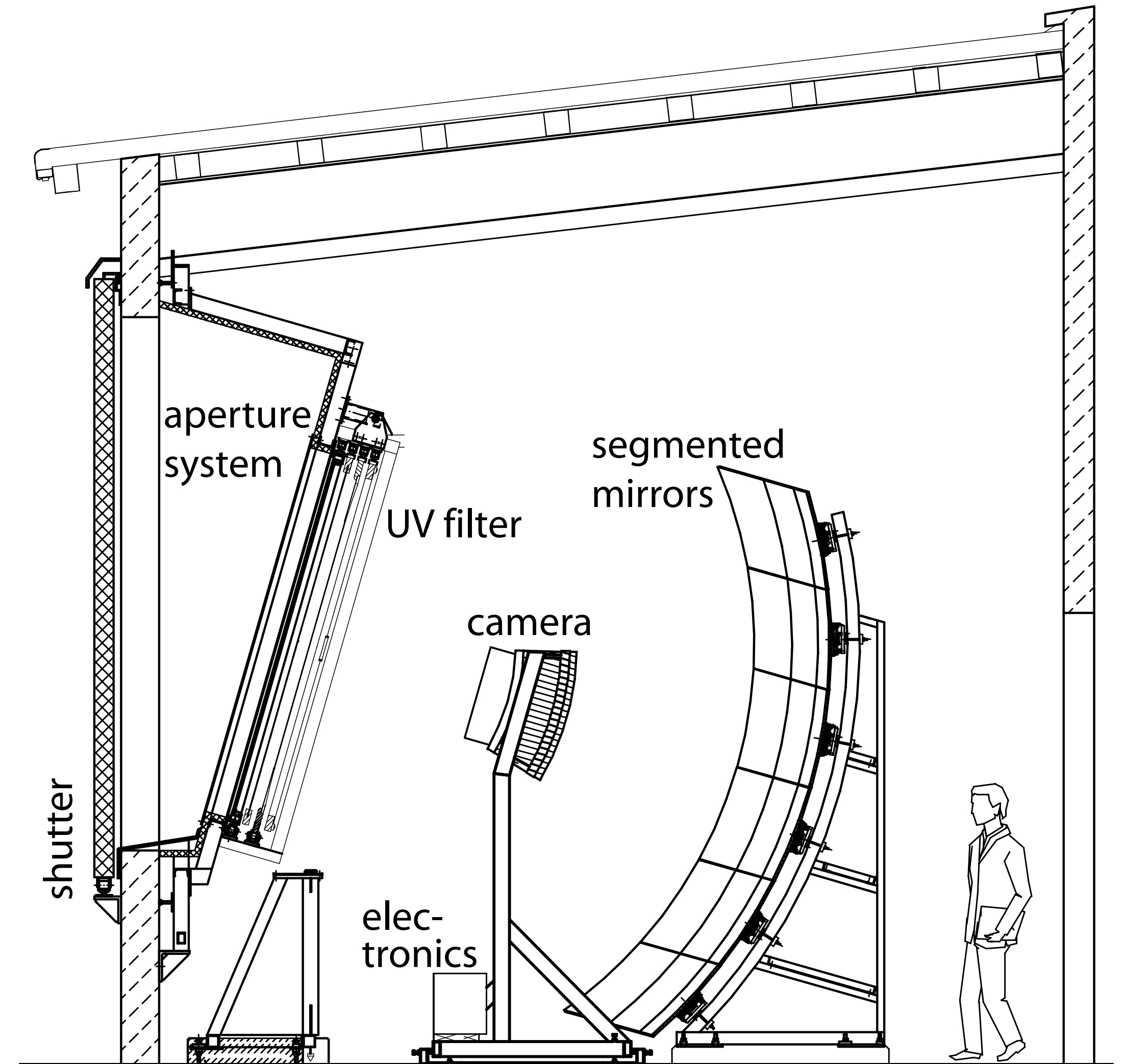
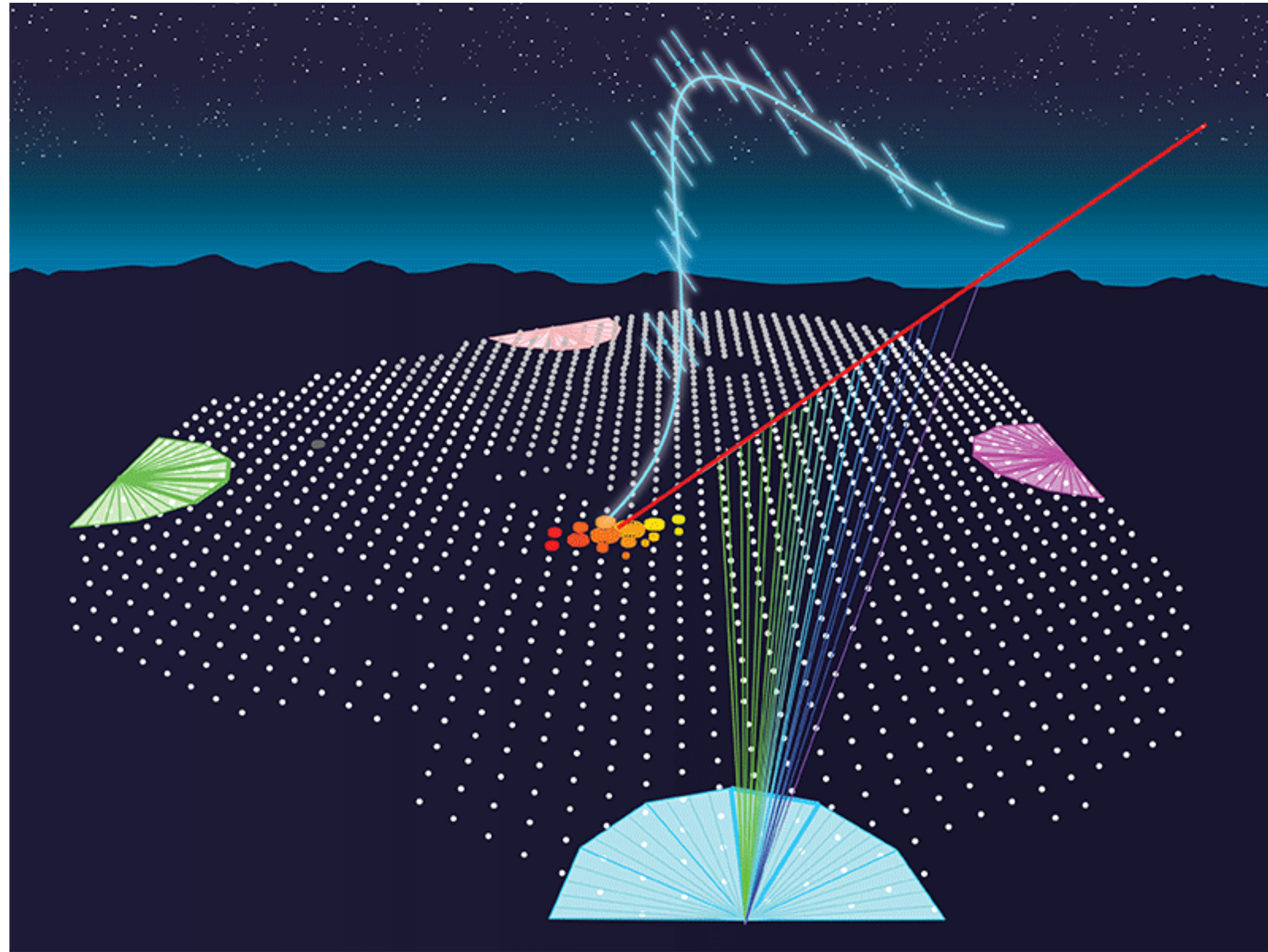
Schema of a cosmic ray detection at the Pierre Auger Obs.



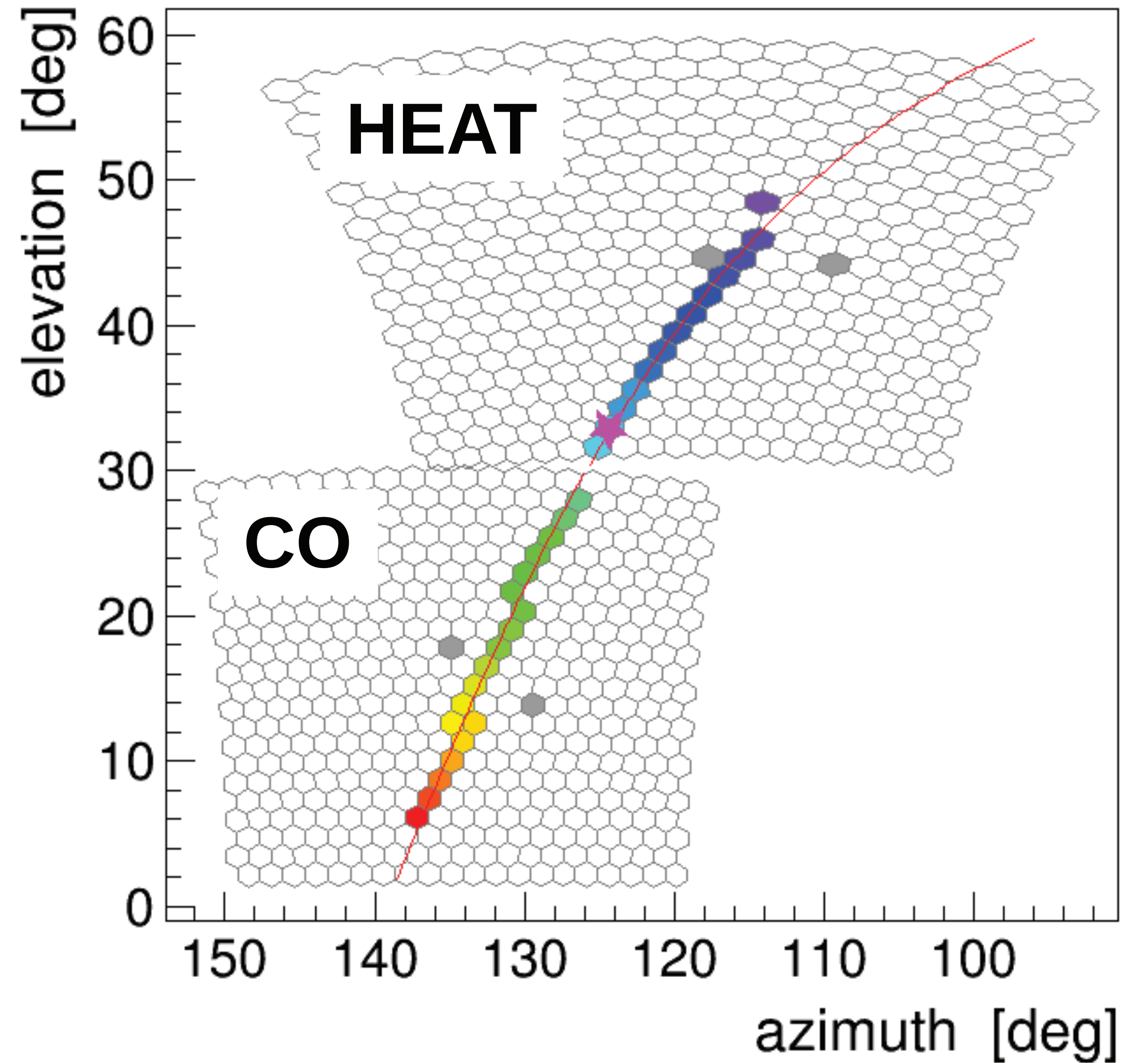
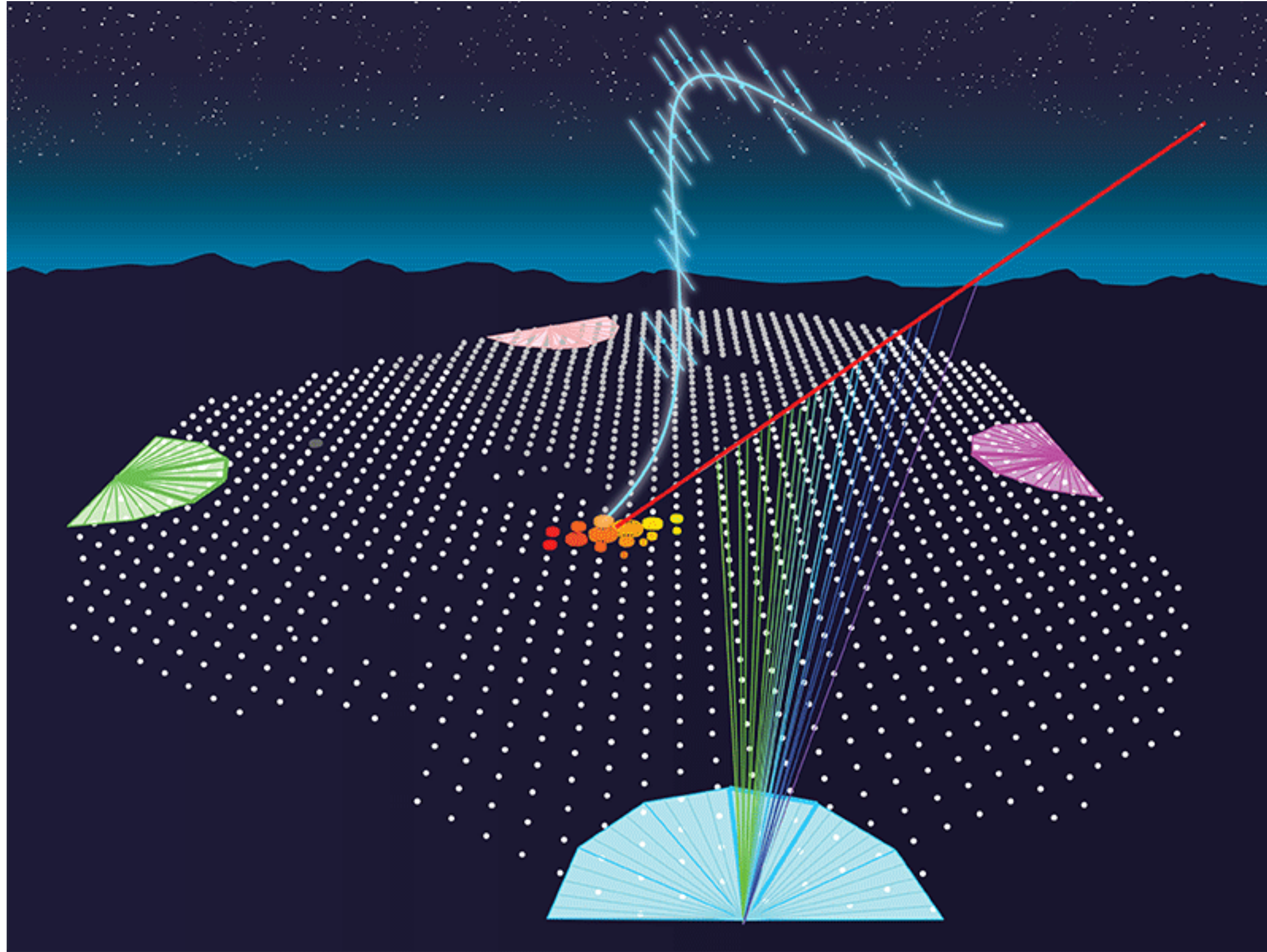
Schema of a cosmic ray detection at the Pierre Auger Obs.



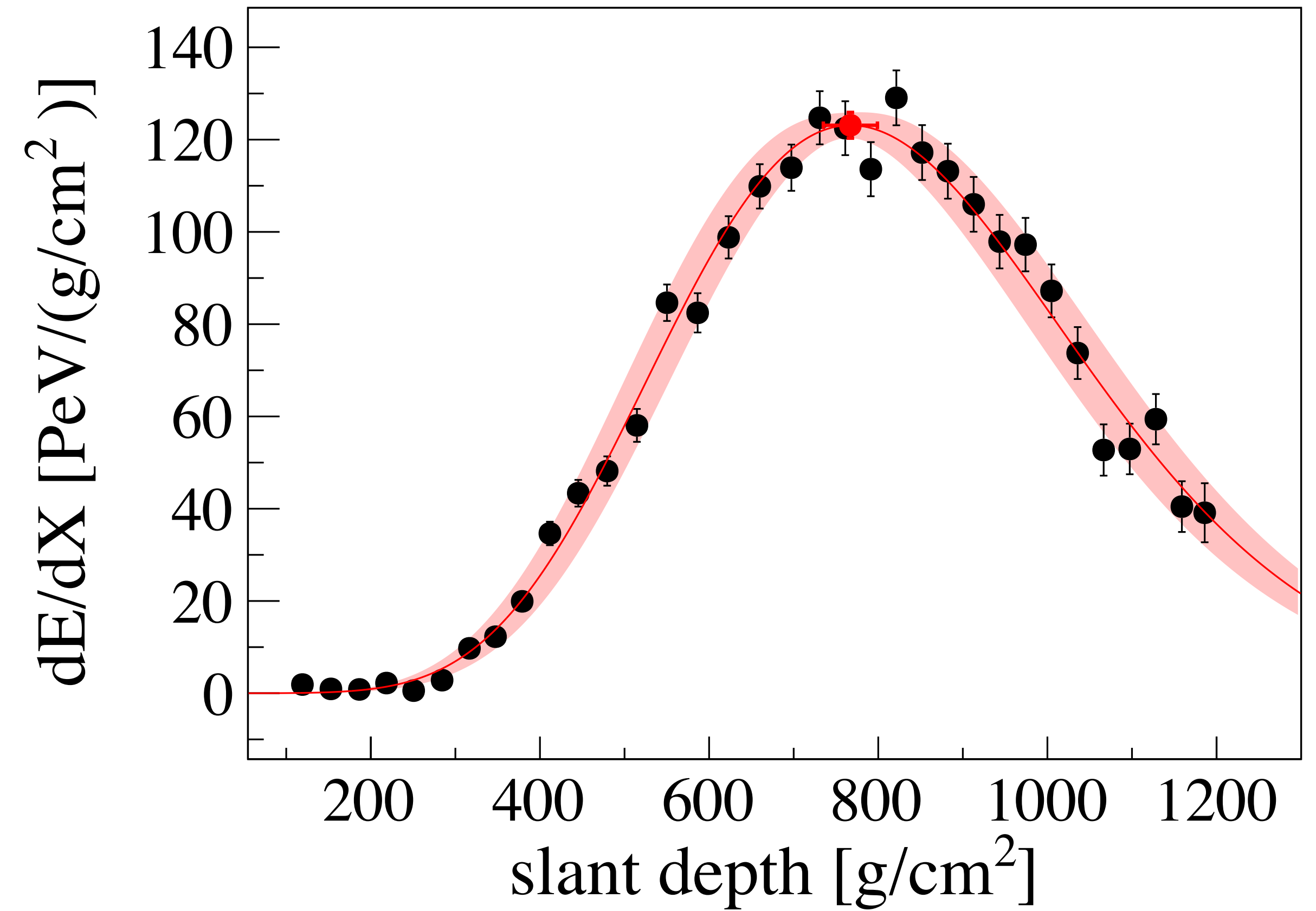
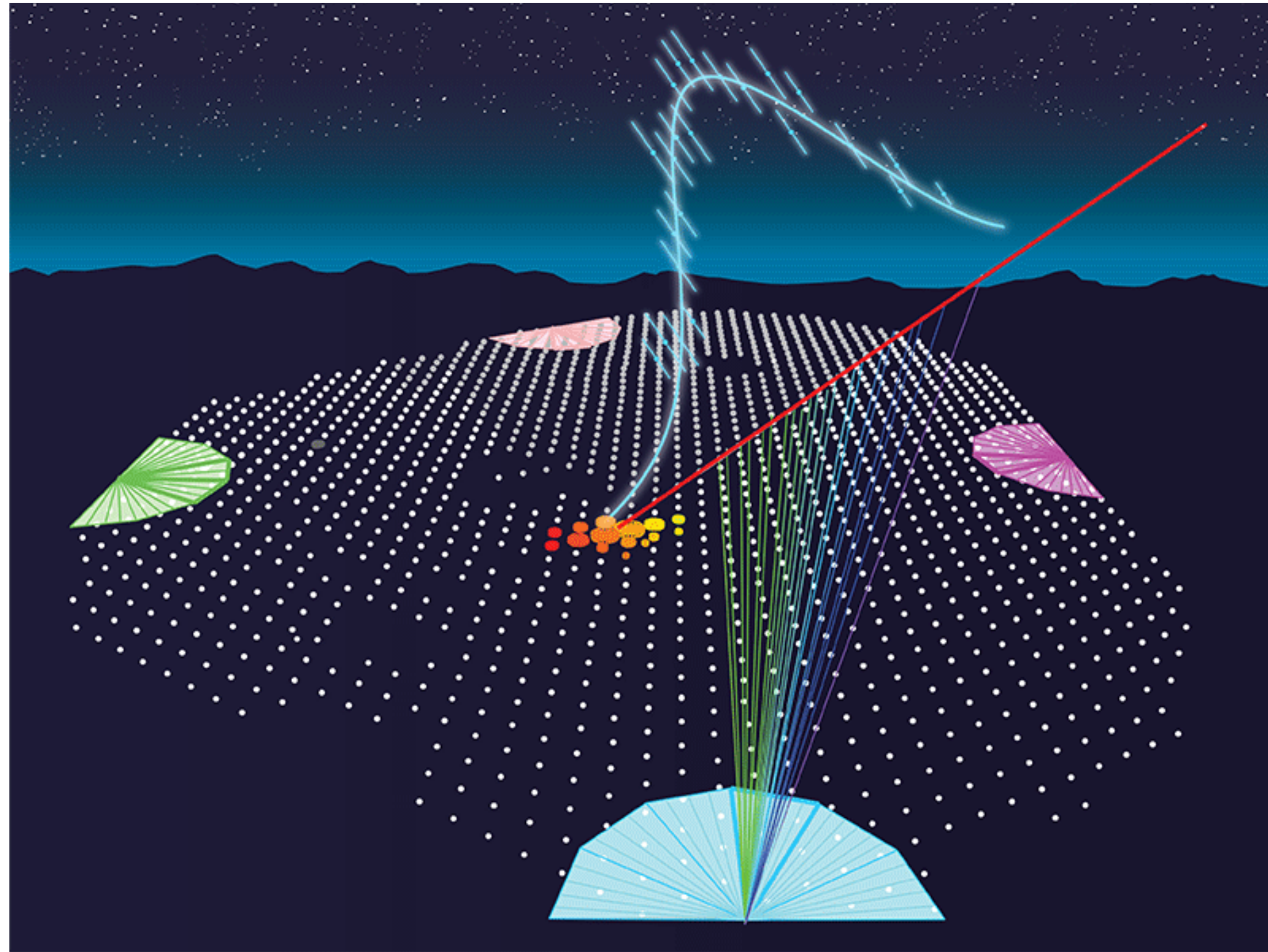
Schema of a cosmic ray detection at the Pierre Auger Obs.



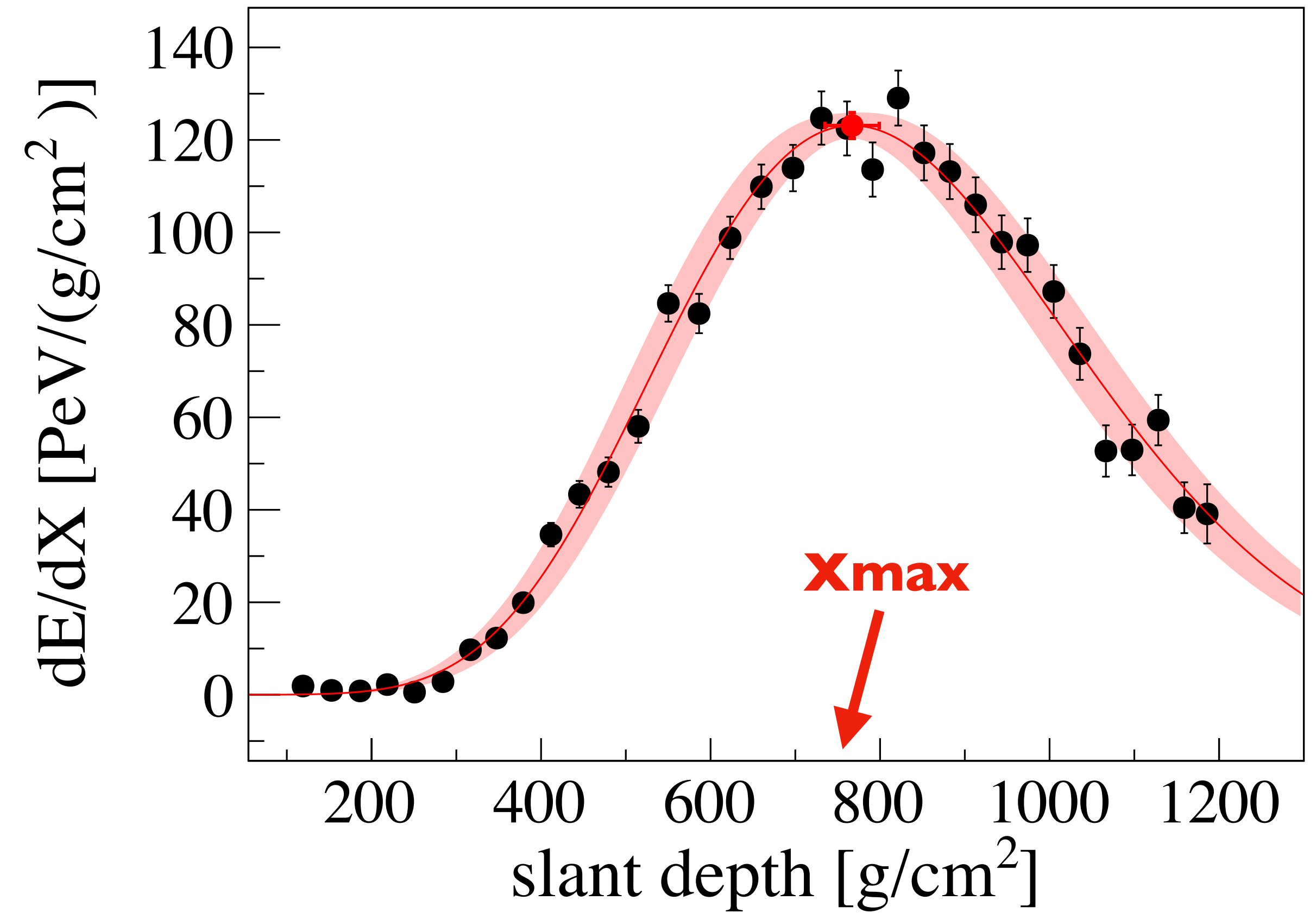
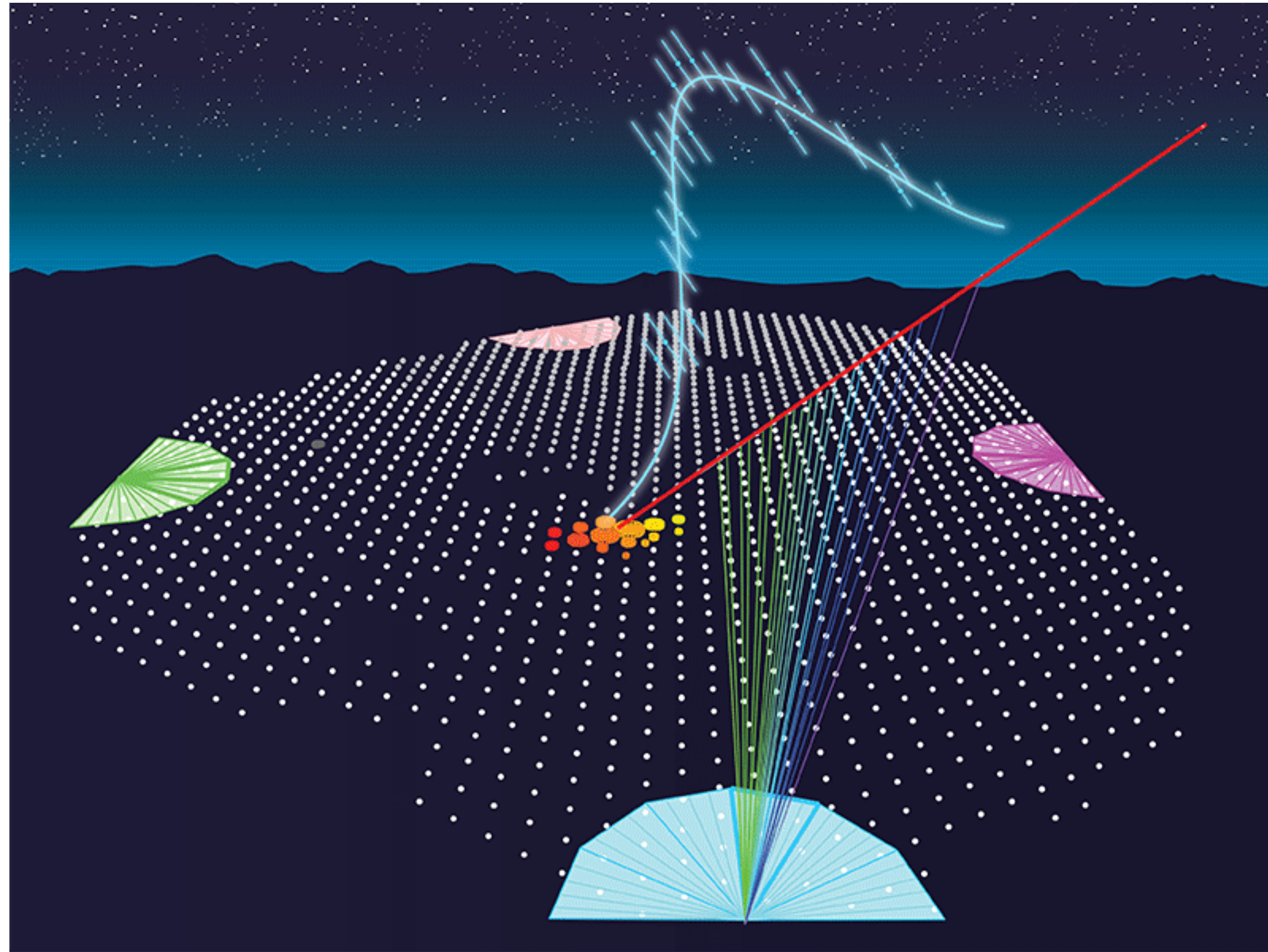
Schema of a cosmic ray detection at the Pierre Auger Obs.



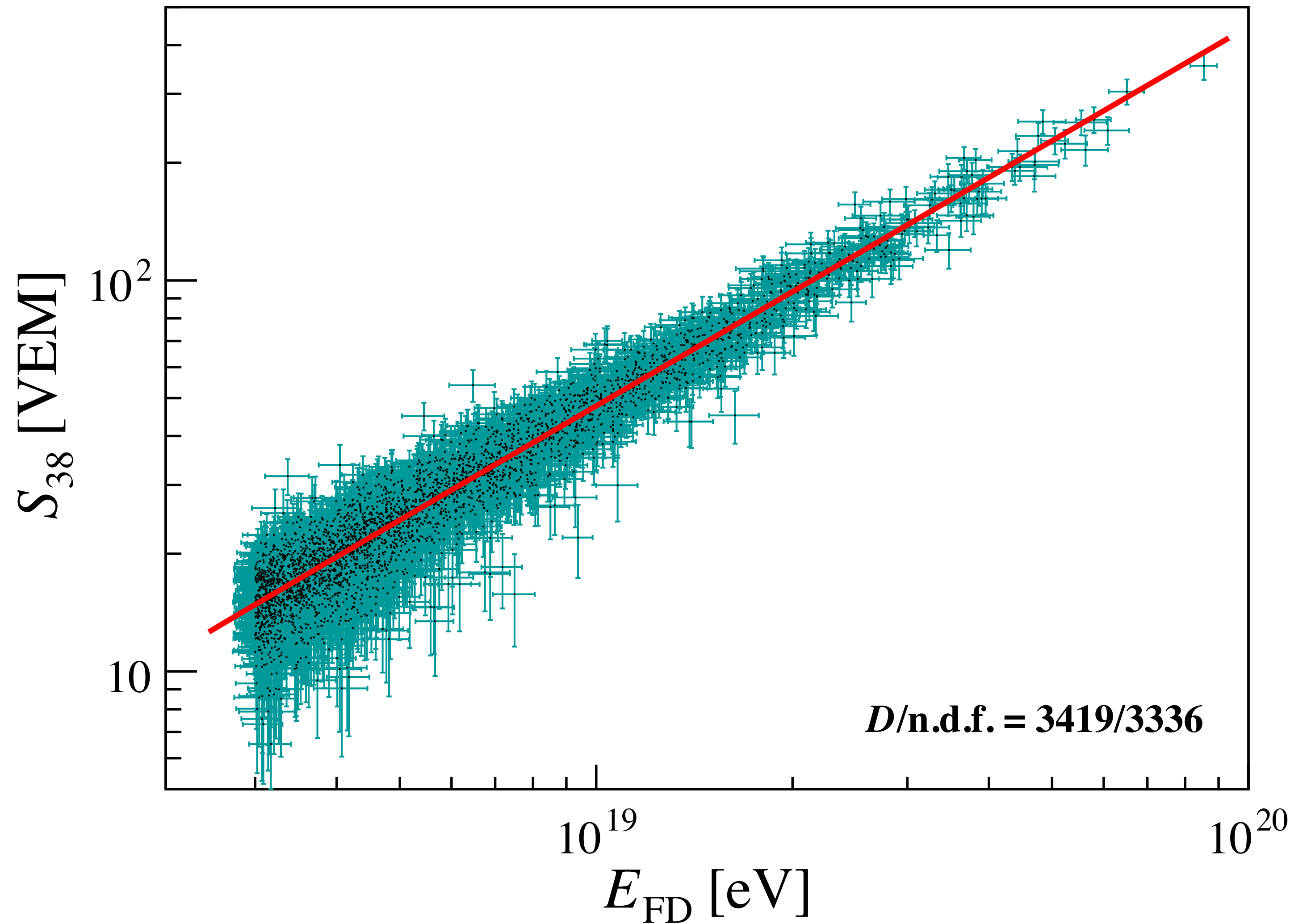
Schema of a cosmic ray detection at the Pierre Auger Obs.



Schema of a cosmic ray detection at the Pierre Auger Obs.



Surface Detector Energy calibration



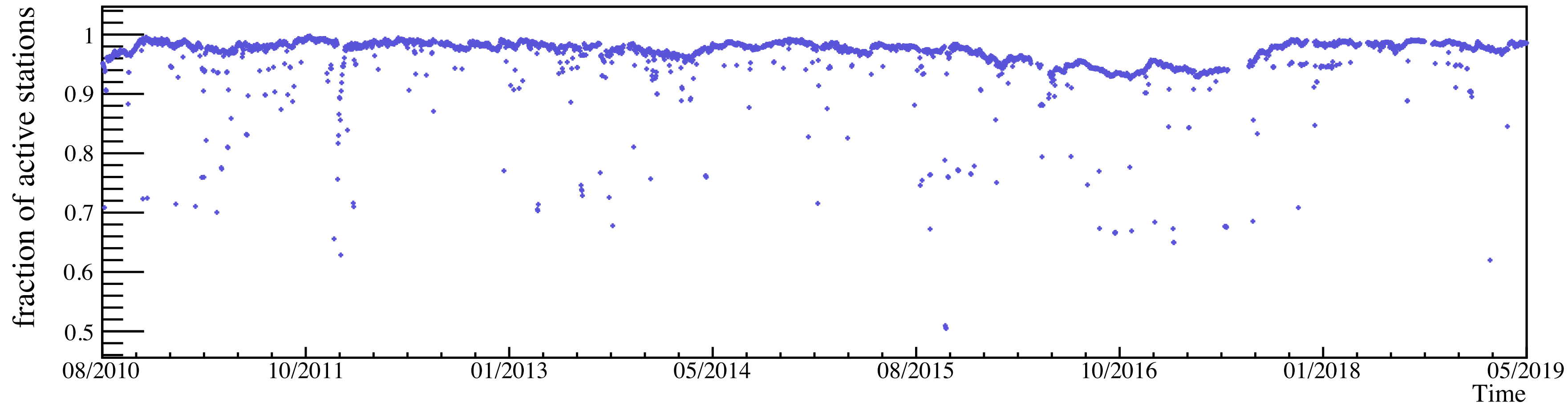
3,338 hybrid events in the fit

$$E_{\text{FD}} = AS_{38}^B$$

$$A = (1.86 \pm 0.03) \times 10^{17} \text{ eV}$$

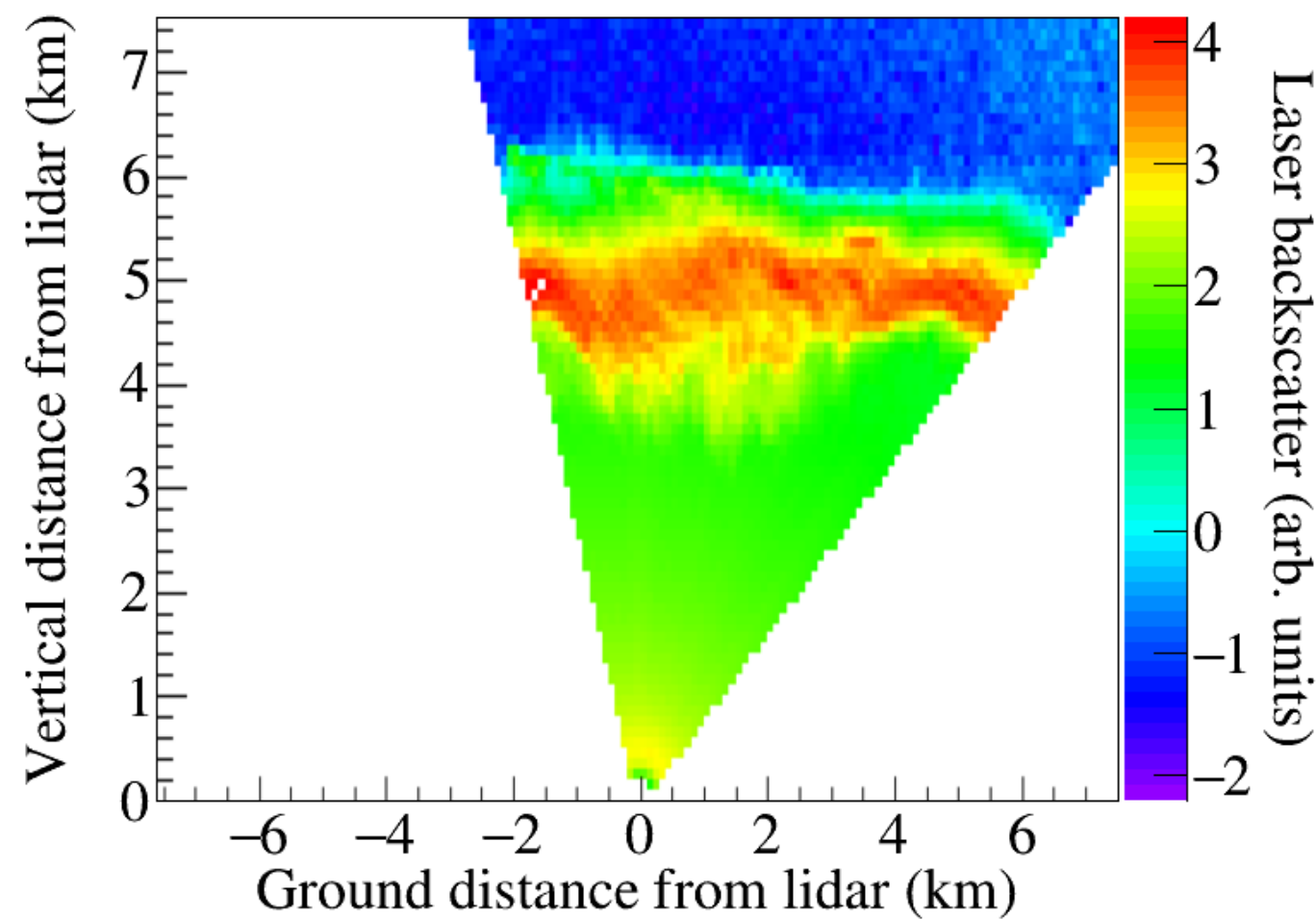
$$B = 1.031 \pm 0.004$$

Long term and real time monitoring



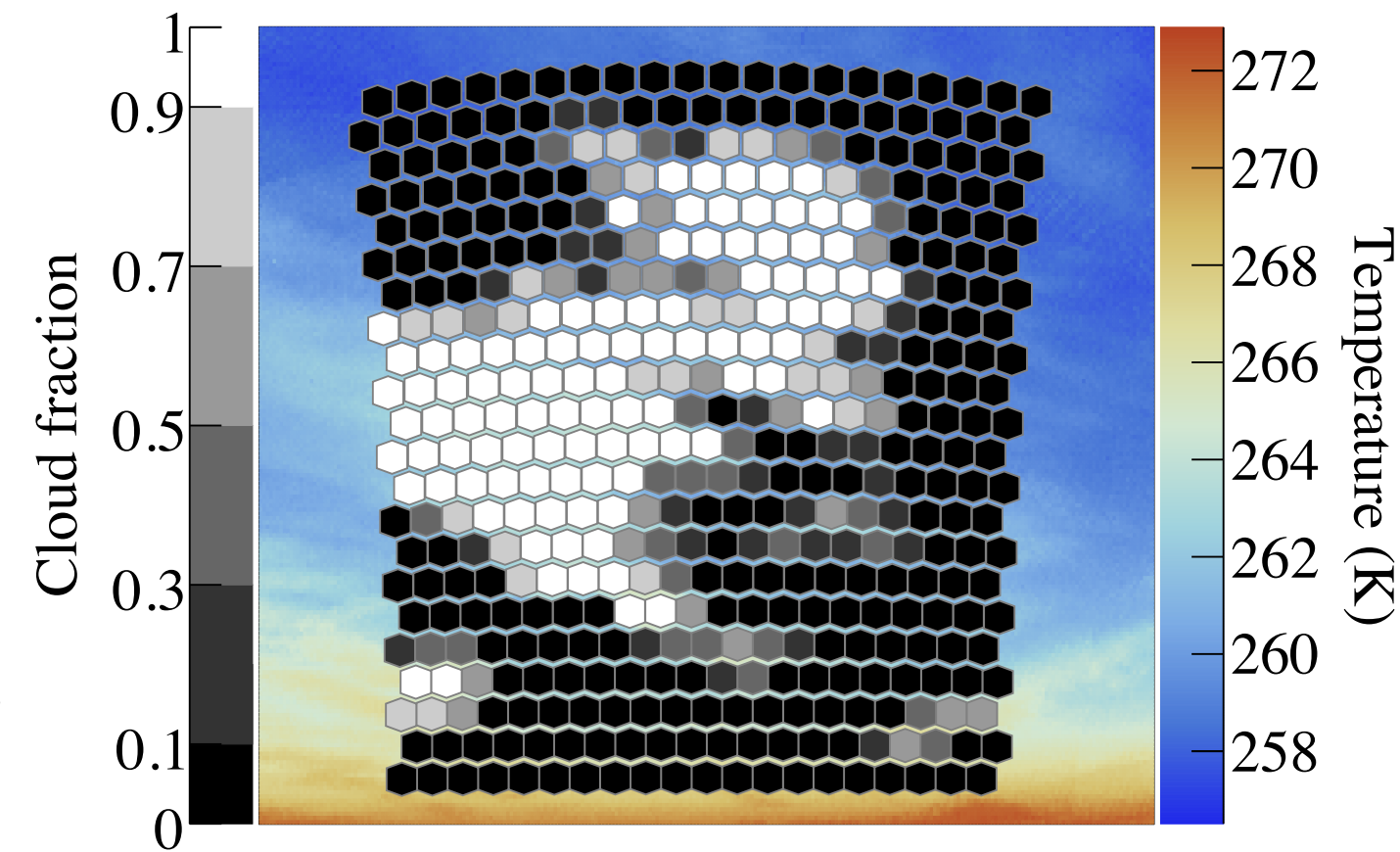
Number of active SD stations normalized to the number of deployed SD stations as a function of time.

2019-06-24T03:13:57Z, LA, zenith scan



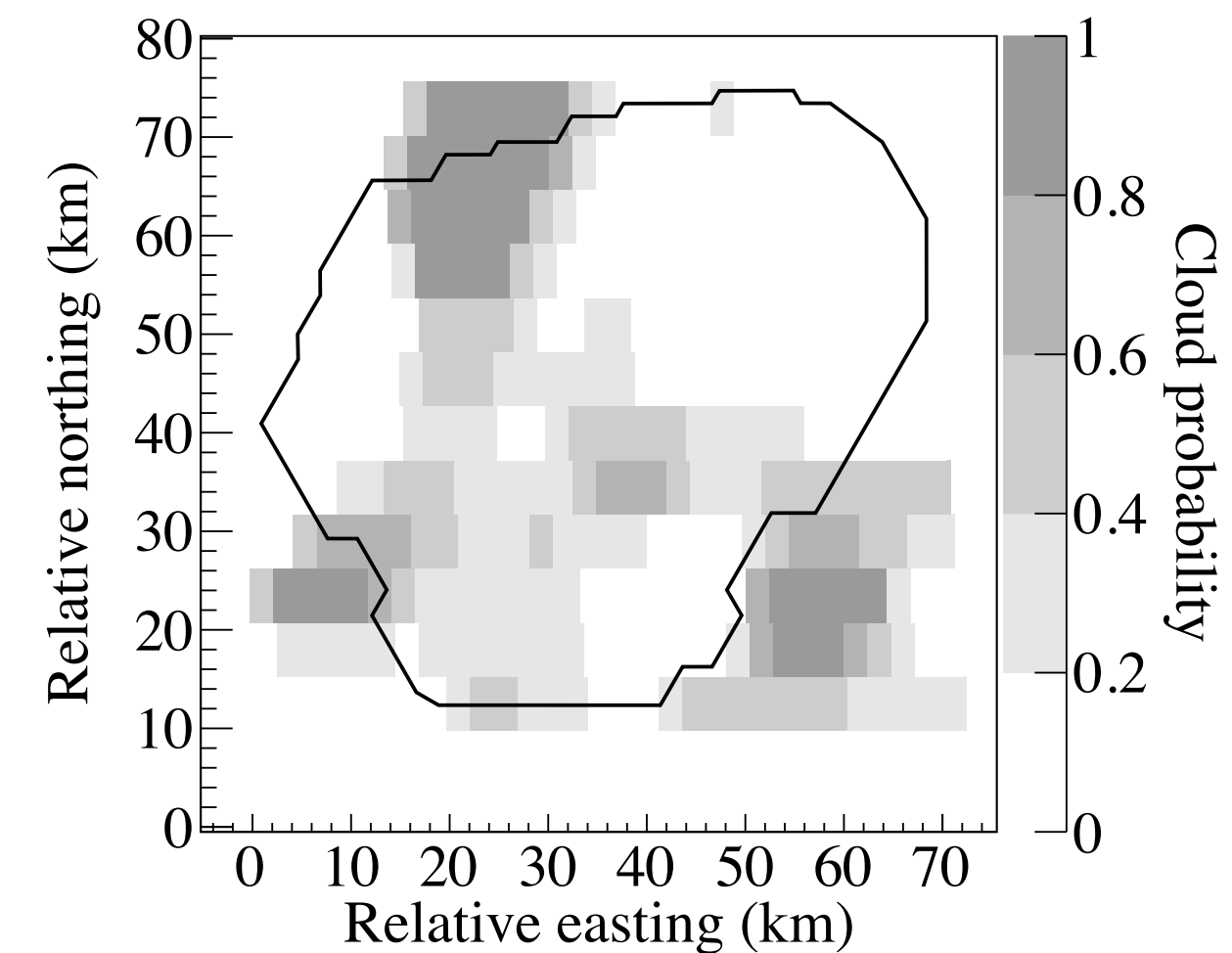
FD lidar scan

2018-07-16T22:58:38Z, LL, telescope 1



Cloud camera image

2017-06-14T20:22:00Z



Satellite cloud probability map

[V. Harvey for the P. Auger Collab. ICRC 2019](#)

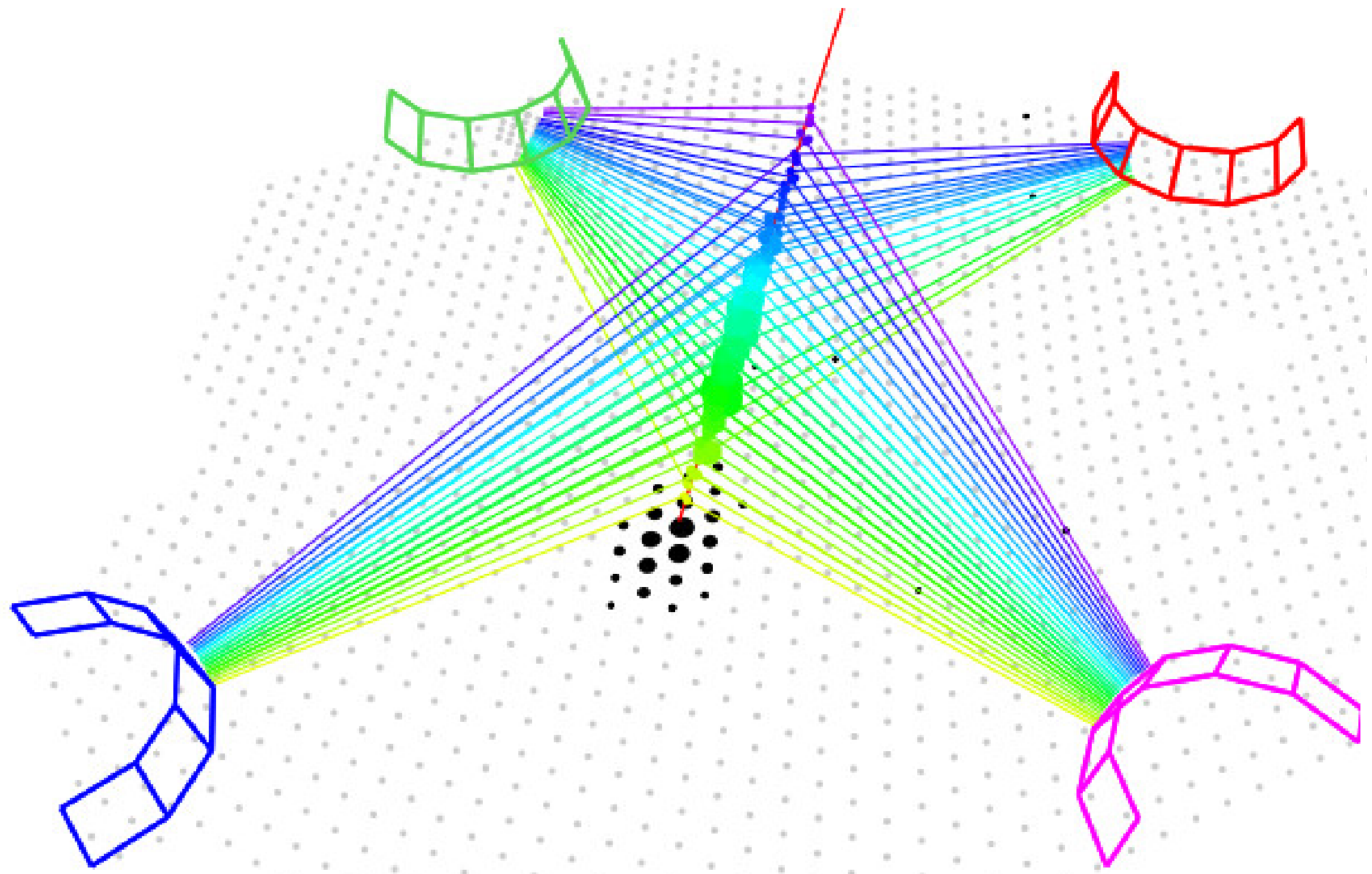
[K. Choi for the P. Auger Collab. ICRC 2019](#)

The Pierre Auger Collaboration

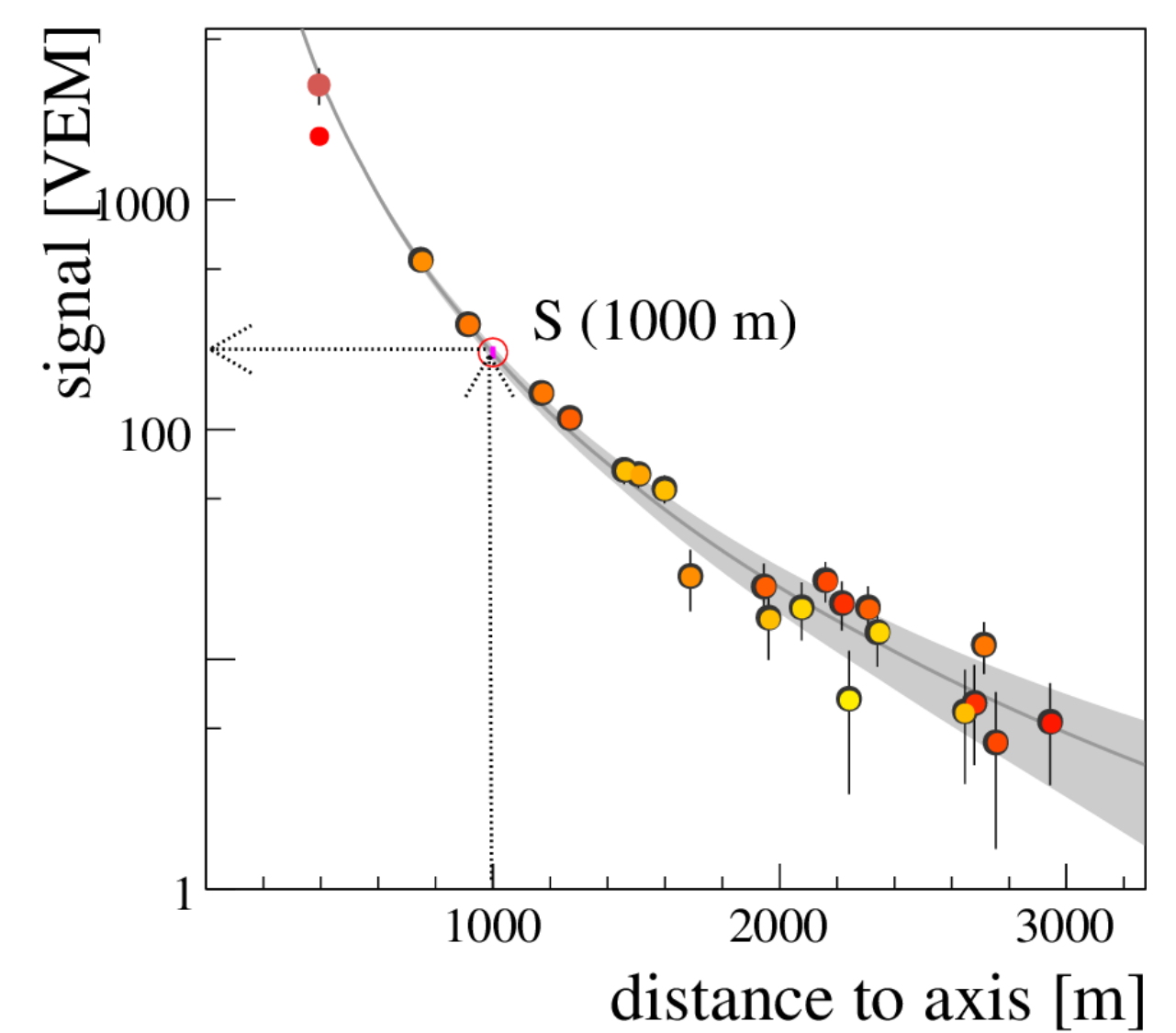
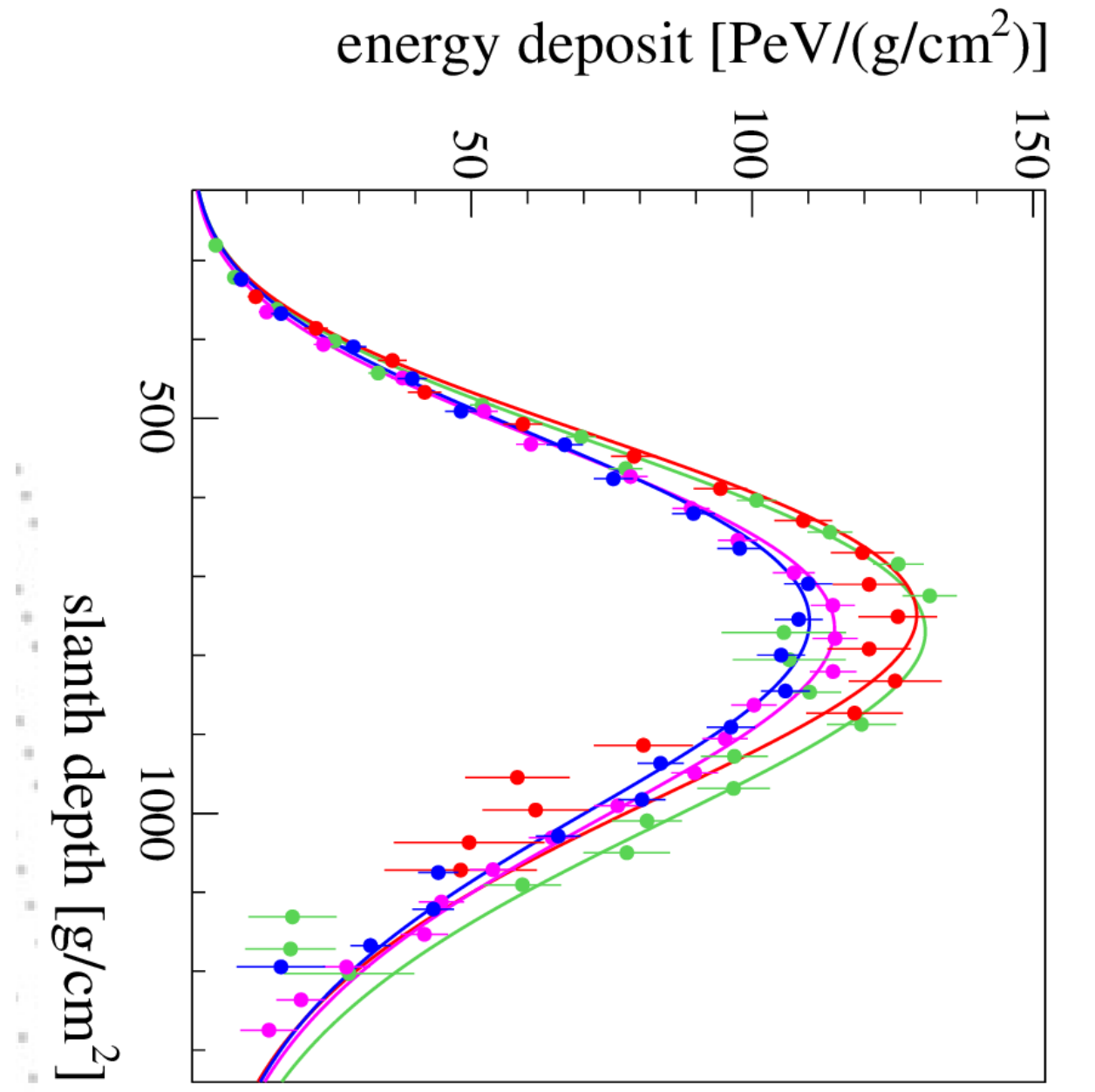
About 400 members from 90 institutions in 16 countries



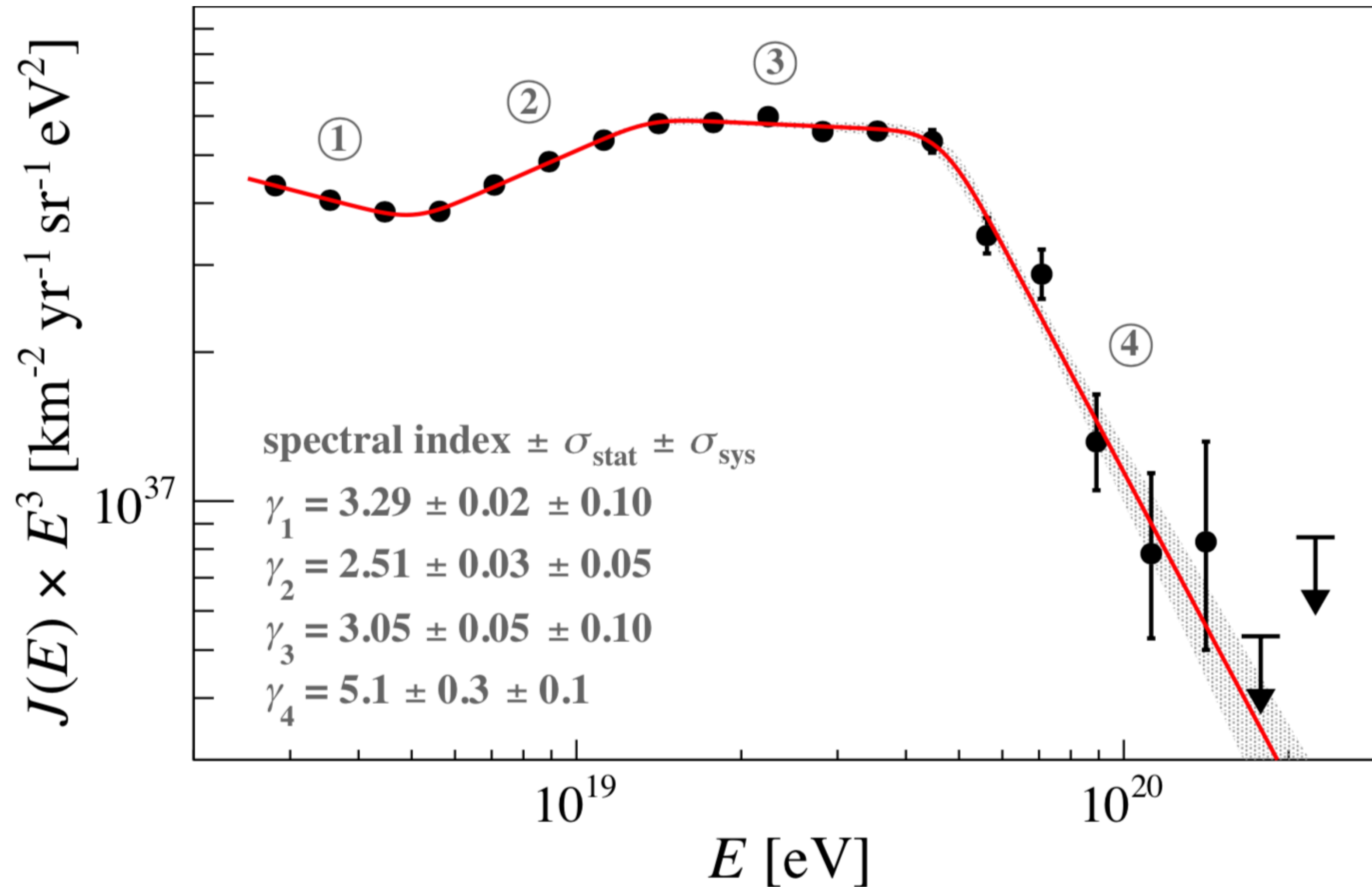
Quadruple hybrid event



65 km between FD



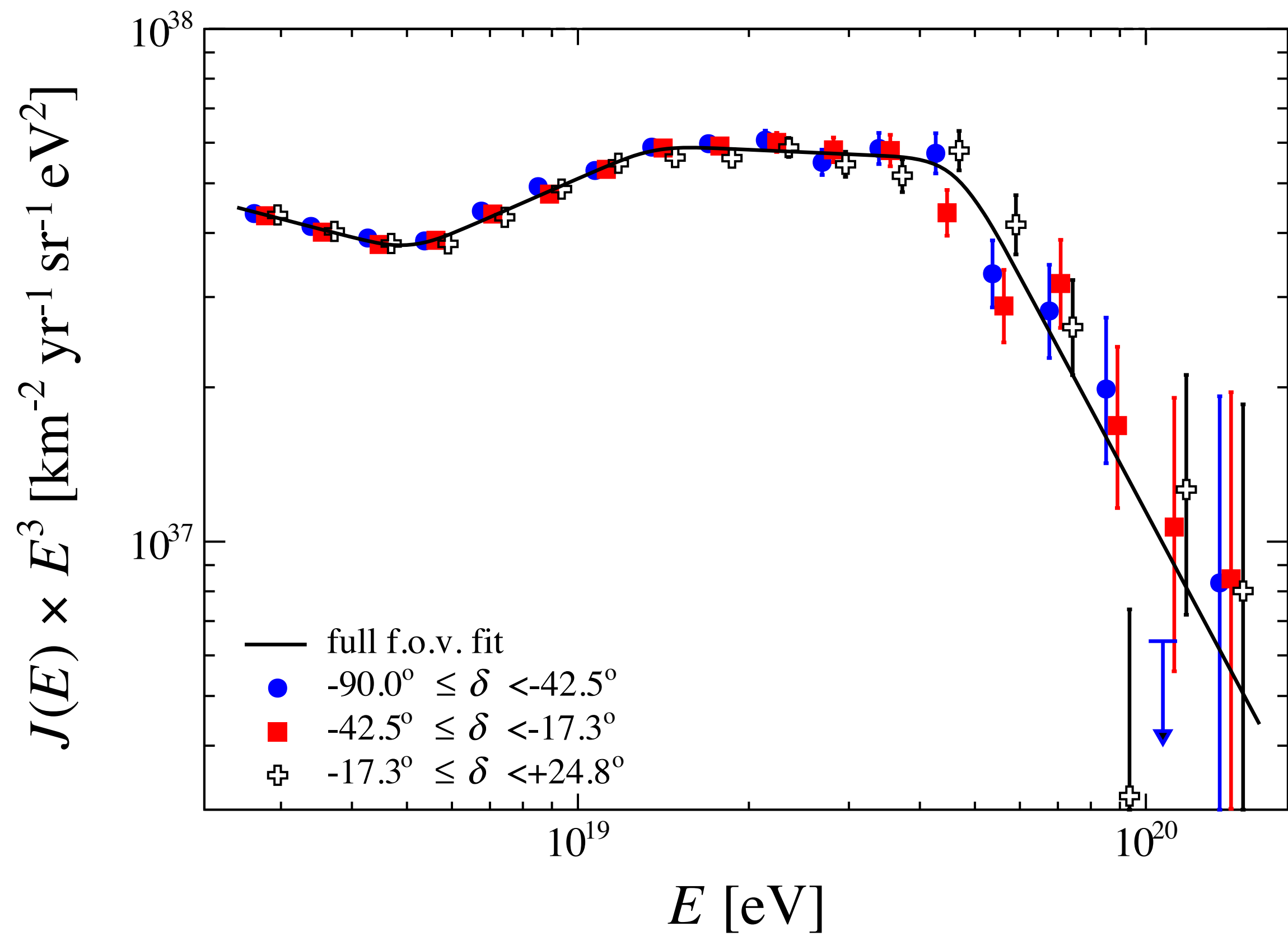
Energy spectrum



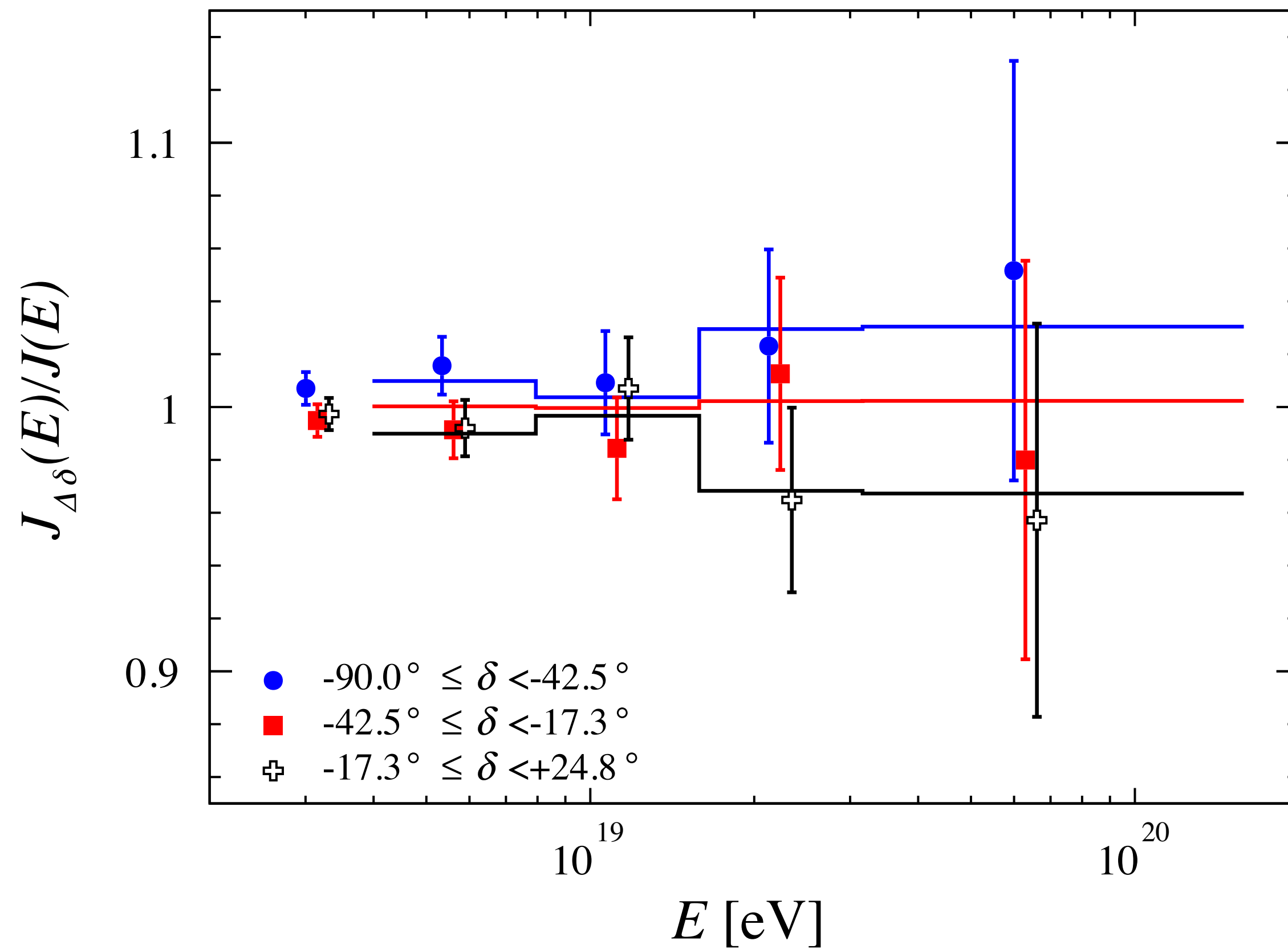
- ★ Data: about 15 years of SD
- ★ 215,030 events
- ★ zenith angles below 60°
- ★ energies larger than 2.5×10^{18} eV

Steepening at 10^{19} eV never observed previously

Energy spectra in three declination bands (SD)

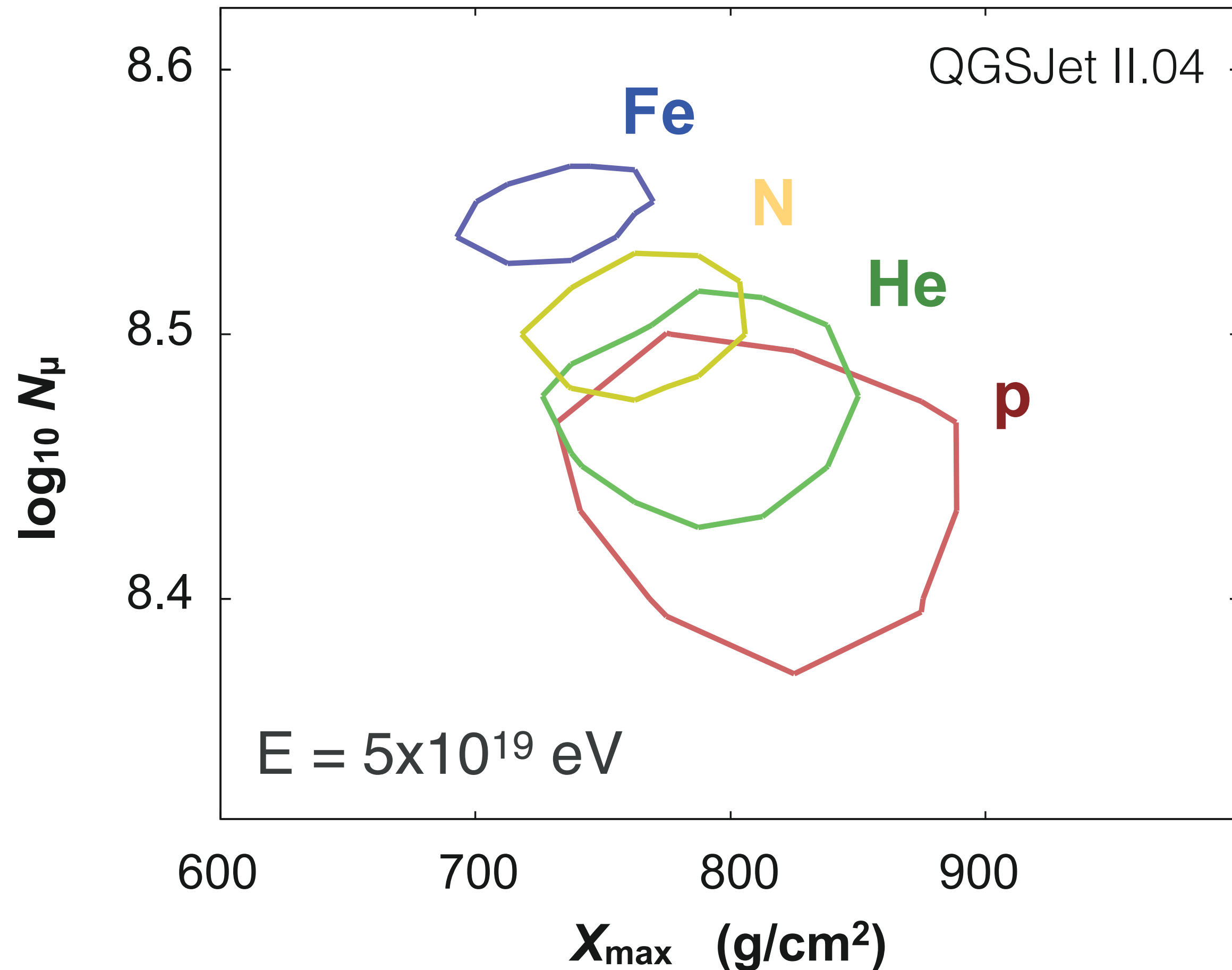


bands of equal exposure



[P. Auger Collab., Phys. Rev. D, 2020](#)

Mass composition sensitivity



Depth of shower maximum

$$\langle X_{\text{max}}^p \rangle \approx \langle X_{\text{max}}^{\text{Fe}} \rangle + (80 - 100) \text{ g cm}^{-2}$$

$$\sigma(X_{\text{max}}^p) / \sigma(X_{\text{max}}^{\text{Fe}}) \approx 3$$

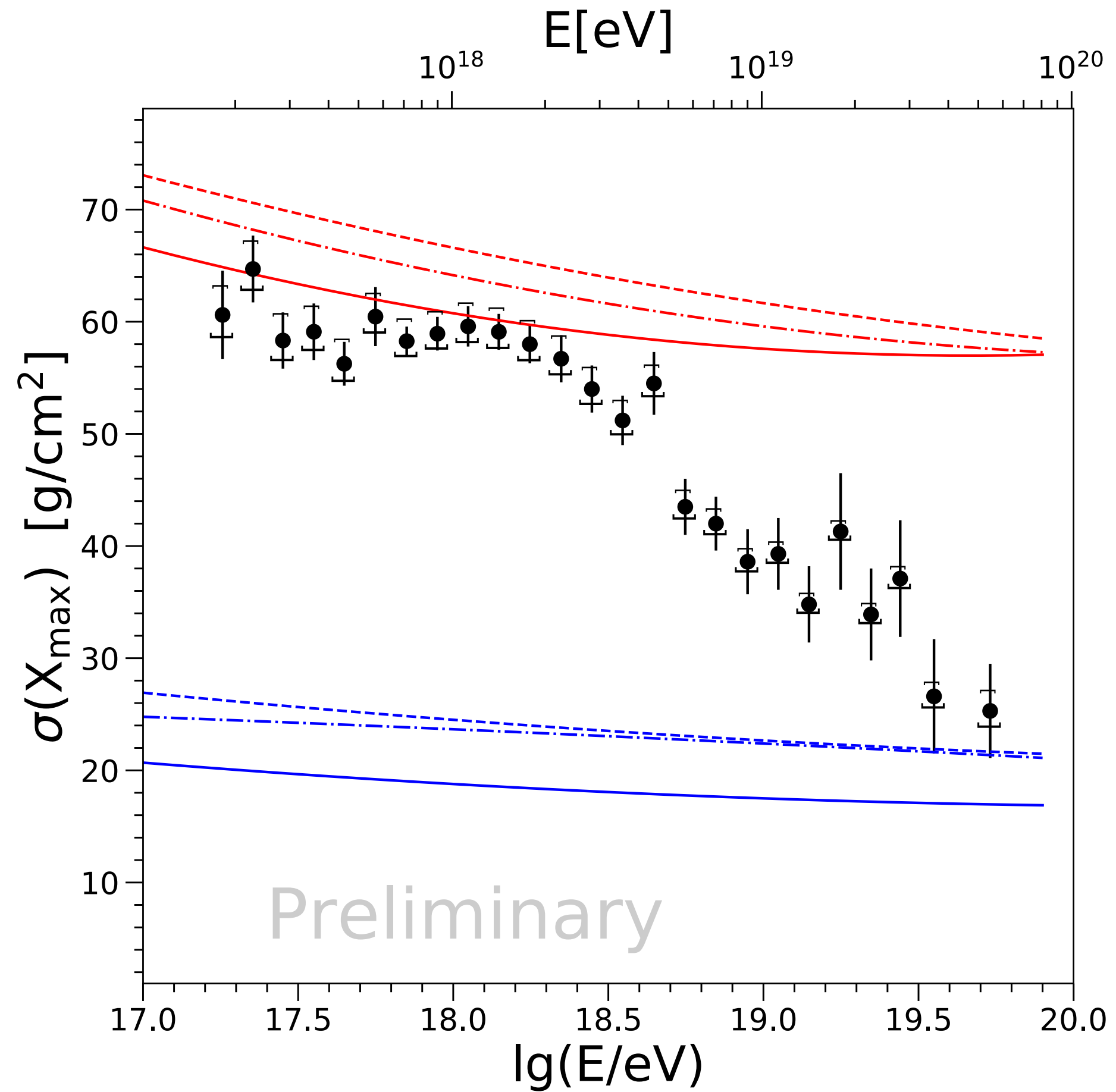
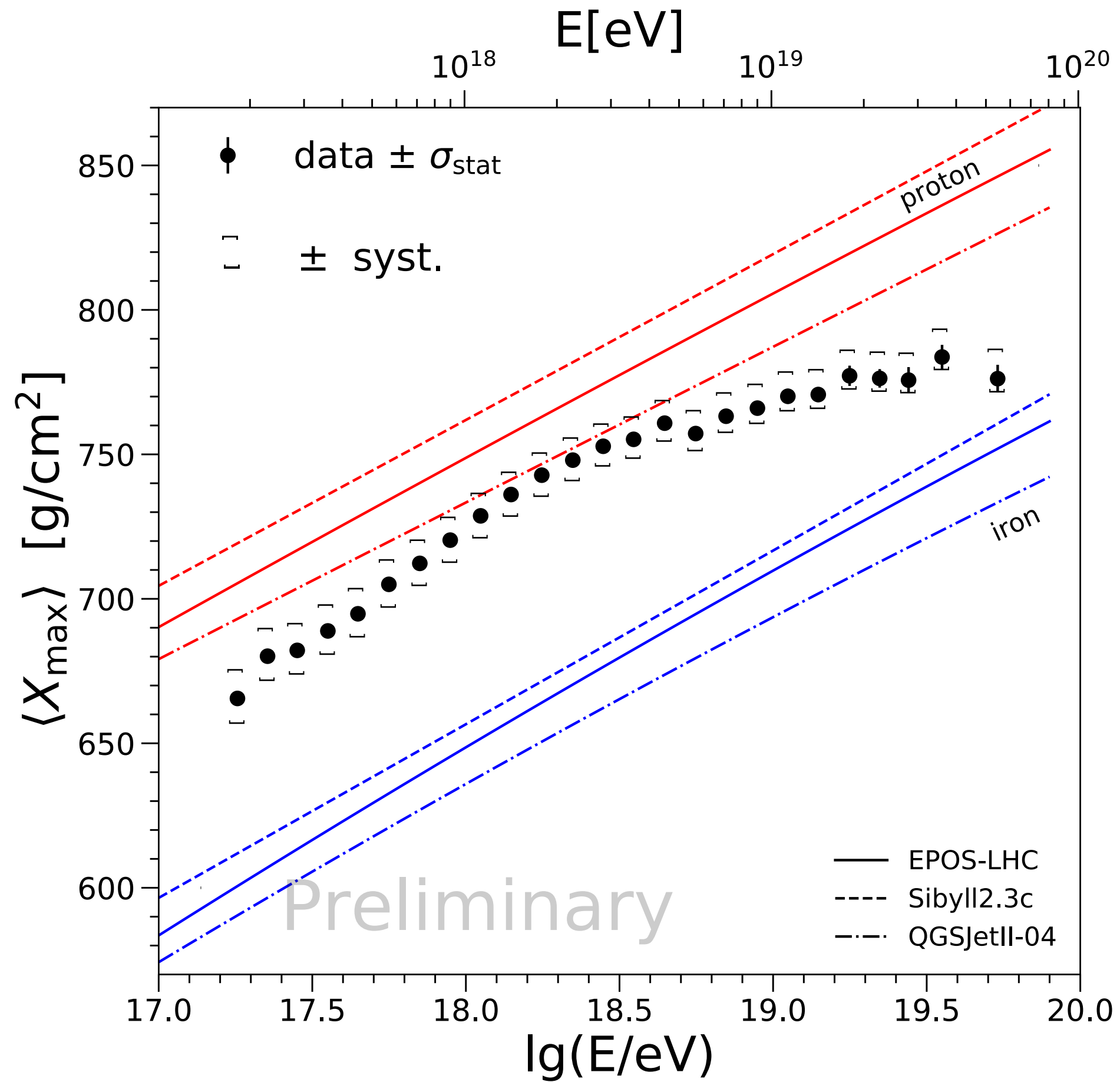
Number of muons

$$N_{\mu}(\text{Fe}) / N_{\mu}(p) \approx 1.4$$

Relative positions and orientation of elements are nearly model-independent.

[The Pierre Auger Observatory Upgrade - Preliminary Design Report](#)
[arXiv:1604.03637](#)

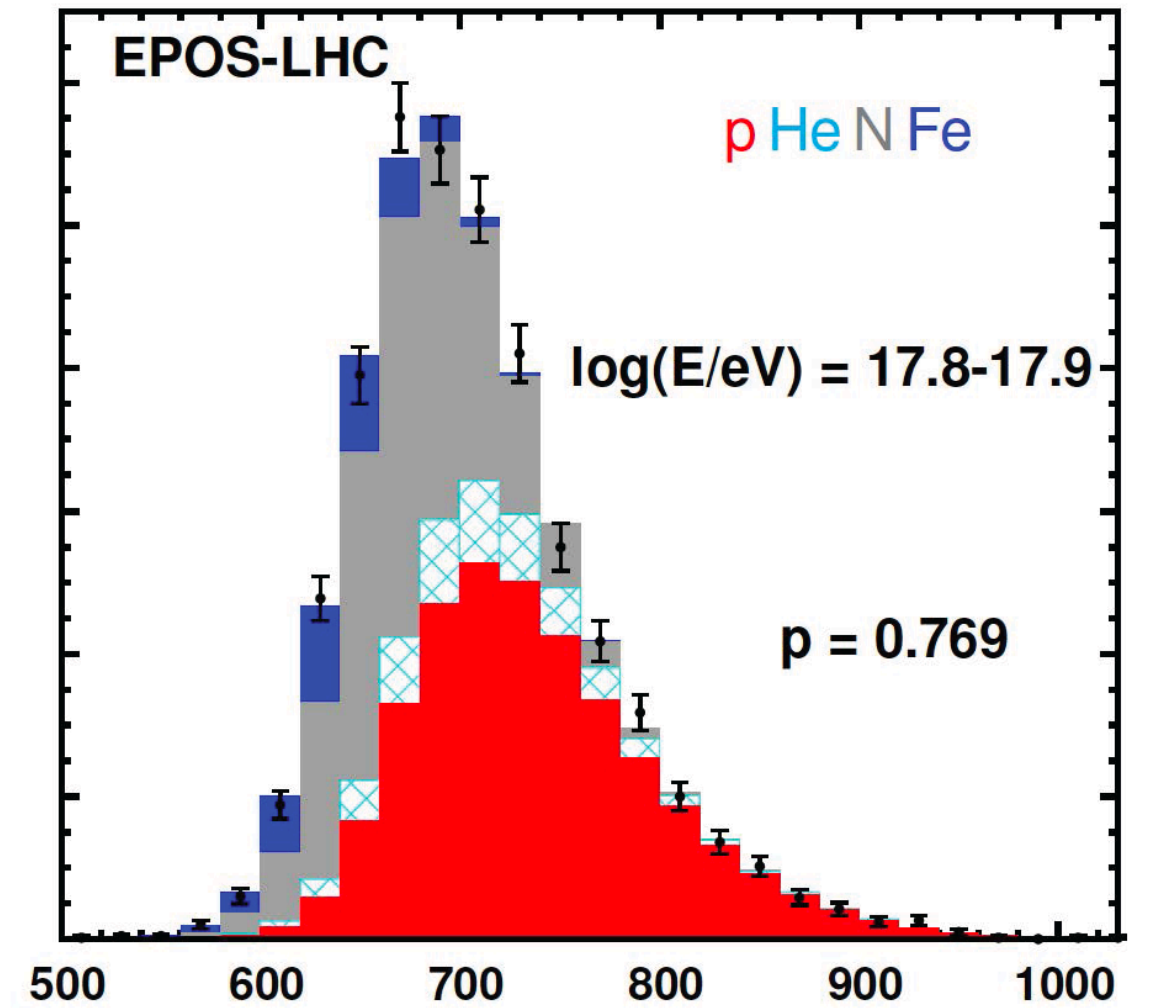
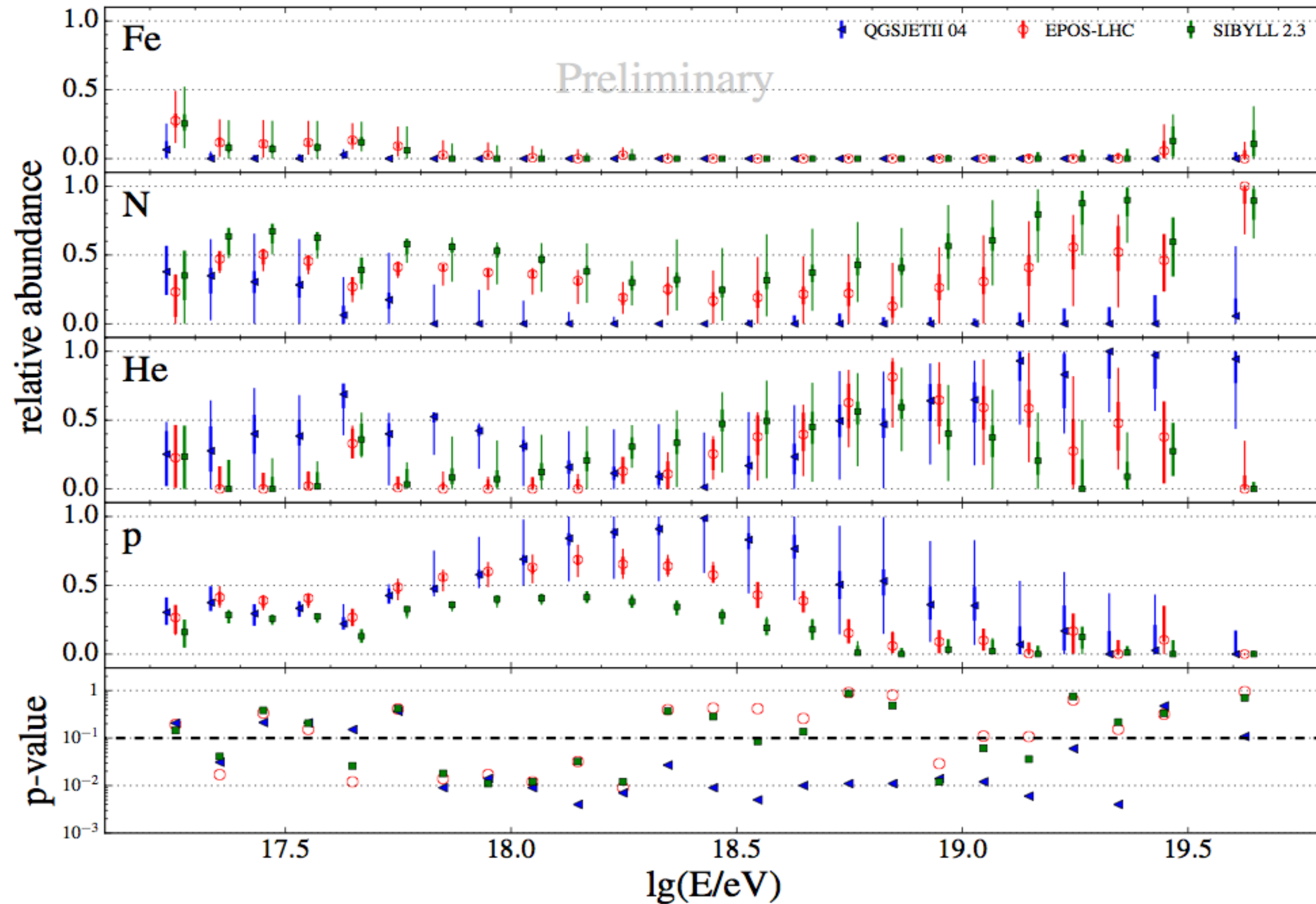
Energy evolution of Xmax



Yushkov for the P. Auger Collab. ICRC 2019

P. Auger Collab. JCAP 2013

Mixed composition – four-component analysis (FD)



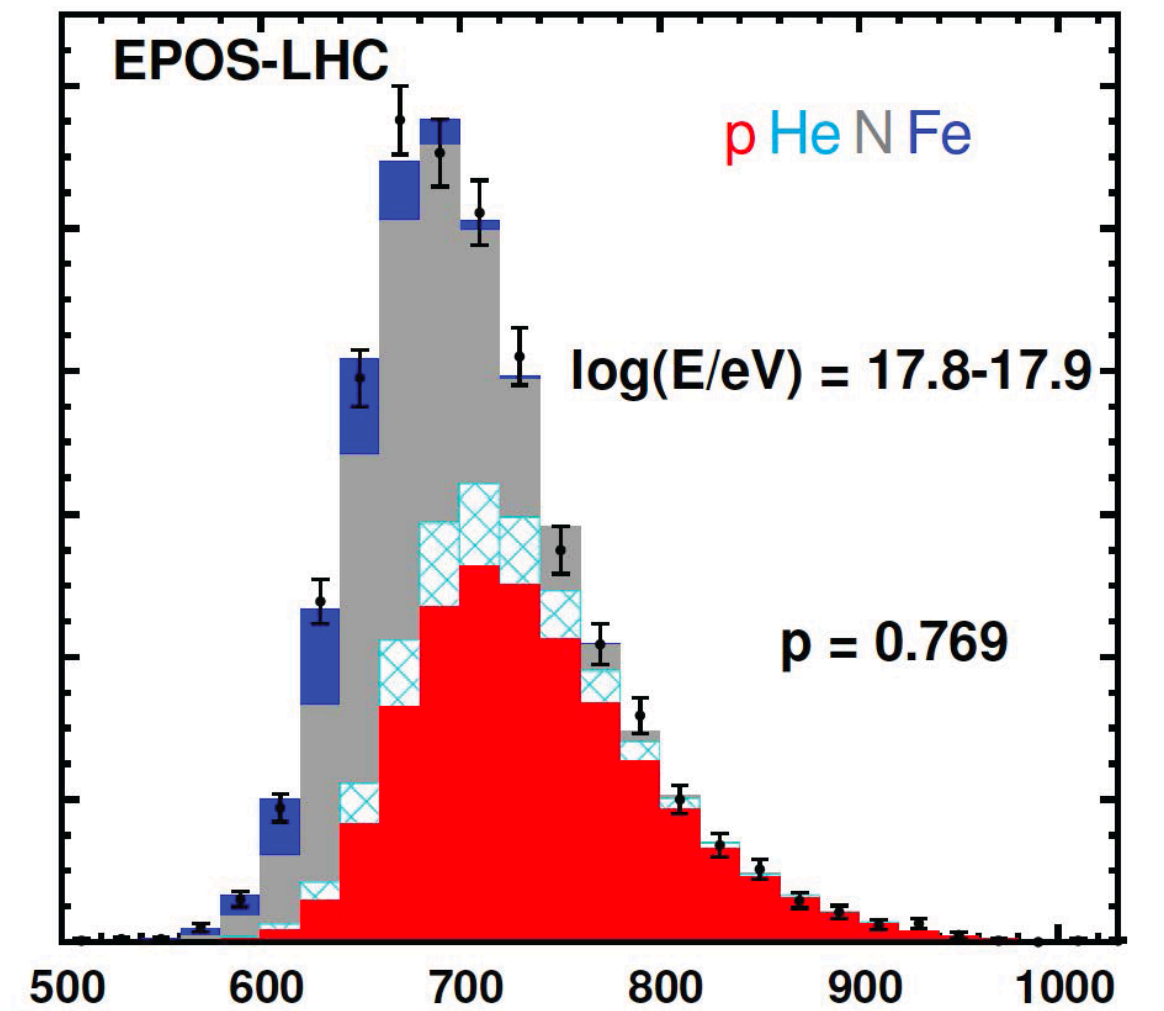
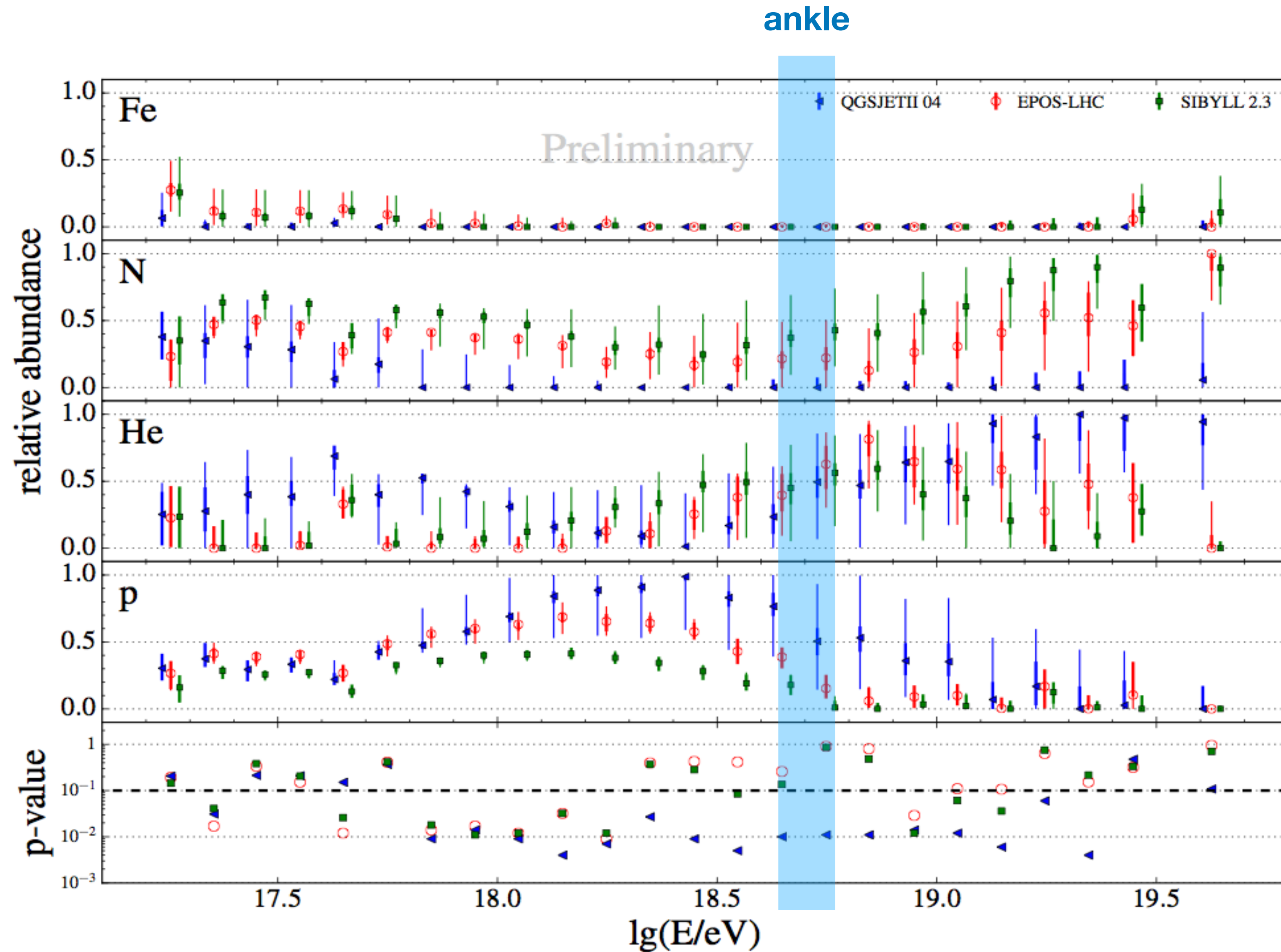
Large proton fraction below the ankle

Mixed composition, heavier at higher energy

Fit quality not always good

Flux suppression beyond $10^{19.5}$ eV

Mixed composition – four-component analysis (FD)



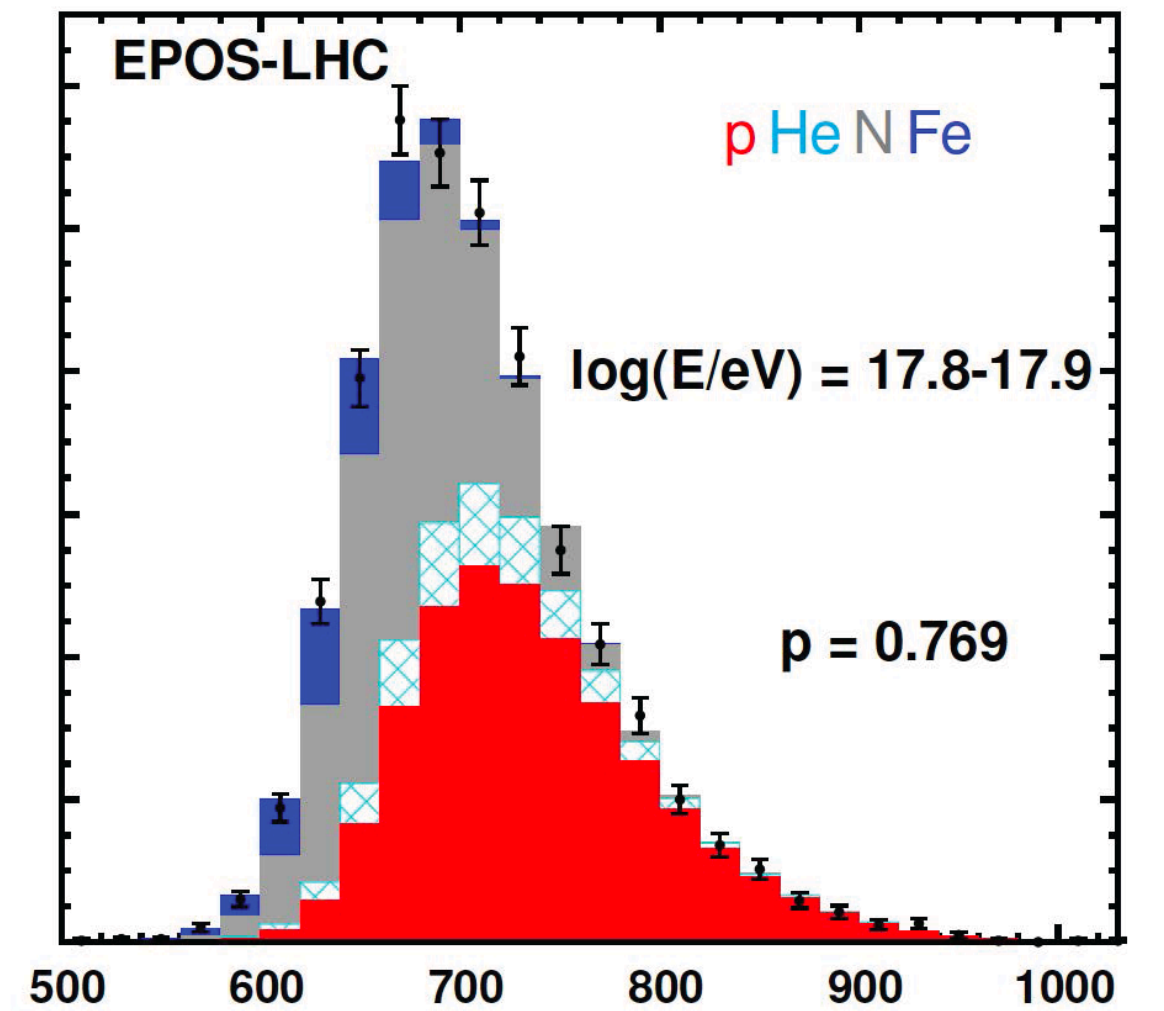
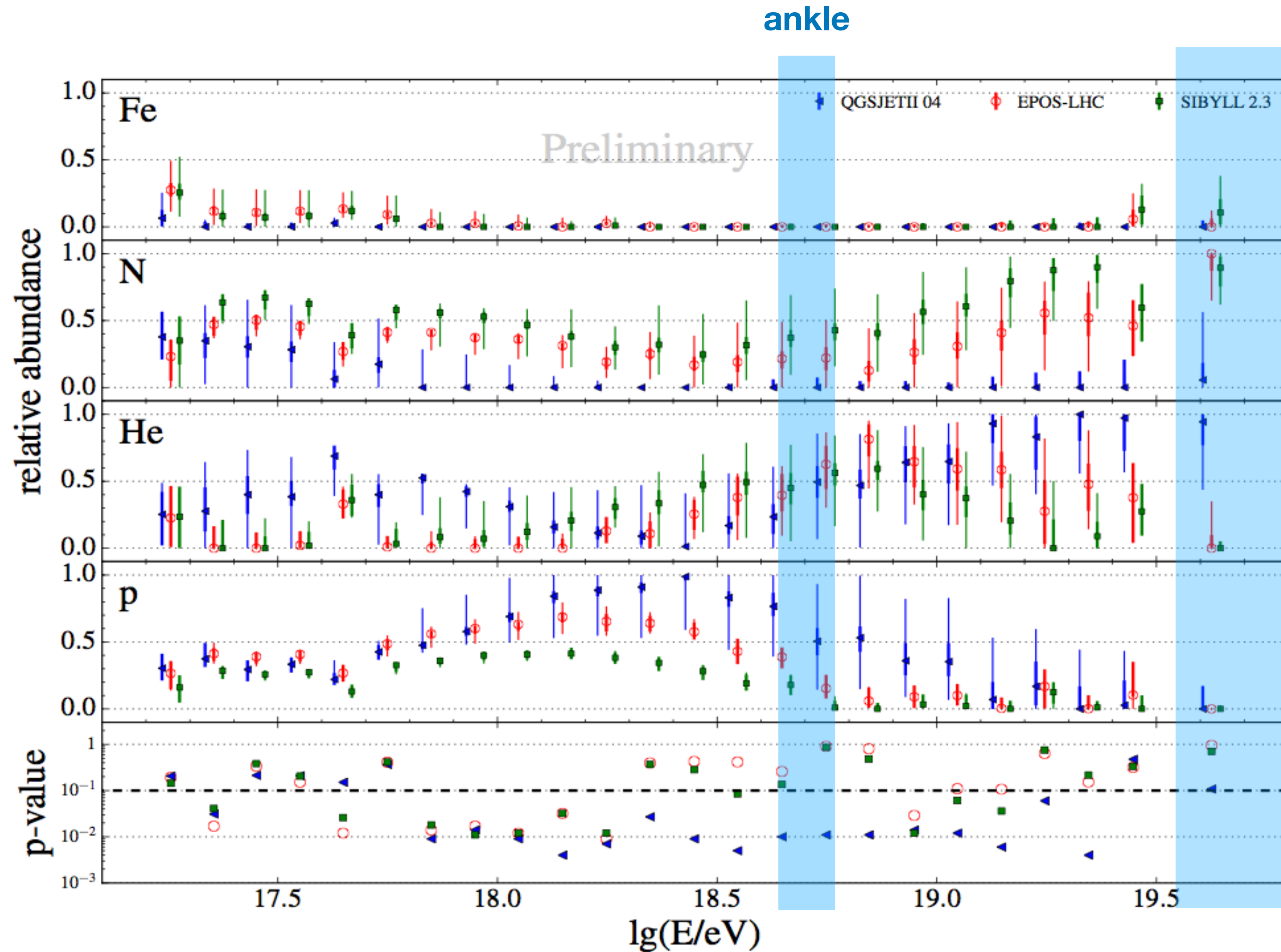
Large proton fraction below the ankle

Mixed composition, heavier at higher energy

Fit quality not always good

Flux suppression beyond $10^{19.5}$ eV

Mixed composition – four-component analysis (FD)



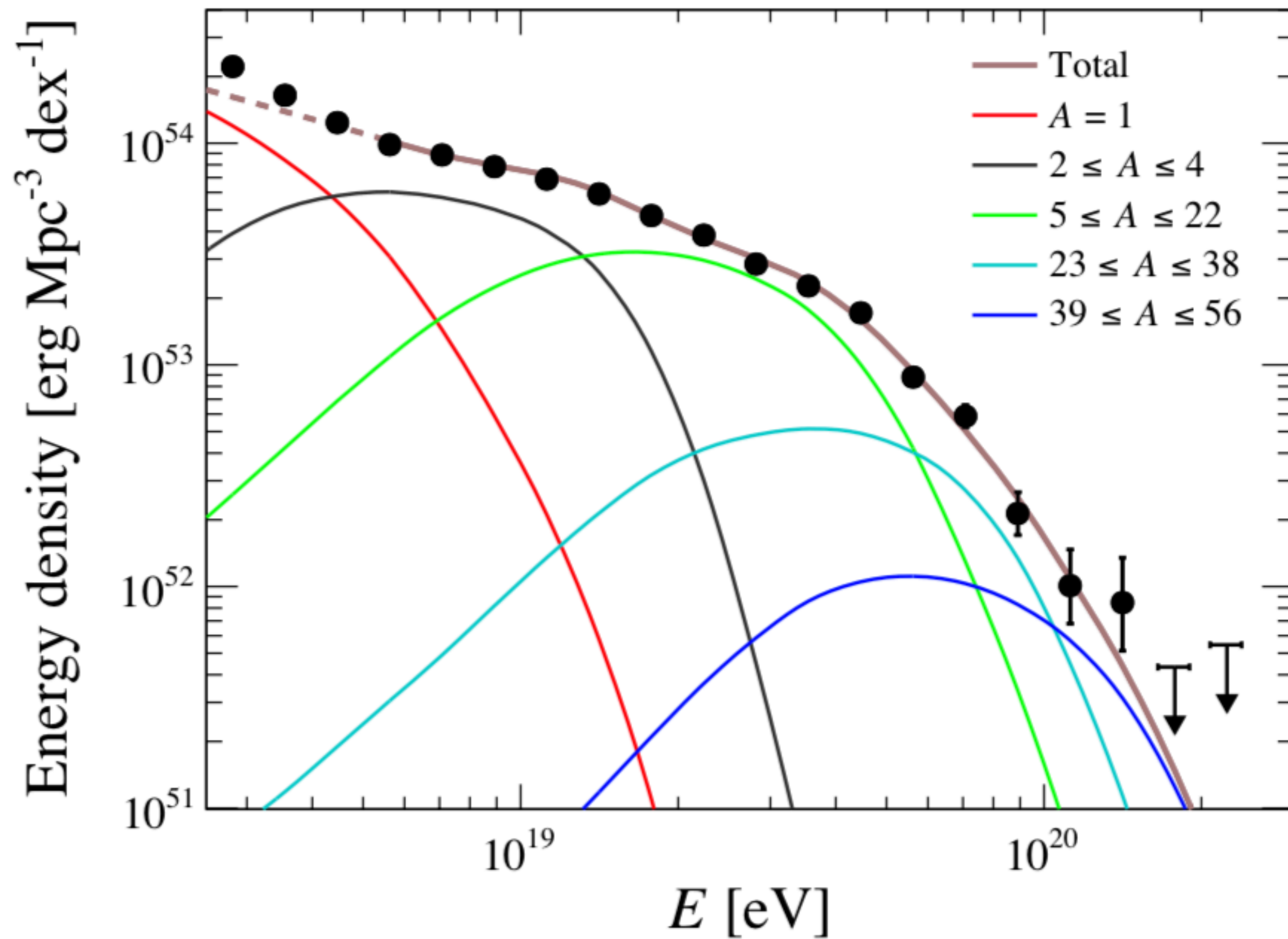
Large proton fraction below the ankle

Mixed composition, heavier at higher energy

Fit quality not always good

Flux suppression beyond $10^{19.5}$ eV

Combined fit of composition and spectrum



Astrophysical Interpretation

Identical sources homogeneously distributed in a comoving volume

Power-law spectrum with rigidity-dependent exponential cutoff

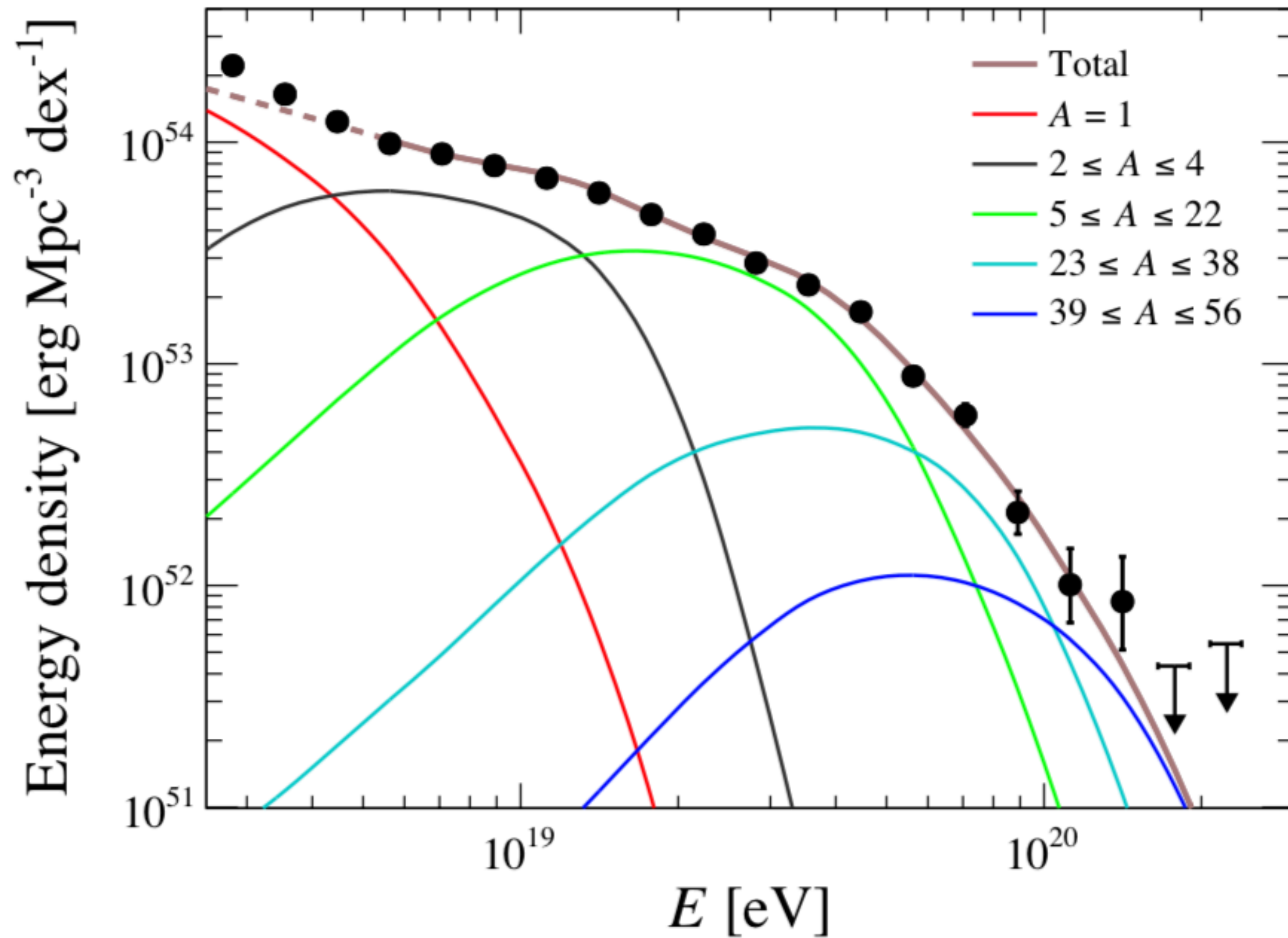
$$\frac{dN_{inj,i}}{dE} = \begin{cases} J_0 p_i \left(\frac{E}{E_0}\right)^{-\gamma}, & E/Z_i < R_{cut} \\ J_0 p_i \left(\frac{E}{E_0}\right)^{-\gamma} \exp\left(1 - \frac{E}{Z_i R_{cut}}\right), & E/Z_i > R_{cut} \end{cases}$$

Seven free parameters

(J_0 , γ , R_{cut} , p_H , p_{He} , p_{Ni} and p_{Si})

[P. Auger Collab., Phys. Rev. Lett, 2020](#)

Combined fit of composition and spectrum



Astrophysical Interpretation

Softening at 1.3×10^{19} eV:

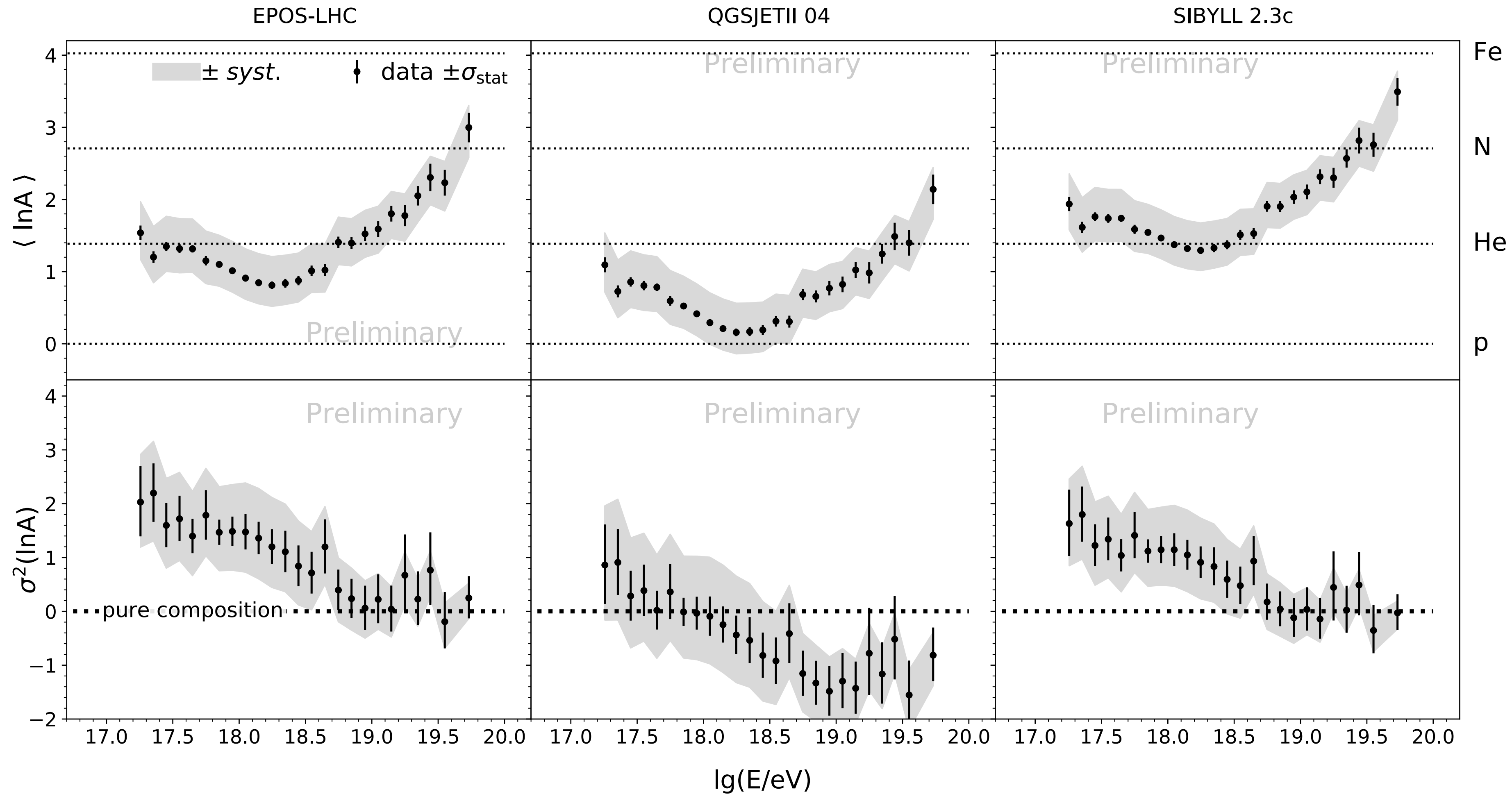
cut-off of helium spectrum with CNO
contribution with photodisintegration effect

Steepening above 5×10^{19} eV:

combination of Greisen-Zatsepin-Kuzmin
effect and cut-off at sources at $5Z \times 10^{19}$ eV

P. Auger Collab., Phys. Rev. Lett, 2020

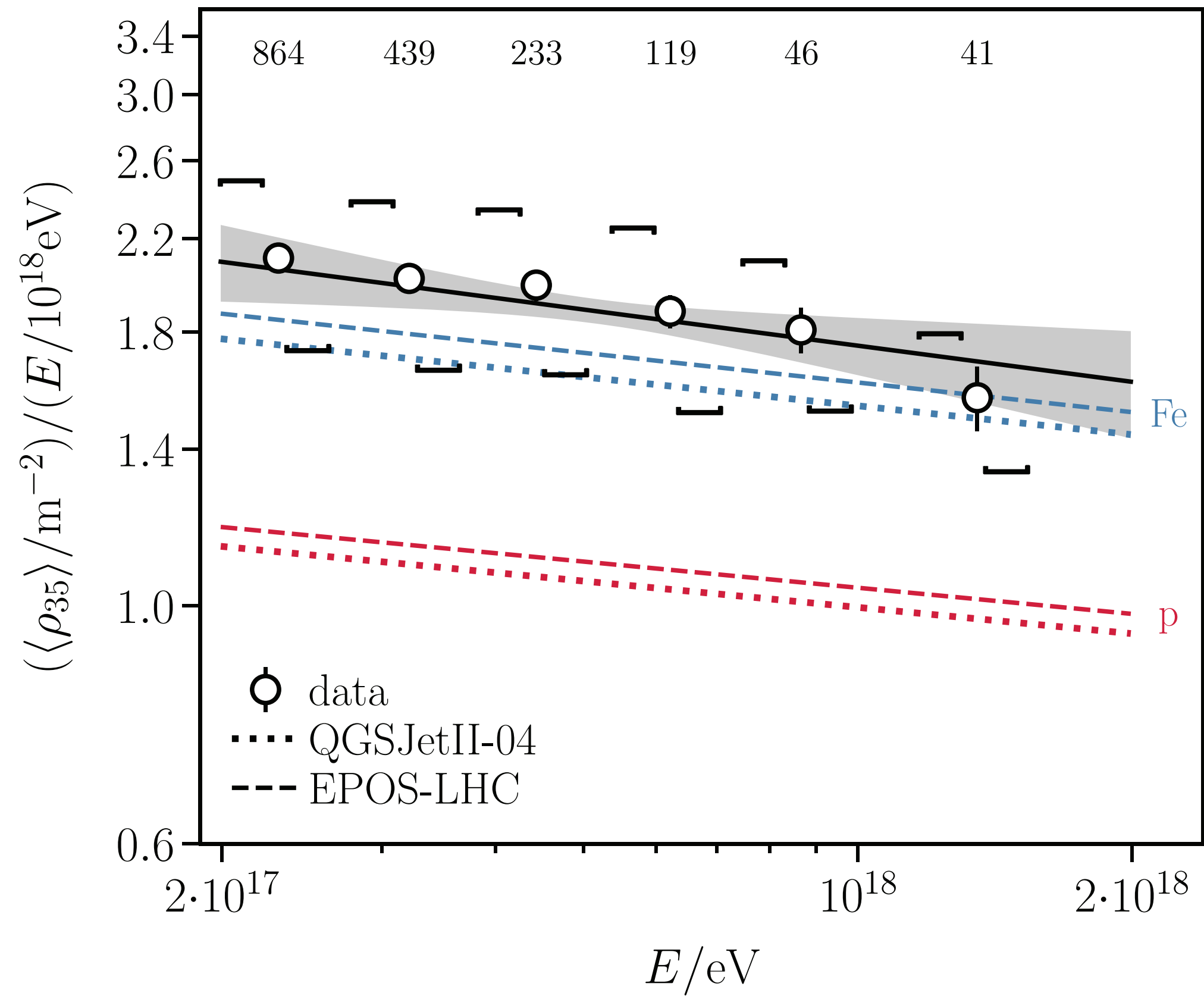
Mean logarithmic mass and spread of masses



Model-independent decrease of $\sigma(\ln A)$ until the ankle ($\sim 10^{18.7}$ eV)

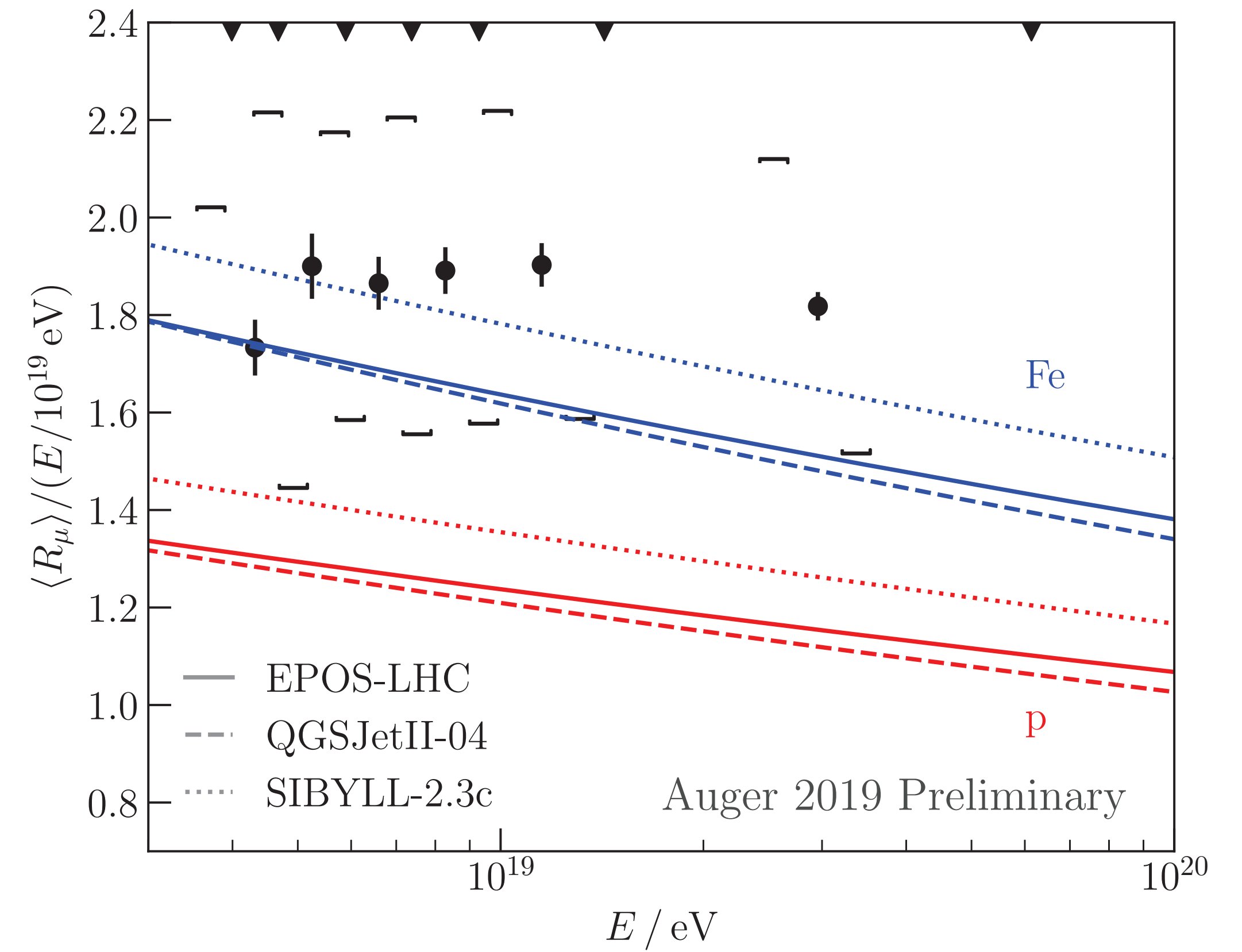
[Yushkov for the P. Auger Collab. ICRC 2019](#)

Deficit of muons in Monte Carlo models



Muon density with underground muon detectors

Data is above MC predictions for iron

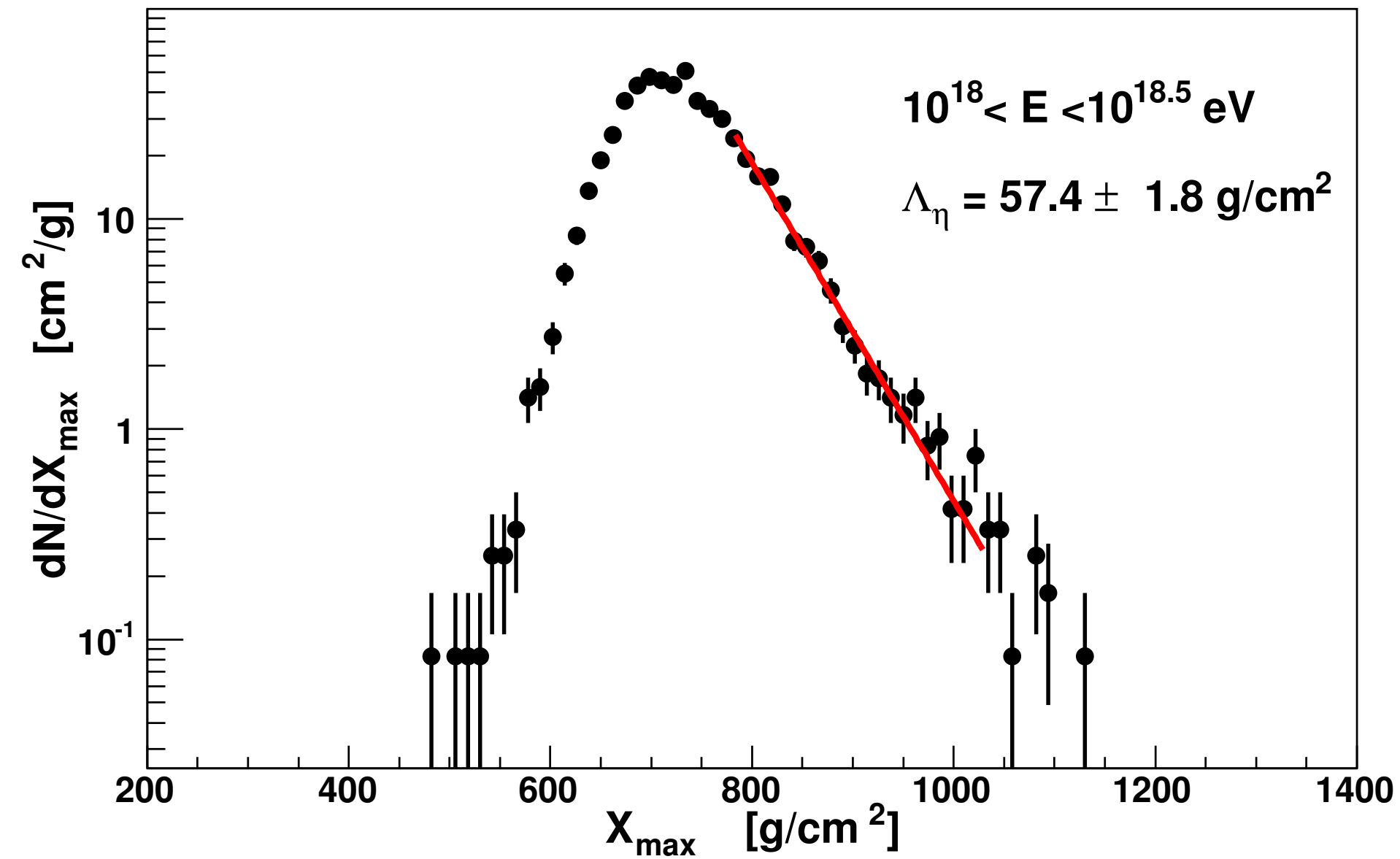


Muon density in inclined showers

[F. Sanchez for the P. Auger Collab., ICRC 2019](#)

[F. Riehn for the P. Auger Collab., ICRC 2019](#)

The p-air cross-section



Tail of the X_{max} distribution is sensitive to $\sigma_{p\text{-air}}^{inel}$

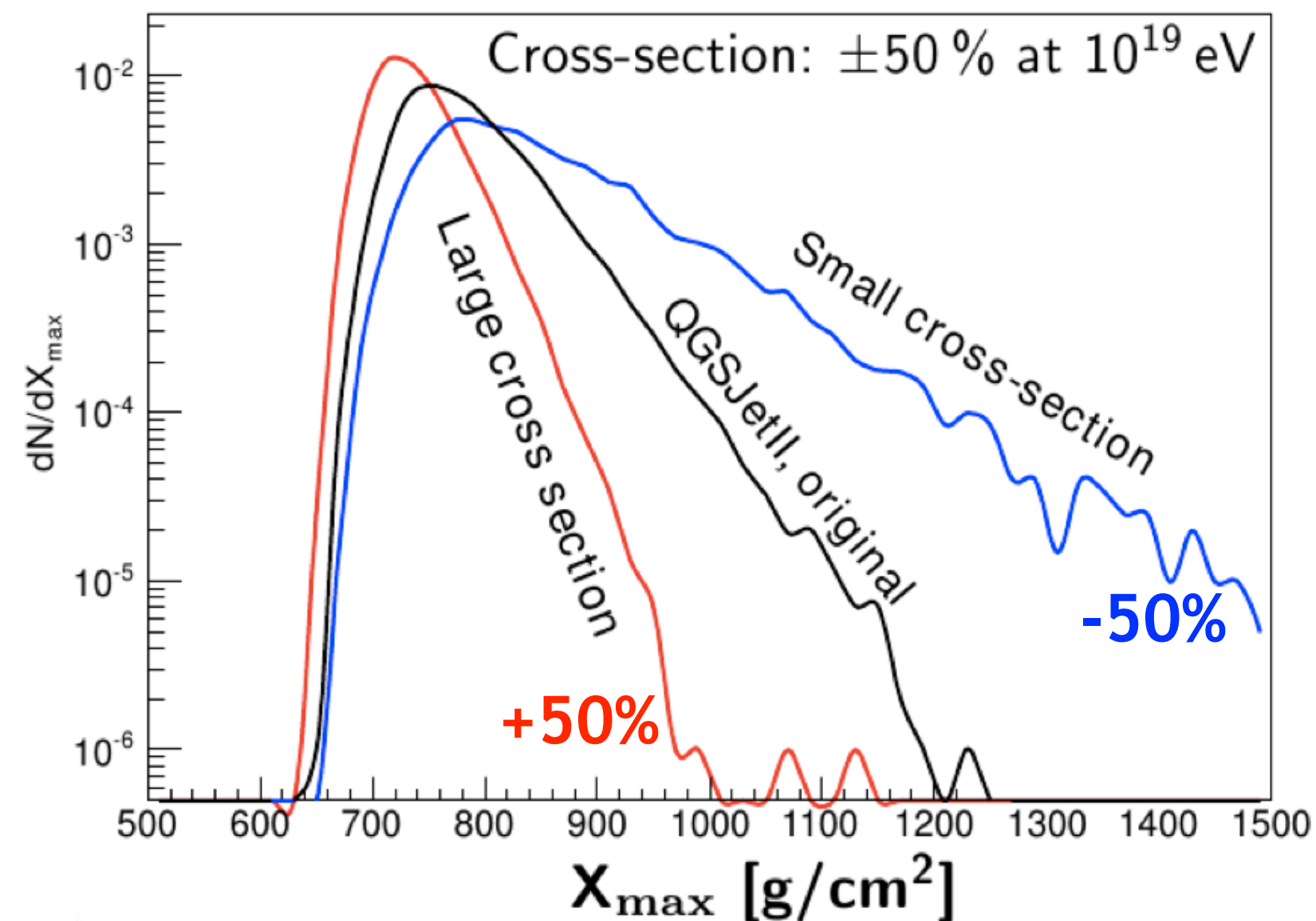
Two energy bins:

$10^{17.8} \text{ eV} < E < 10^{18} \text{ eV}$

$10^{18} \text{ eV} < E < 10^{18.5} \text{ eV}$

tail dominated by protons

$$\frac{dN}{dX_{max}} \sim \exp\left(-\frac{X_{max}}{\Lambda_\eta}\right)$$



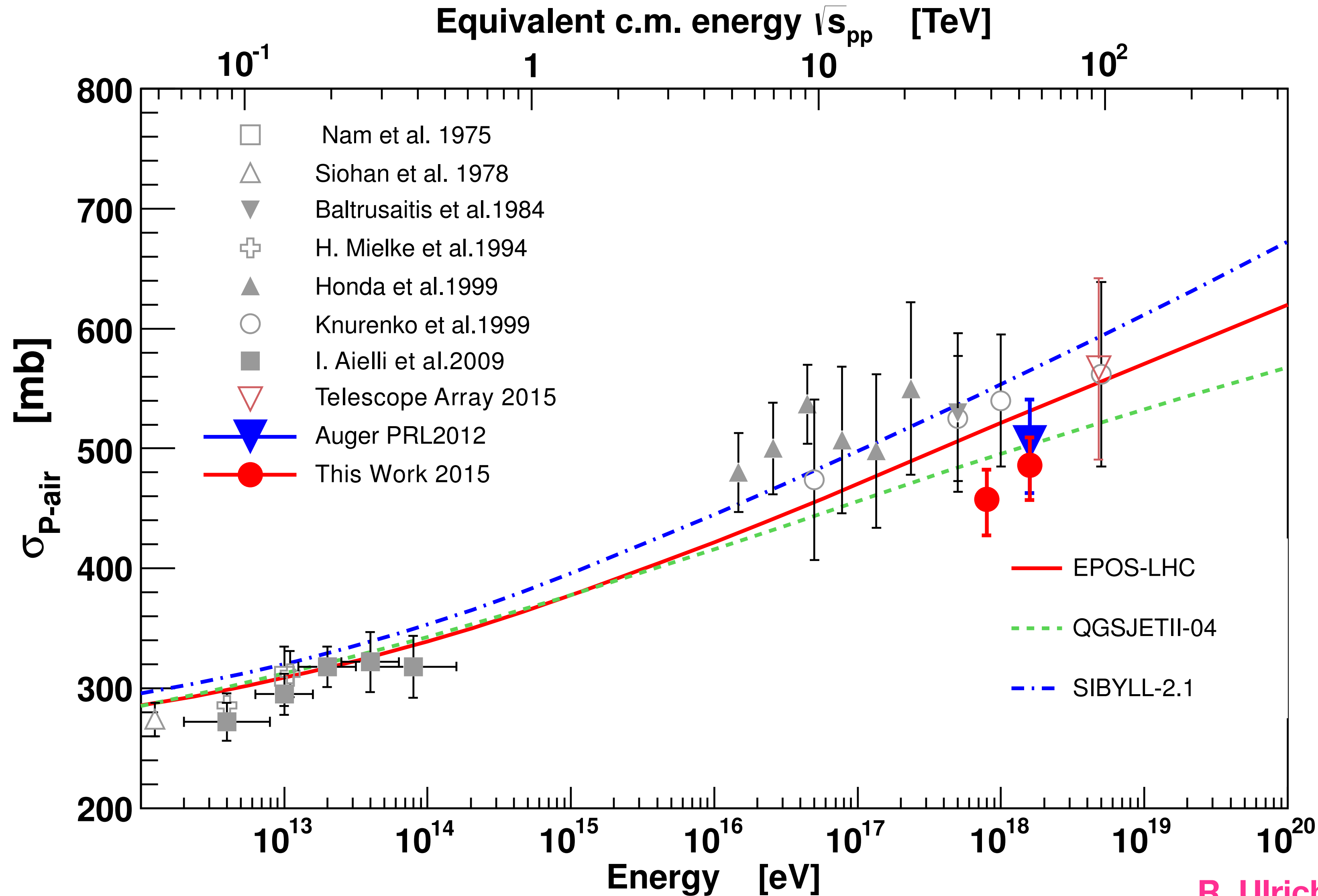
$\Lambda_\eta \rightarrow \sigma_{p \rightarrow \text{Air}}$

by tuning models to reproduce tail seen in data

[R. Ulrich, Auger Coll., ICRC 2015, ArXiv 1509.03732](#)

[P. Auger Coll., Phys. Rev. Let. 2012](#)

Cross section measurement



Intervals of energy used:

LAB $10^{17.8} - 10^{18}$ eV. $10^{18} - 10^{18.5}$ eV

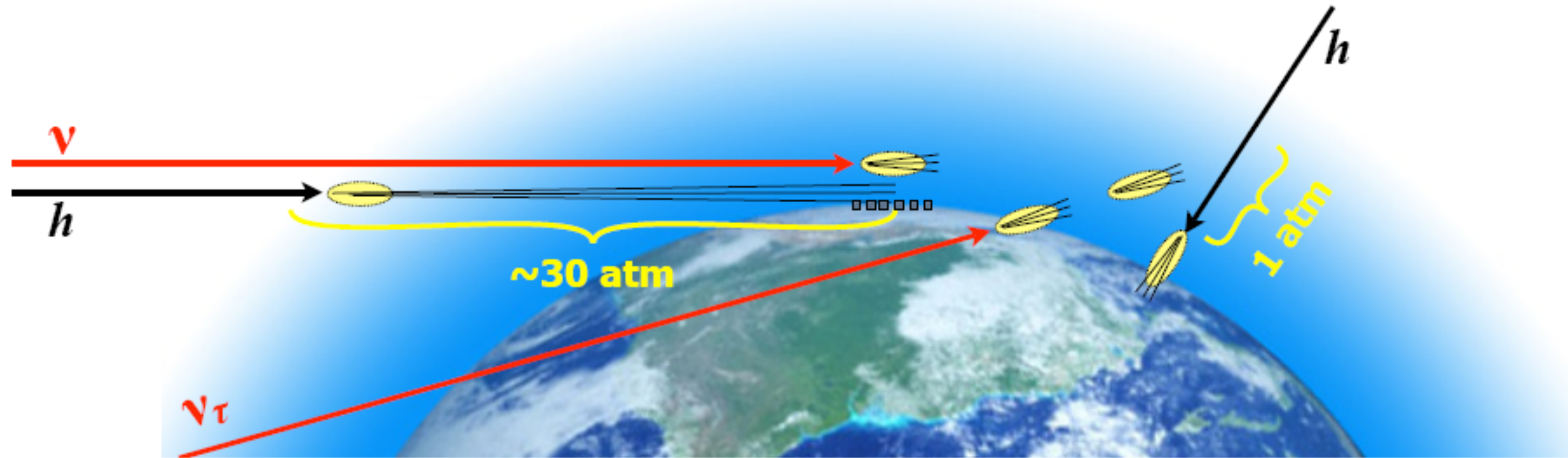
COM pp 38.7 TeV 55.5 TeV

- ★ Glauber theory used to convert p-air to inelastic pp cross section
- ★ Largest source of systematic uncertainty is helium fraction
- ★ Amounts to 6% bias in calculated values if fraction at 25%
- *
- ★ The data is consistent with a rising cross section with energy.

[R. Ulrich, Auger Coll., ICRC 2015, ArXiv 1509.03732](#)

[P. Auger Coll., Phys. Rev. Let. 2012](#)

Neutrino search: old and young showers



shower front

after 1 atm

after 3 atm

electromagn.
cascade

hard muons

+ 20% electrons
in equil. with muons

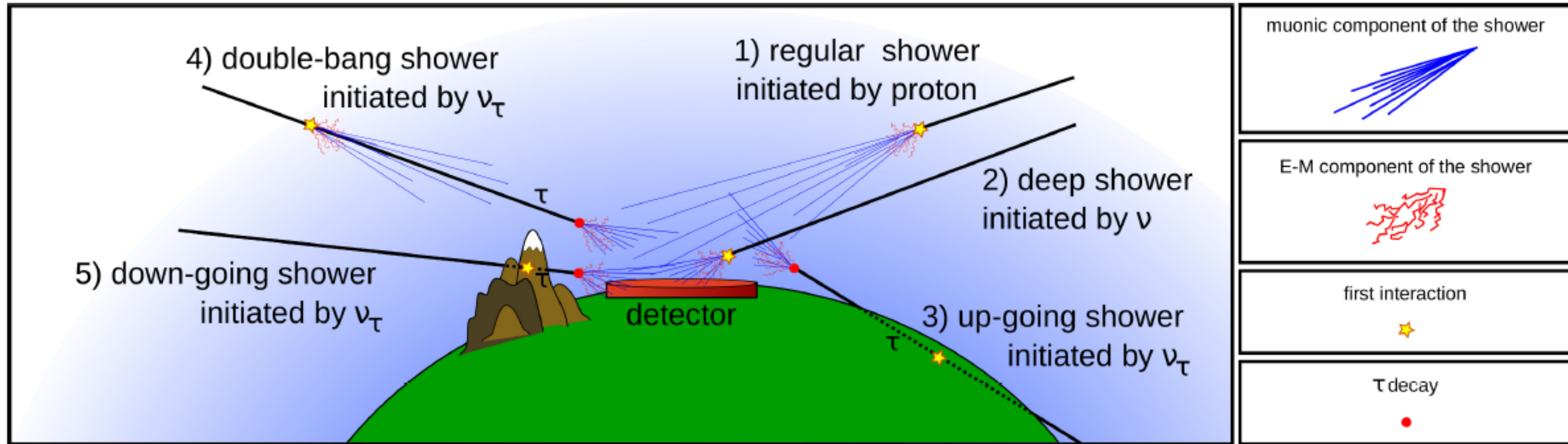
Young shower:

large curvature
large em. component
extended time structure

Old shower:

small curvature
small em. component
compressed time structure

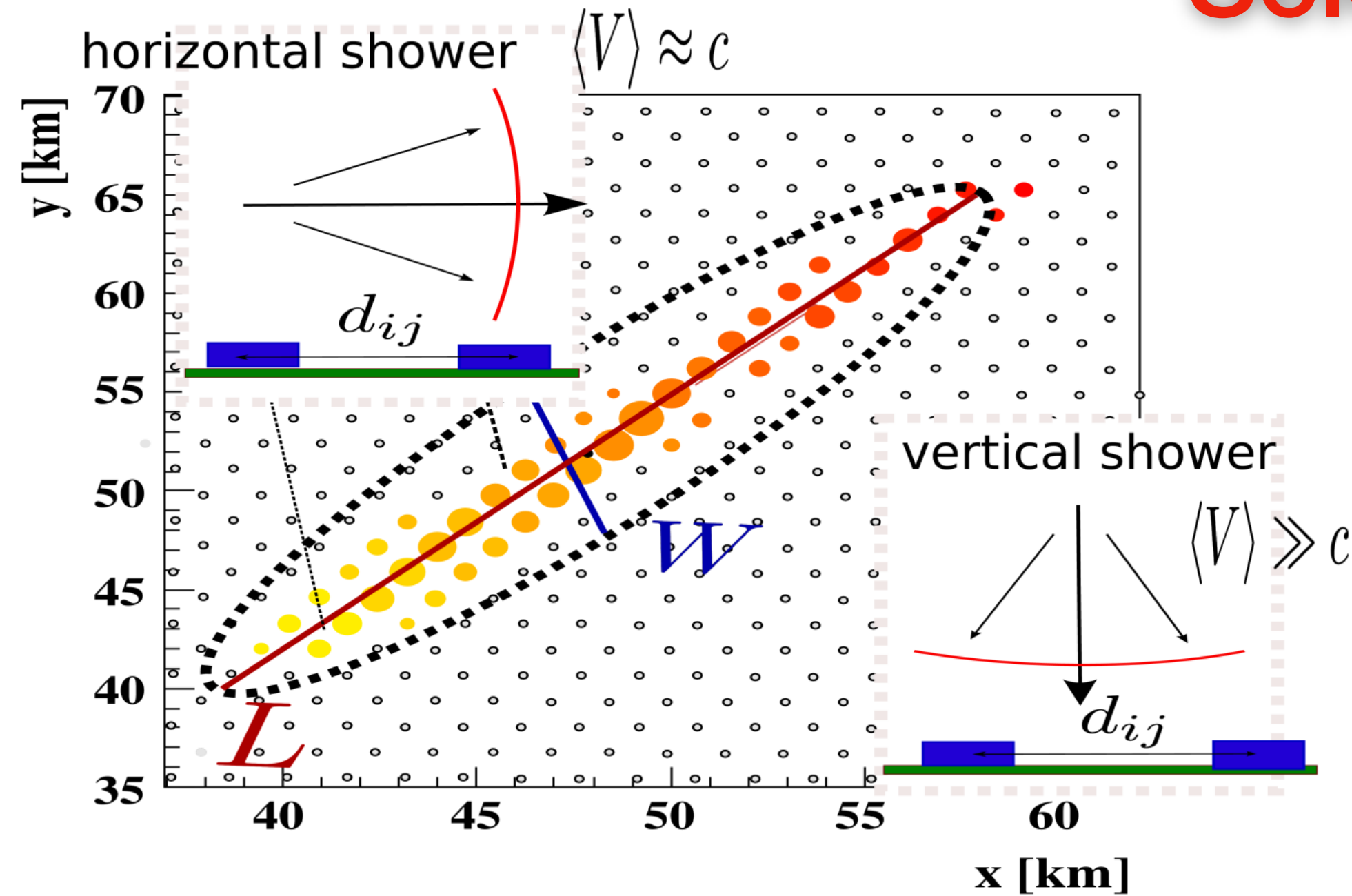
Sensitivity: all flavours and channels



Three selection criteria

- ★ Downward-going low zenith (2 and 4) DGL (60° - 75°)
- ★ Downward-going high zenith (2, 4 and 5) DGH (75° - 90°)
- ★ Earth-skimming (3) ES (90° - 95°)

Selecting ν in data



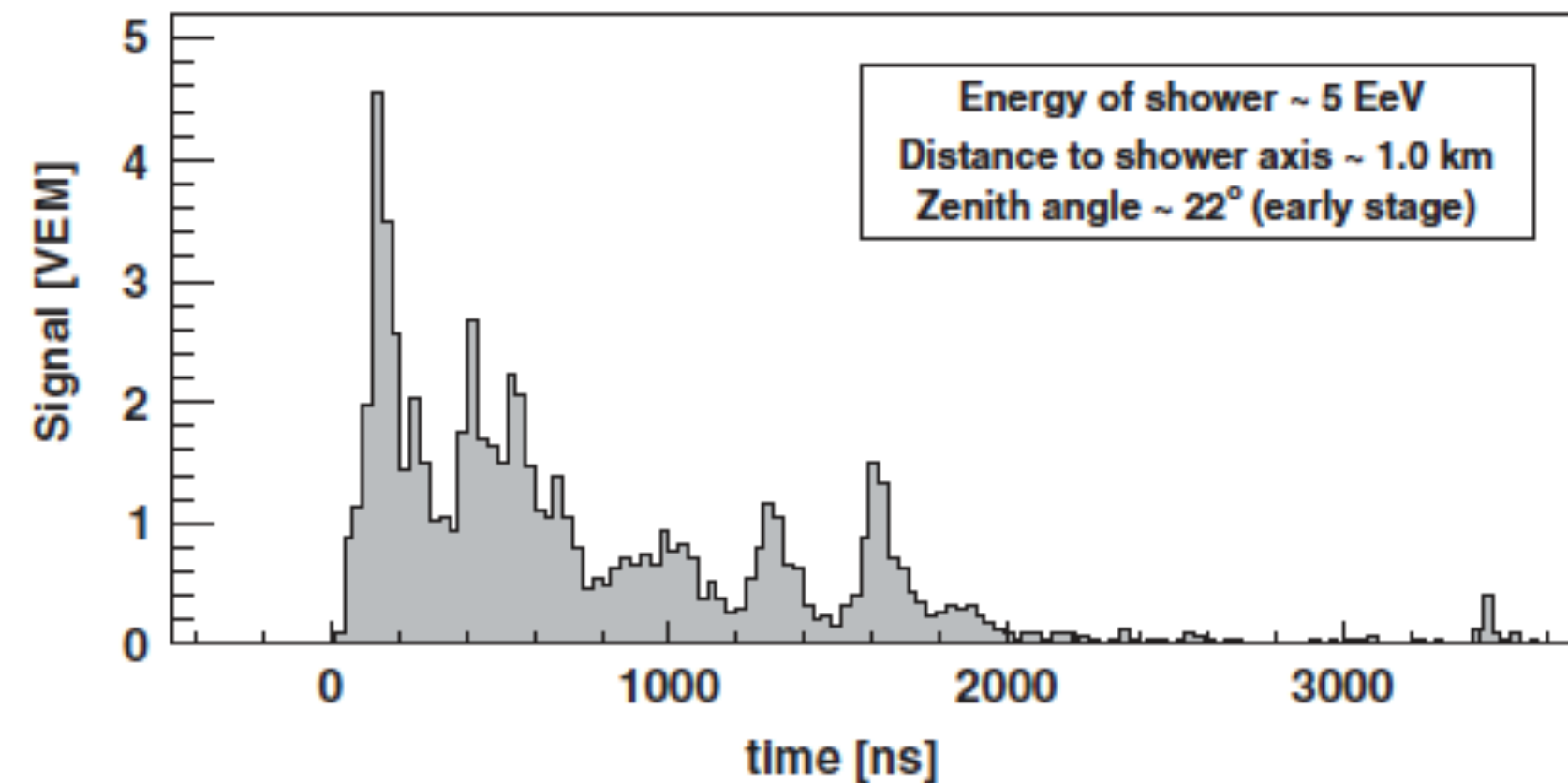
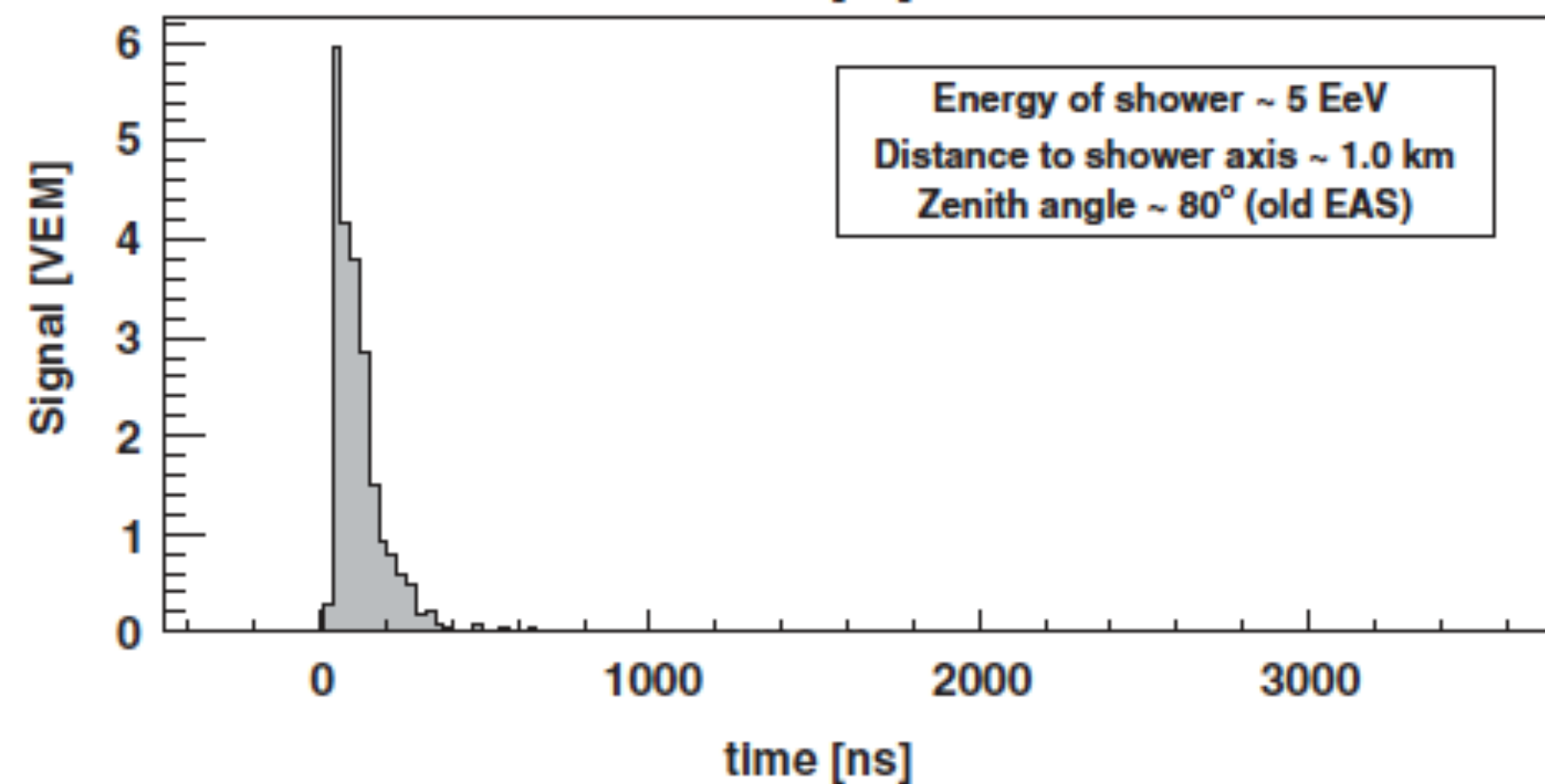
Inclined selection

- ★ Elongated pattern: $L > W$
- ★ Apparent speed signal $\approx c$
- ★ Angular reconstruction $60^\circ - 75^\circ$ & $75^\circ - 90^\circ$

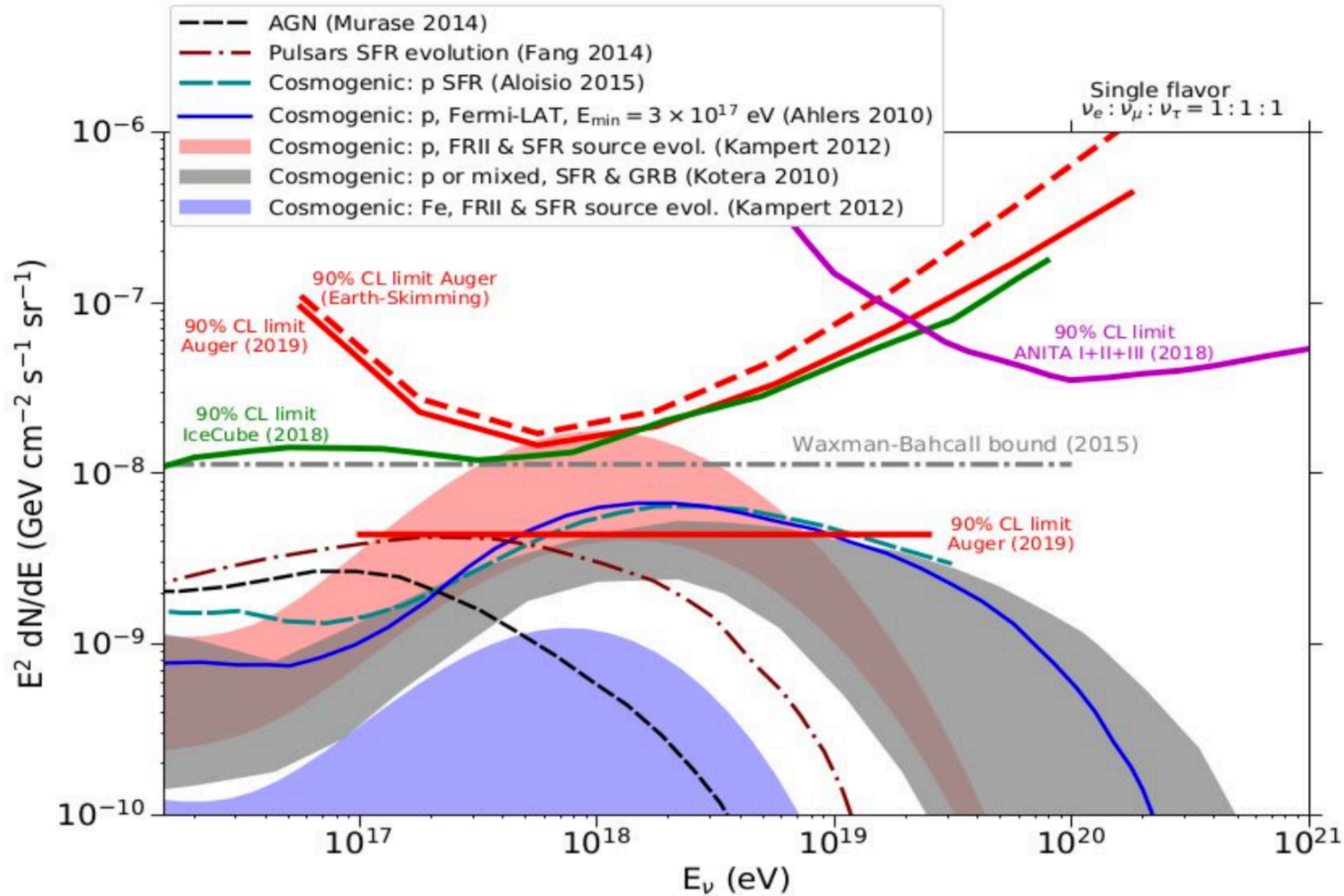
Select young showers

- ★ Broad EM component

<AOP> area over peak of digitized signal

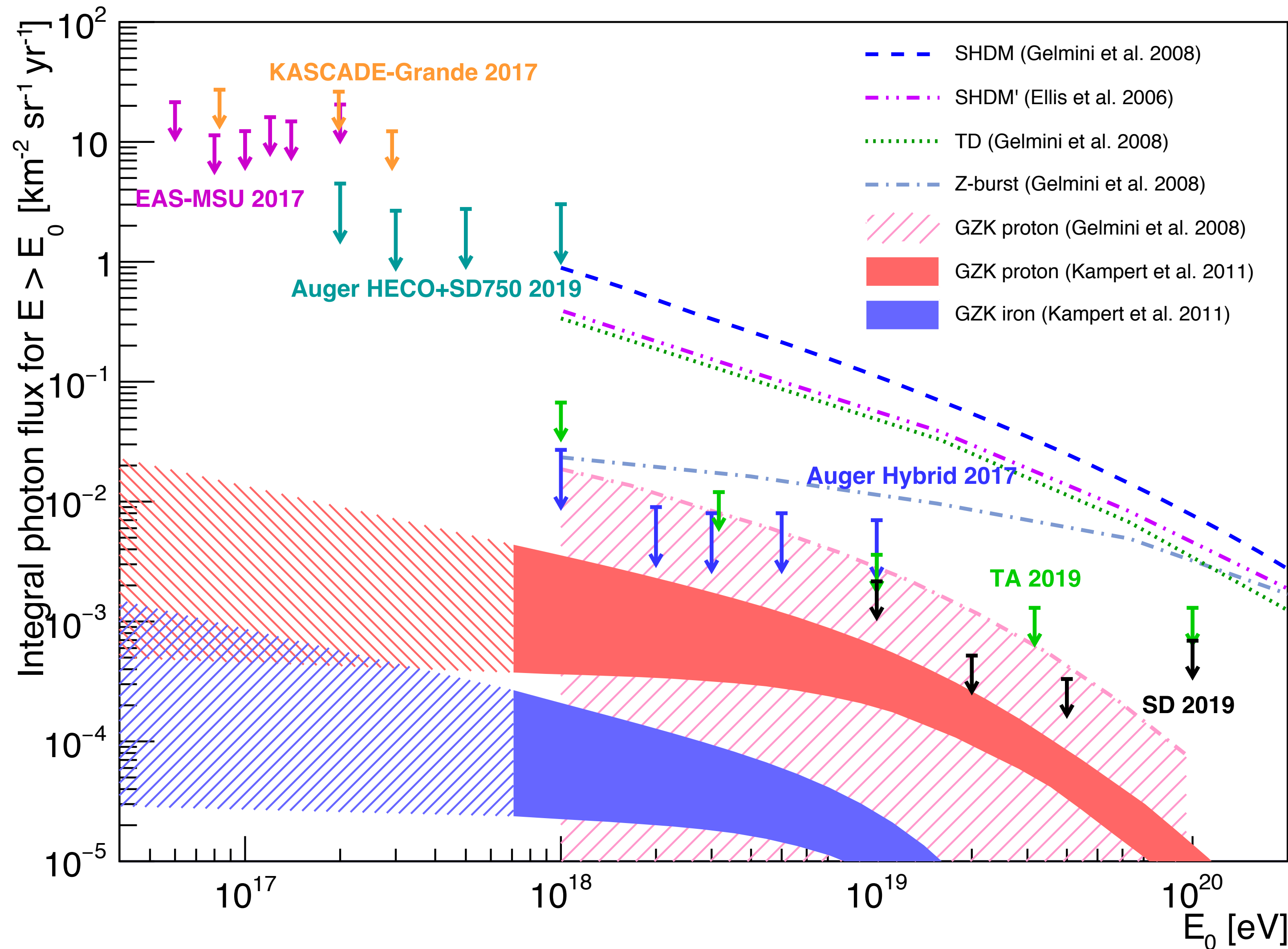


Neutrino limits



No candidates: **constraints** on proton-dominated astrophysical models and source evolution

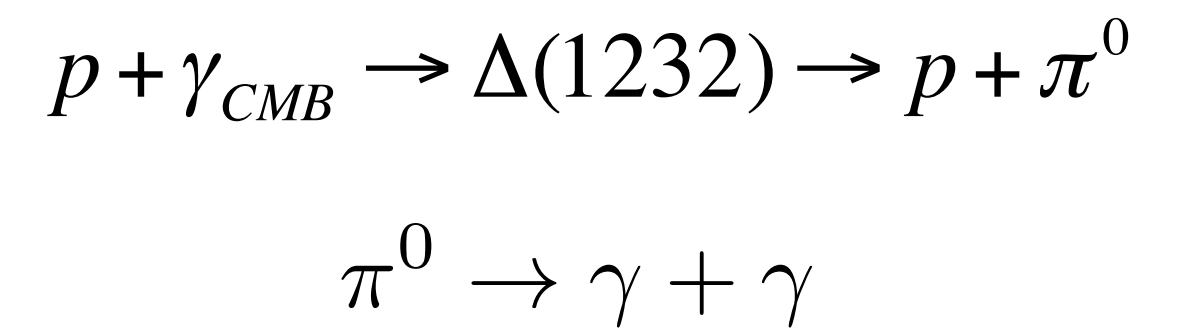
Photon limits



Photons characterized by:

- ★ deep Xmax in FD
- ★ small signal in SD

SHDM models barely compatible to hybrid and strongly constrained by SD limits

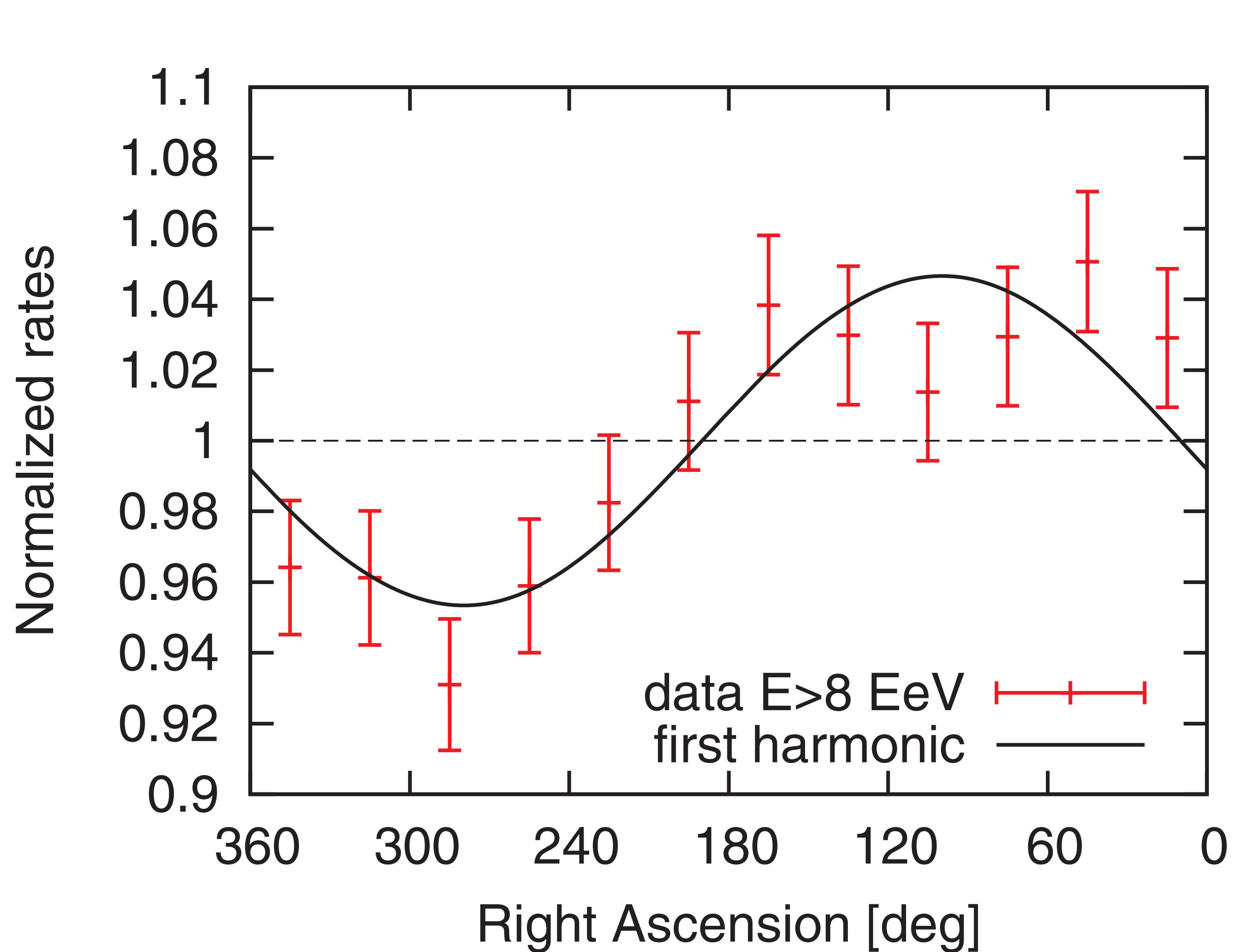


Significant increase of exposure needed to constrain recent GZK proton scenarios

J. Rautenberg for the P. Auger Collaboration ICRC 2019

P. Auger Collab. JCAP 2017

Modulation in flux of ultrahigh energy cosmic rays with $E \geq 8$ EeV



Exposure $> 92000 \text{ km}^2 \text{ sr yr}$
for events with $\theta < 80^\circ$

Rayleigh analysis in right ascension

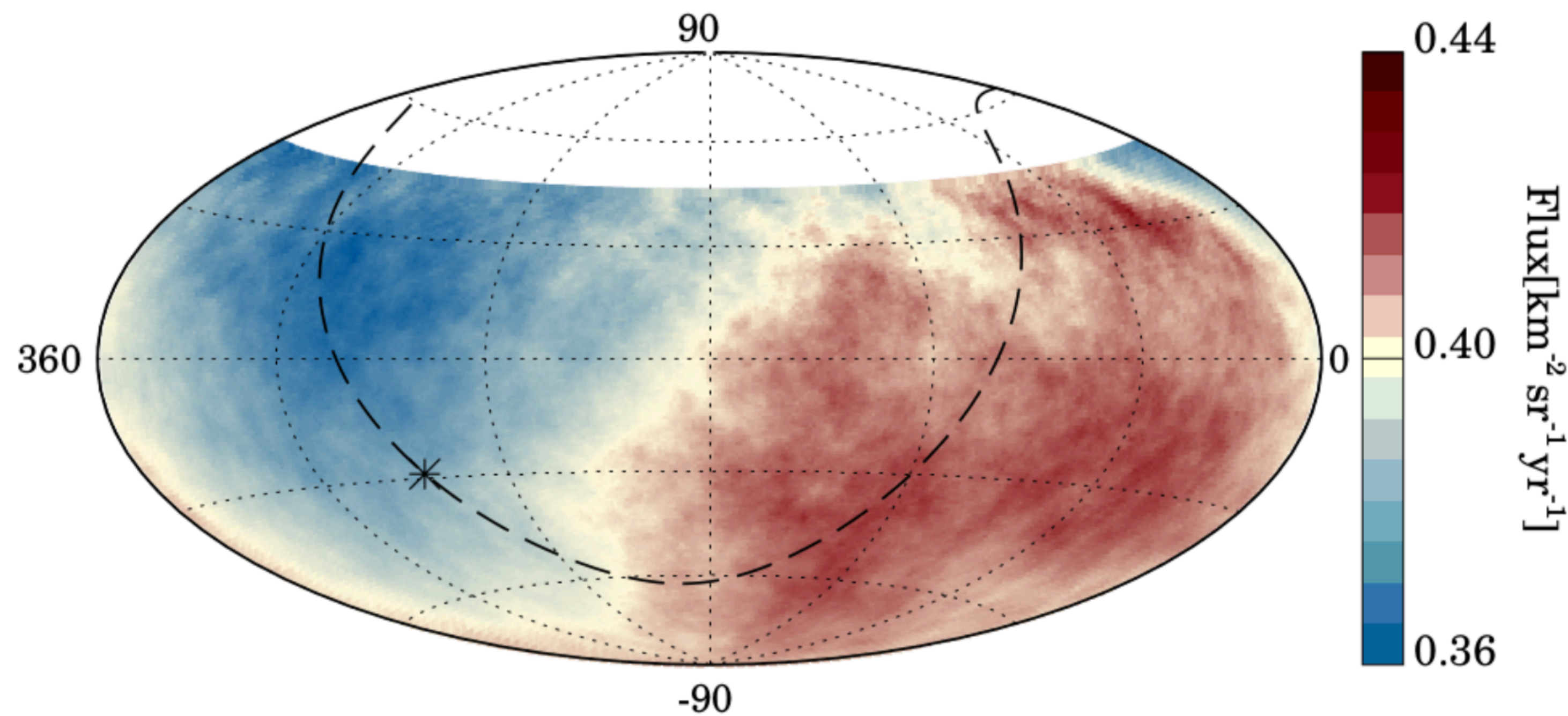
The effective aperture of the array is determined every minute.

P. Auger Collab., Science, 2017

E. Roulet for the P. Auger Collab., ICRC 2019



Large scale anisotropy



Phase in R.A. $\alpha_d = 98^\circ \pm 9^\circ$
is nearly opposite to the
Galactic center $\alpha_{GC} = -94^\circ$

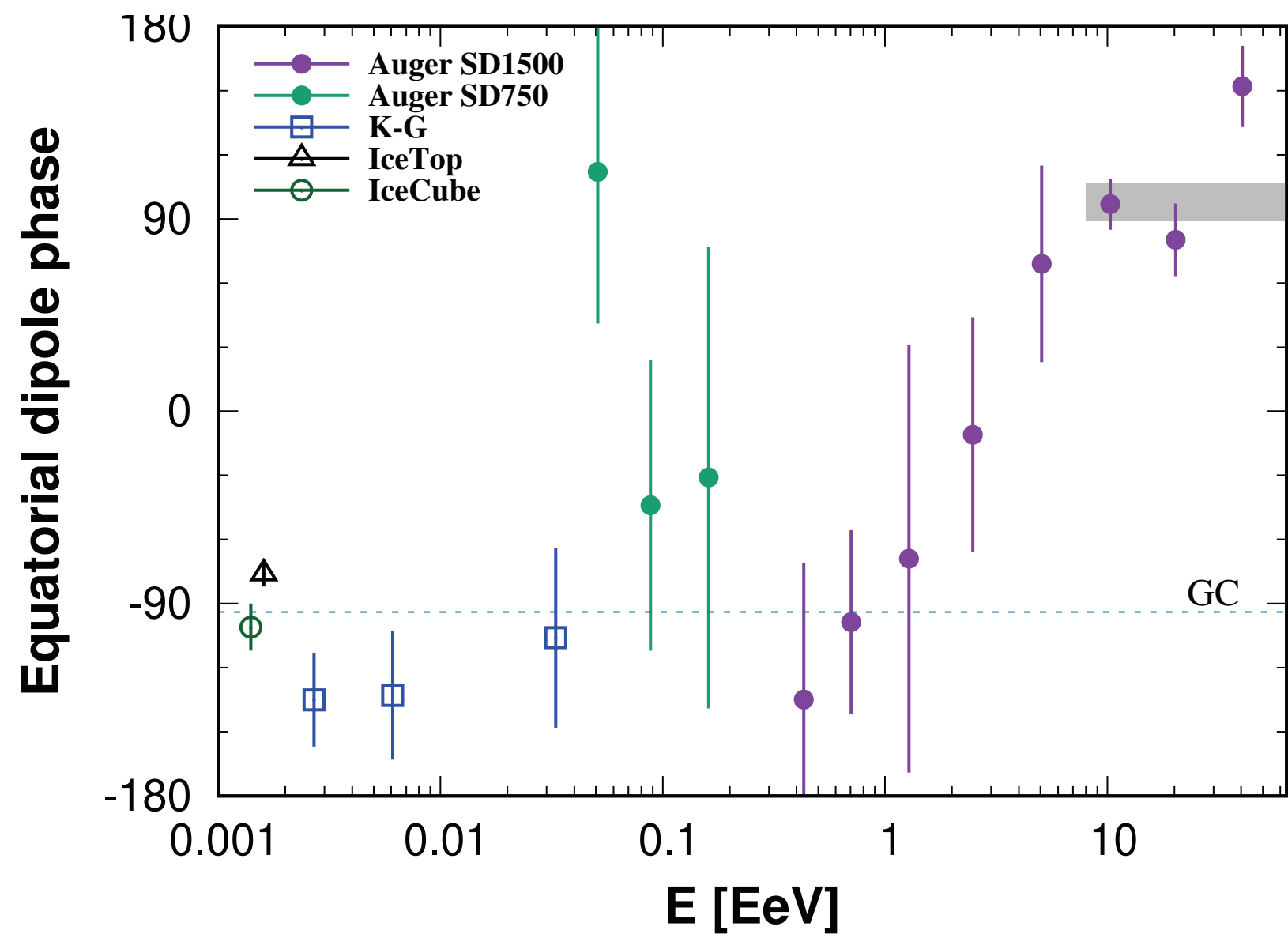
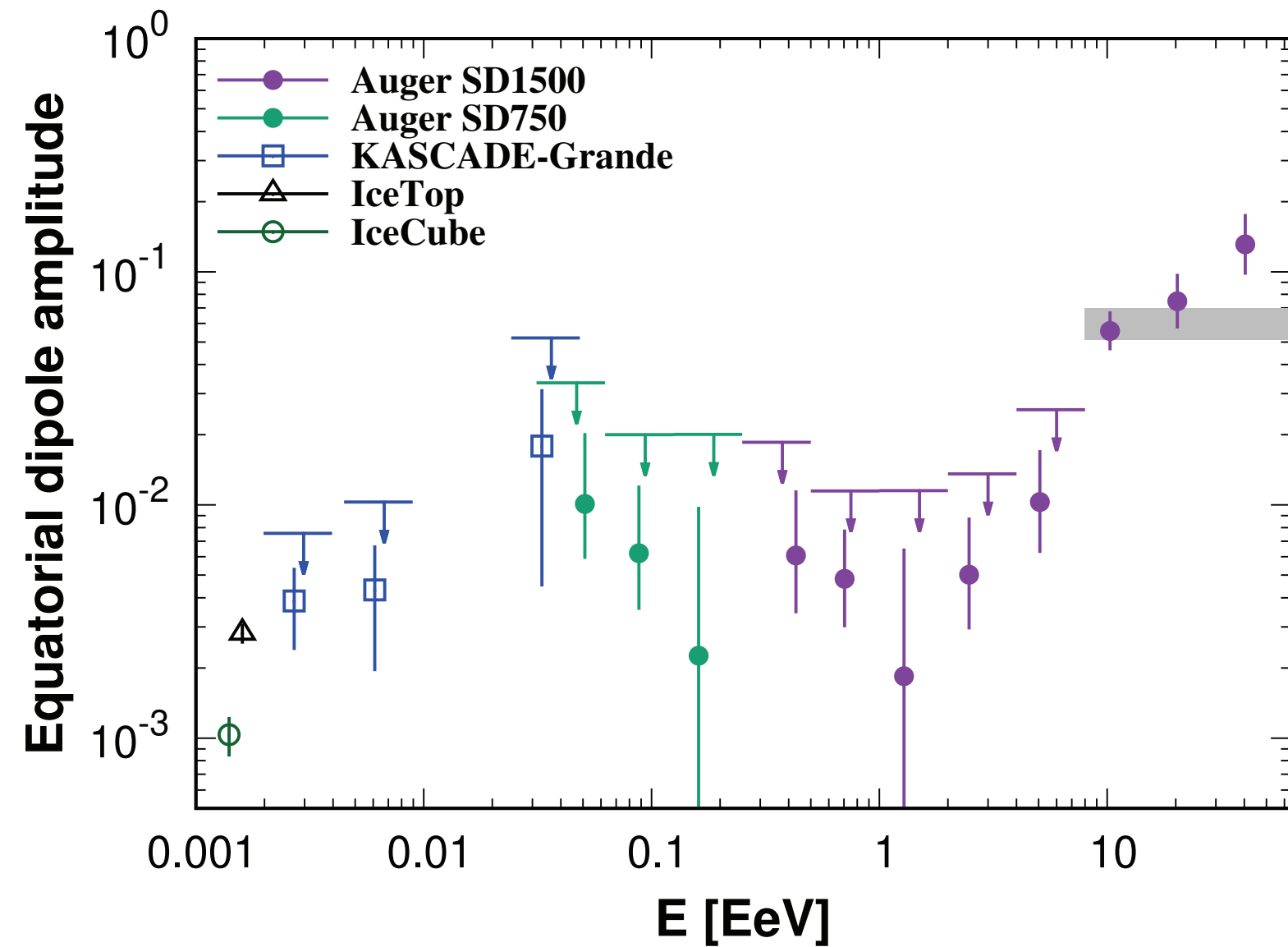
Magnitude and direction of
dipole support extragalactic
origin of UHECRs with $E > 4$ EeV

3-D Dipole above 8 EeV at $(\alpha, \delta) = (98^\circ, -25^\circ)$

$$d = (6.0_{-0.8}^{+1.2}) \% \quad \text{at } 6\sigma \text{ from isotropy}$$

E. Roulet for the P. Auger Collab., ICRC 2019

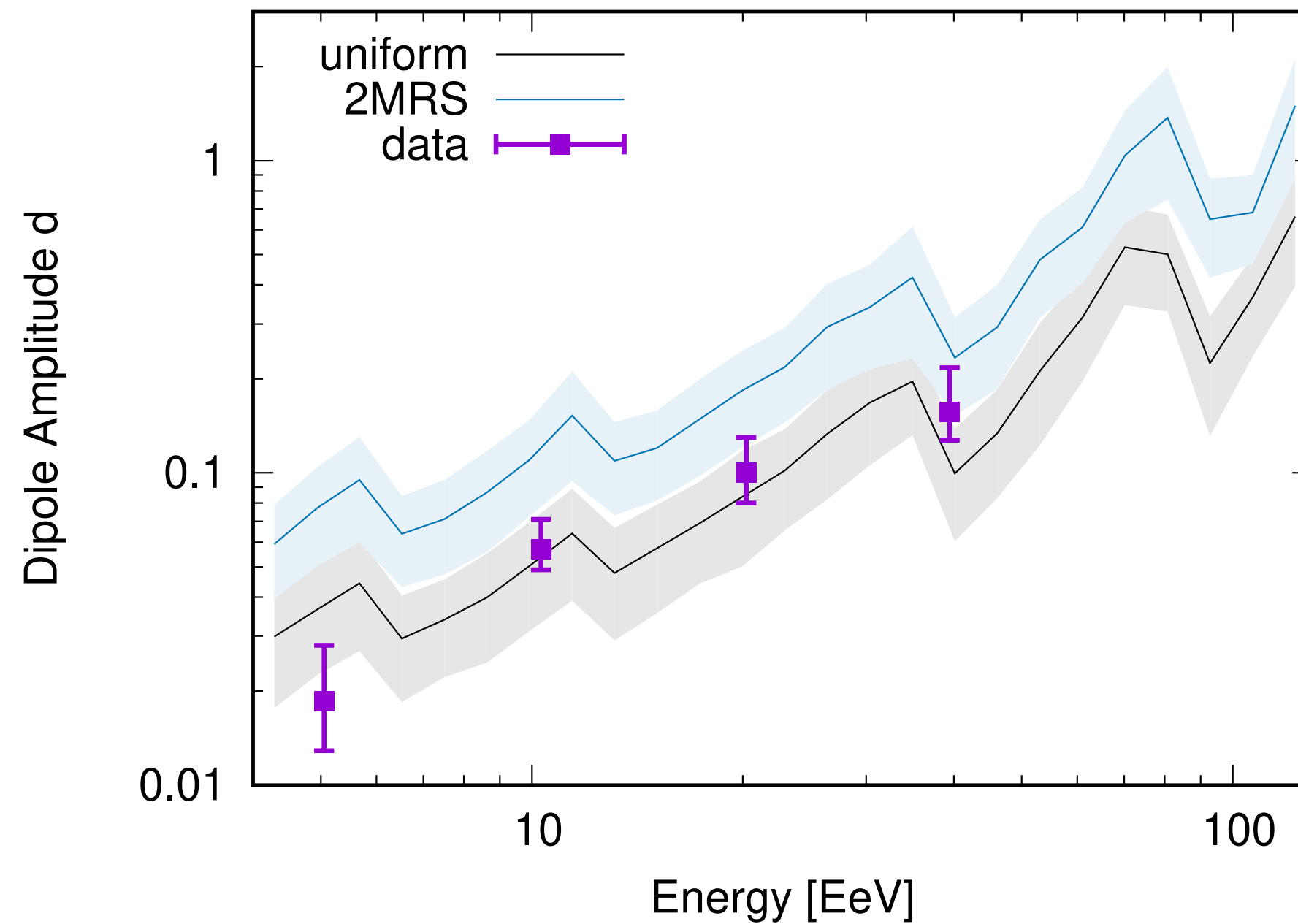
Energy evolution of the dipole



gray band: integrated bin $E > 8$ EeV

Both amplitude and deviation of phase from the GC increase with energy

Dipole amplitude with energy and scenarios of extragalactic sources with a mixed CR composition



[E. Roulet for the P. Auger Collab., ICRC 2019](#)

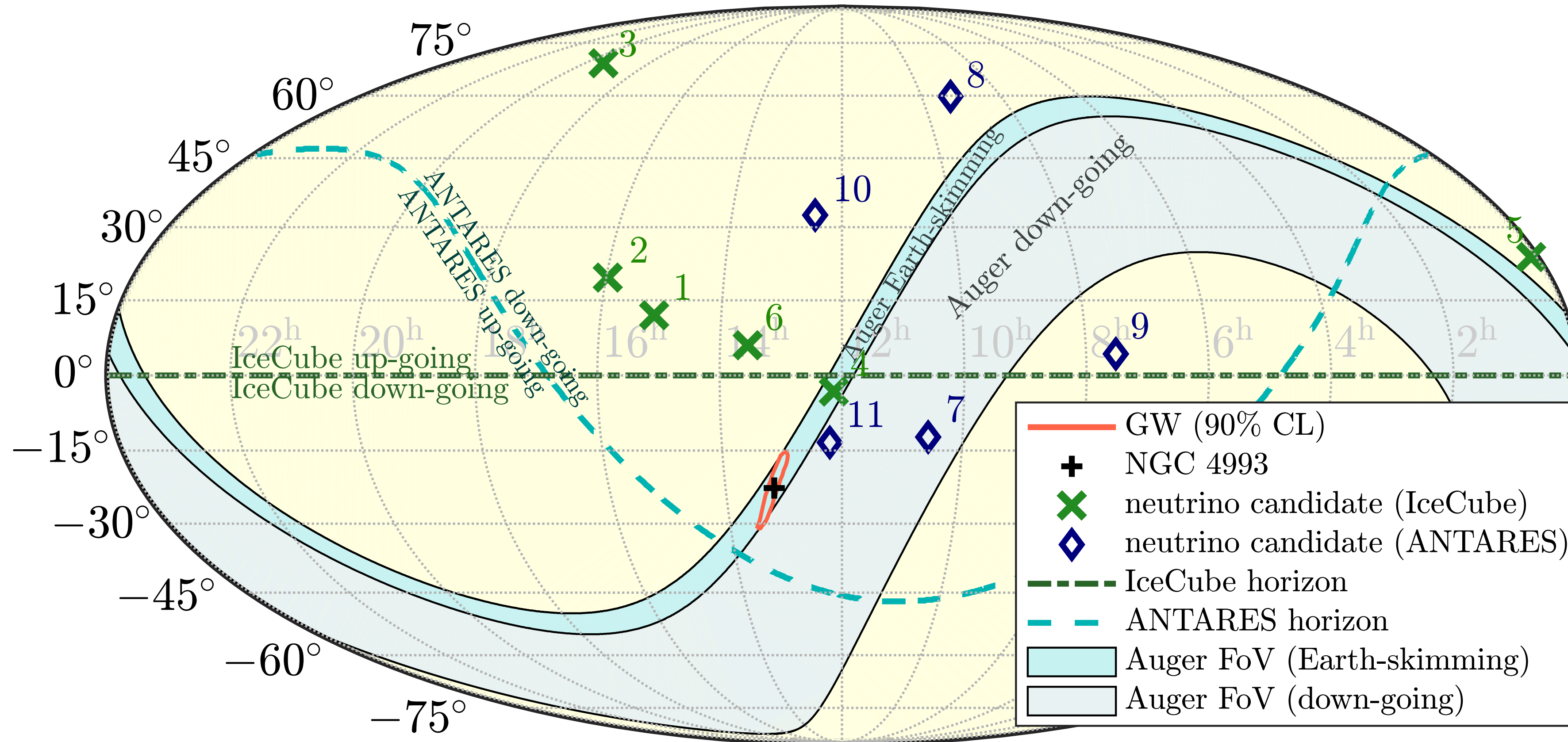
[P. Auger Collab. Astroph. J., 2020](#)

ν in coincidence with GW170817

- ★ ν follow up: Antares, IceCube and Pierre Auger Observatory
- ★ At time of GW trigger: event in region of maximum sensitivity for Auger

Energy range of Auger: $E_\nu > 10^{17}$ eV

Zenith angle of optical counterpart within ± 500 s: $(90.4^\circ; 93.3^\circ)$, Earth-skimming



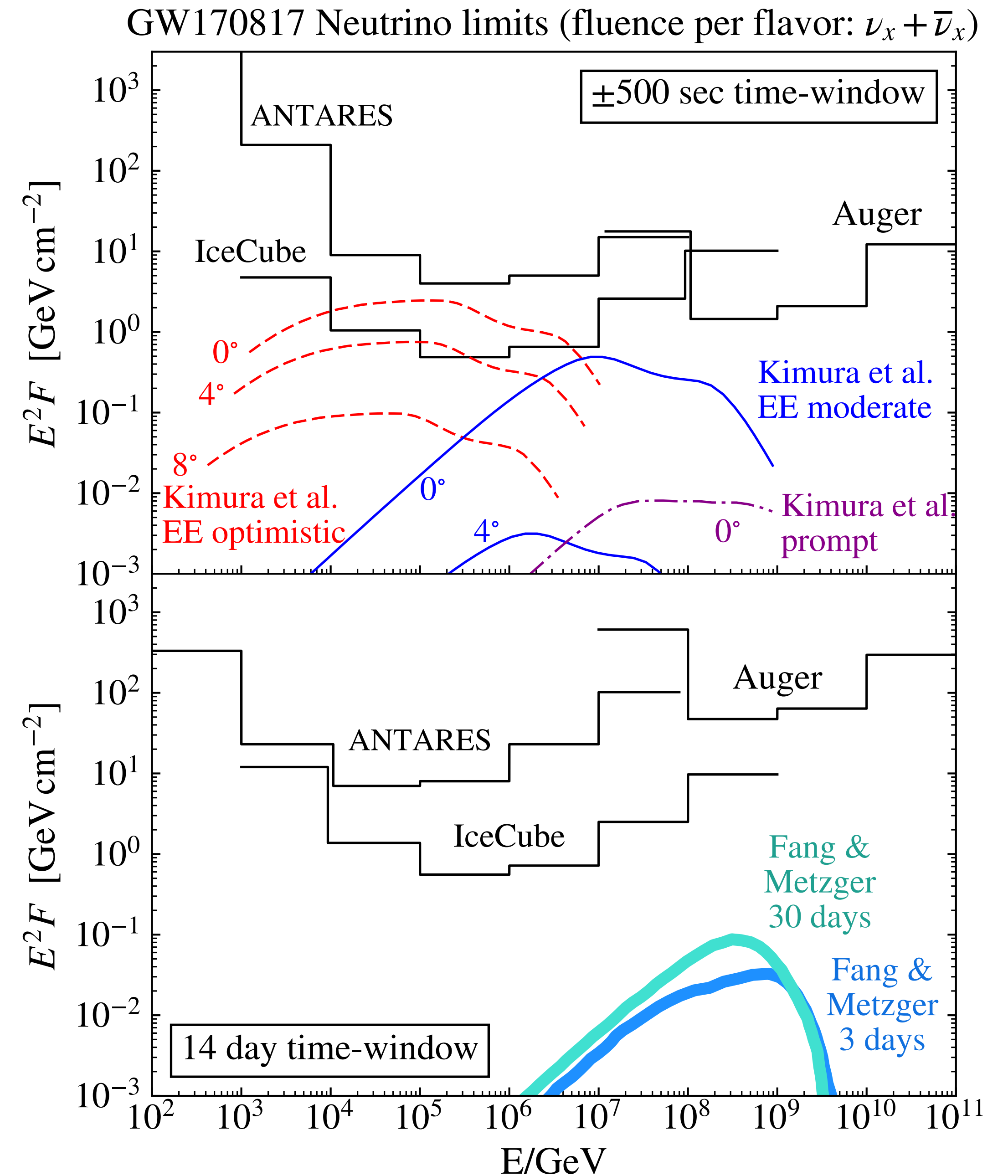
ANTARES, IceCube and the Pierre Auger Observatory, AJL, 2017

GW170817 ν limits

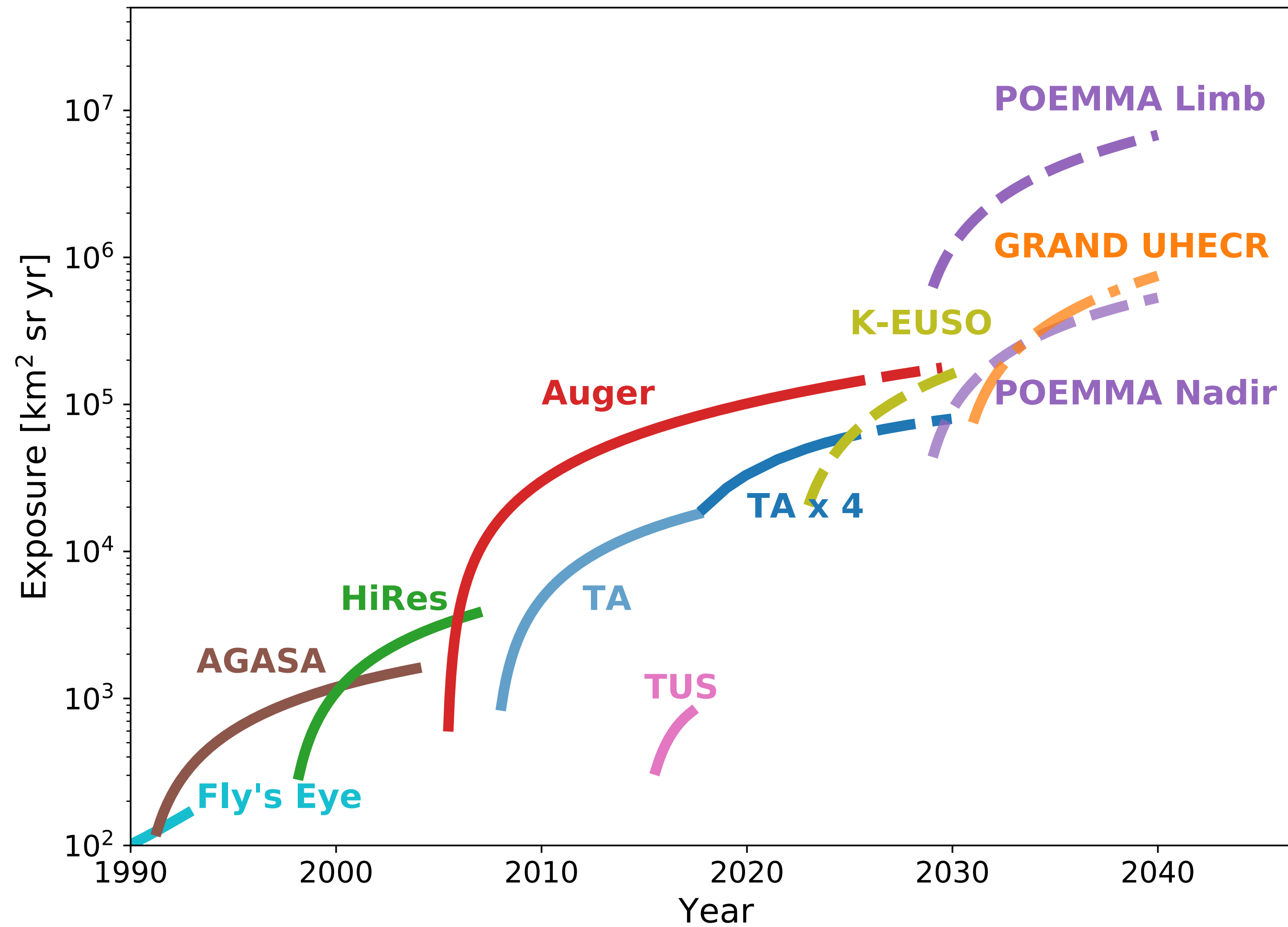
- ★ Time windows: ± 500 s, 14-days
- ★ No neutrino candidate found
- ★ Only optimistic model constraint by observations
- ★ Consistent with model predictions of short GRB observed off-axis and low luminosity GRB

- ★ Complementary searches
- ★ An unprecedented joint effort of experiments sensitive to high-energy neutrino

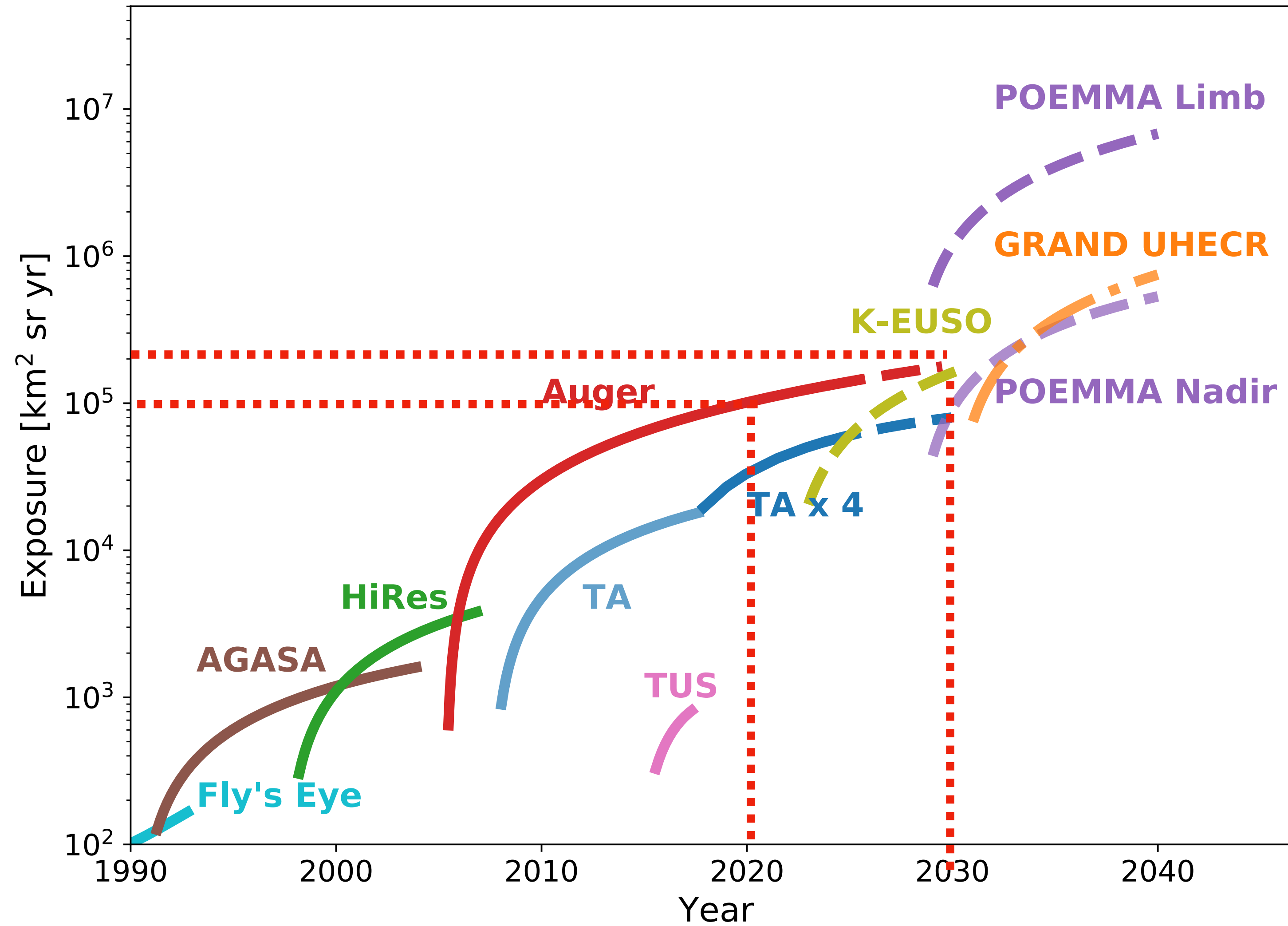
[ANTARES, IceCube and the P. Auger Observatory, AJL, 2017](#)



Future of UHECR physics



Future of UHECR physics



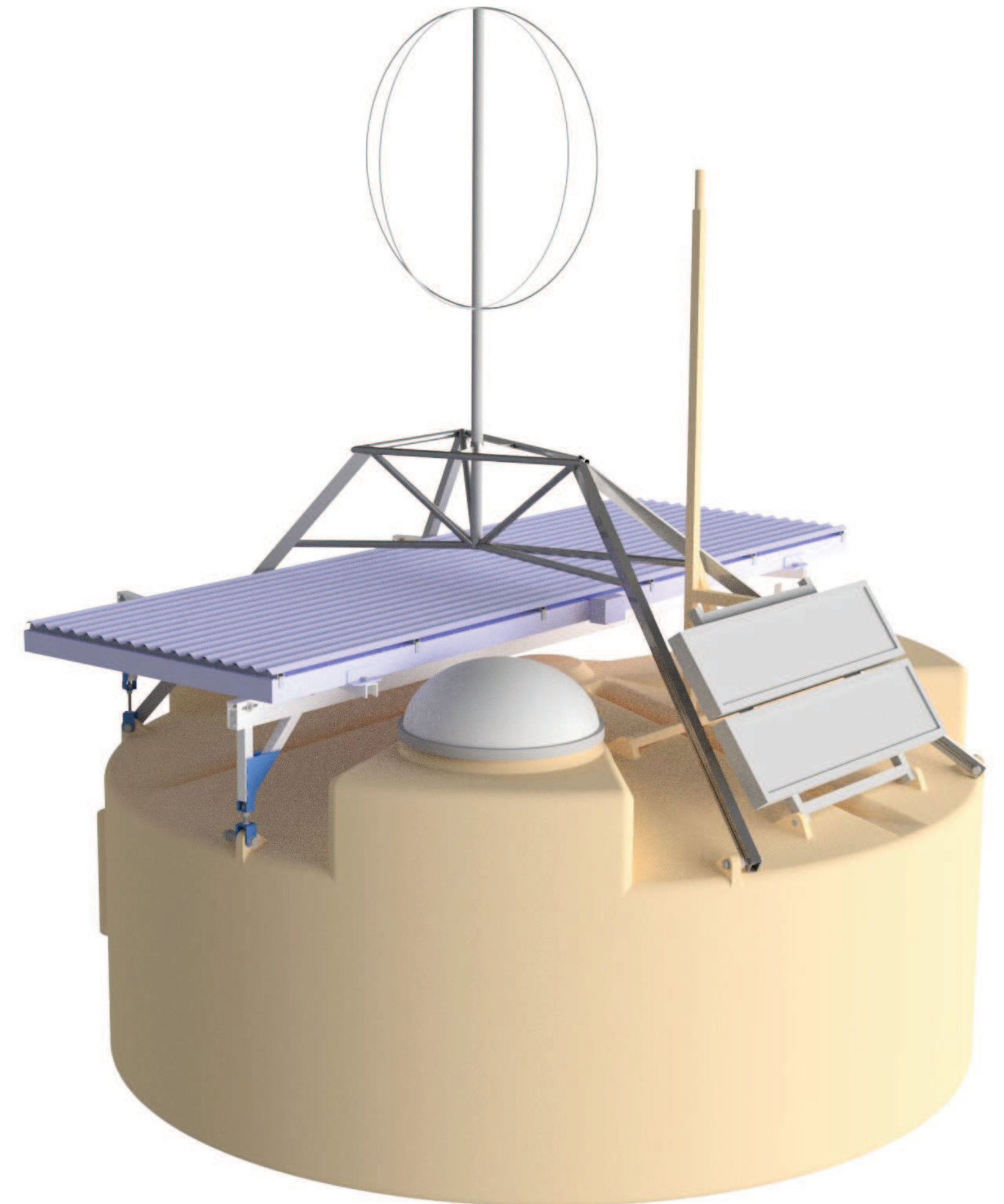
The Pierre Auger Observatory Upgrade (AugerPrime)

Physics goals

- ★ composition measurement at 10^{20} eV
- ★ composition-enhanced anisotropy studies
- ★ particle physics with air showers

Components of upgrade

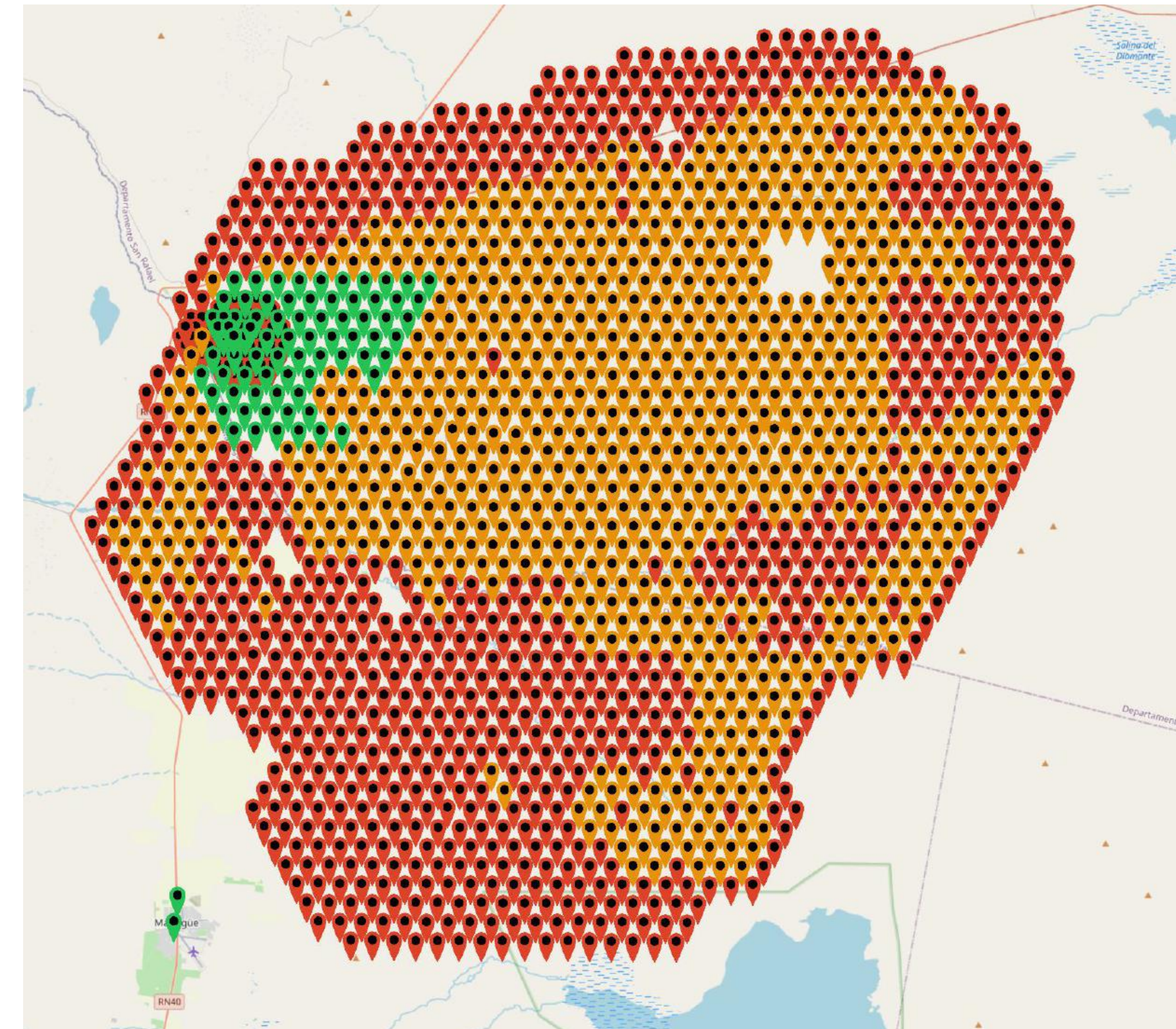
- ★ New Surface Scintillator Detector (SSD) on top of SD stations
- ★ Radio Detector at each SD station
- ★ SD electronics improvements
- ★ Upgrade of the Underground Muon Detector (23.5 km^2)
- ★ Increase of the FD operation time



Status of AugerPrime



SD station with new scintillator and new radio antenna



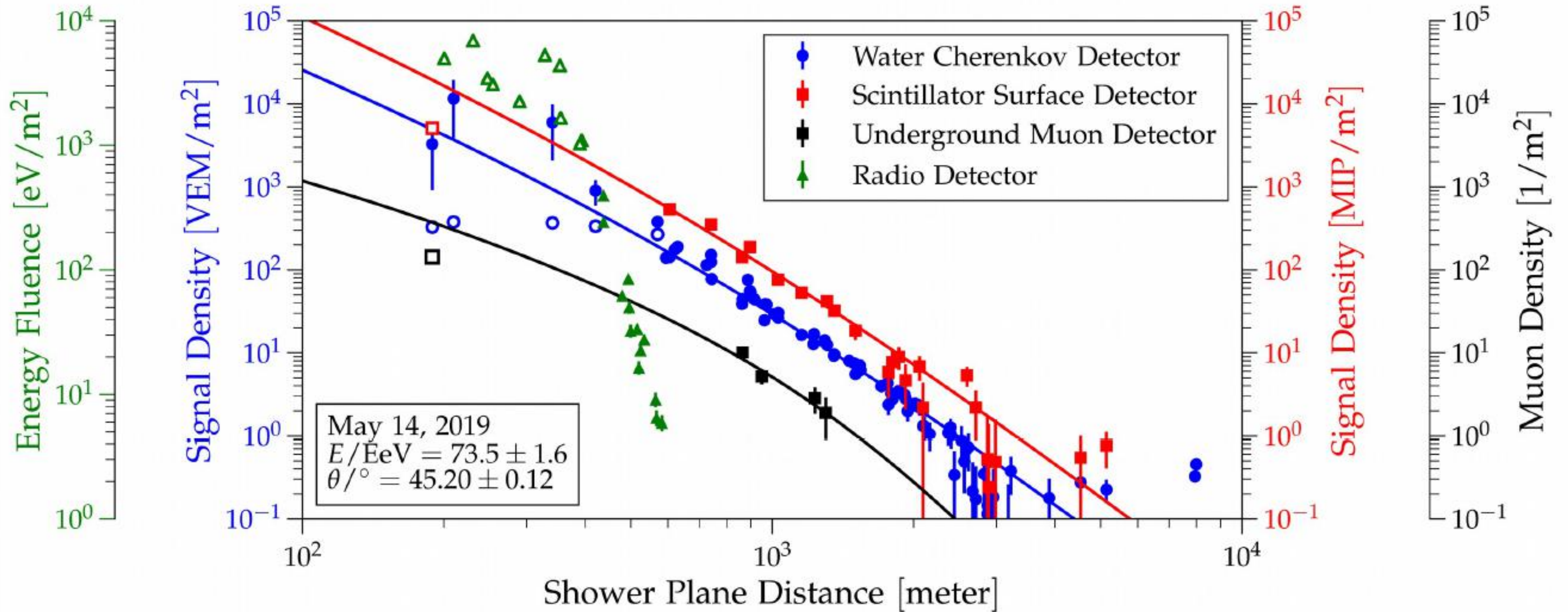
Engineering array (12 stations) data since 2016

Pre-production SSD array (77 stations) since March 2019

866 SSD stations deployed (October 2020)

[J. Stasielak for the P. Auger Collab. ICNFP 2020](#)

AugerPrime data



Lateral distribution of signals measured by different detectors of a real event, as a function of the distance to the shower core

